Title

Search for heavy resonances decaying into a W or Z boson and a Higgs boson in final states with leptons and b-jets in 36 fb−1 of s=13 TeV pp collisions with the ATLAS detector

Journal

Journal of High Energy Physics, 2018(3)

ISSN

1126-6708

Authors

The ATLAS collaboration
Aaboud, M
Aad, G
et al.

Publication Date

2018-03-01

DOI

10.1007/jhep03(2018)174

EUROPEAN ORGANISATION FOR NUCLEAR RESEARCH (CERN)

JHEP 03 (2018) 174
DOI: DOI:10.1007/JHEP03(2018)174

CERN-EP-2017-250
10th May 2018

Search for heavy resonances decaying into a W or Z boson and a Higgs boson in final states with leptons and b-jets in 36 fb^{-1} of $\sqrt{s}$ = 13 TeV pp collisions with the ATLAS detector

The ATLAS Collaboration

A search is conducted for new resonances decaying into a W or Z boson and a 125 GeV Higgs boson in the $\nu\bar{\nu}b\bar{b}$, $\ell^{\pm}\nu b\bar{b}$, and $\ell^{+}\ell^{-}b\bar{b}$ final states, where $\ell^{\pm} = e^{\pm}$ or $\mu^{\pm}$, in pp collisions at $\sqrt{s} = 13$ TeV. The data used correspond to a total integrated luminosity of 36.1 fb^{-1} collected with the ATLAS detector at the Large Hadron Collider during the 2015 and 2016 data-taking periods. The search is conducted by examining the reconstructed invariant or transverse mass distributions of Wh and Zh candidates for evidence of a localised excess in the mass range of 220 GeV up to 5 TeV. No significant excess is observed and the results are interpreted in terms of constraints on the production cross-section times branching fraction of heavy W' and Z' resonances in heavy-vector-triplet models and the CP-odd scalar boson A in two-Higgs-doublet models. Upper limits are placed at the 95% confidence level and range between 9.0×10^{-4} pb and 7.3×10^{-1} pb depending on the model and mass of the resonance.

1 Introduction

The ATLAS [1] and the CMS [2] collaborations discovered a Higgs boson (h) with a mass near 125 GeV and properties consistent with the Standard Model (SM) predictions [3–5]. Two of the most important questions that remain are how the Higgs boson mass is protected against large radiative corrections (the naturalness problem [6–8]) and whether the Higgs boson is part of an extended scalar sector [9], thus making this particle important for searches for new physics beyond the SM.

Various models with dynamical electroweak symmetry breaking scenarios attempt to solve the naturalness problem by assuming a new strong interaction at a higher energy scale. These models generically predict the existence of new vector resonances that naturally decay into a vector boson and a Higgs boson, for example in Minimal Walking Technicolour [10–12], Little Higgs [13], and composite Higgs models [14, 15]. The decays into a vector-boson and Higgs boson final state are frequently enhanced in these models.

Another possible extension of the SM includes the addition of a second Higgs doublet [16]. A second Higgs doublet arises in many theories beyond the SM, collectively called two-Higgs-doublet models (2HDMs), such as the minimal supersymmetric SM [17–21], axion models [22], and baryogenesis models [23]. In 2HDMs with a CP-conserving Higgs potential, the scalar sector of the theory consists of five Higgs bosons: two charged ($H^{\pm}$), two neutral CP-even (h, H) and one neutral CP-odd (A).

This paper describes a search for the production of new heavy vector bosons, denoted hereafter by W' and Z', that decay into a W or a Z boson and an h boson and a search for a heavy CP-odd scalar boson A that decays into a Z and an h boson. The analyses described here target leptonic decays of the vector bosons ($W^{\pm} \to \ell^{\pm}\nu$, $Z \to \ell^{+}\ell^{-}/\nu\bar{\nu}$; $\ell^{\pm} = e^{\pm}, \mu^{\pm}$) and decays of the h boson into a b-quark pair. This results in three search channels: $W' \to W^{\pm}h \to \ell^{\pm}\nu b\bar{b}$, $Z'/A \to Zh \to \ell^{+}\ell^{-}b\bar{b}$, and $Z'/A \to Zh \to \nu\bar{\nu}b\bar{b}$.

Resonance searches are typically not sensitive to all free parameters of the underlying theory, thus simplified models [24] can be used to parameterise a broad class of models, wherein only the relevant couplings and mass parameters are retained in the Lagrangian. For the interpretation of the results in the context of models with heavy vector triplets (HVT), a simplified model [25, 26], based on a phenomenological Lagrangian is used as a benchmark. This model incorporates an $\mathrm{SU}(2)_{\mathrm{L}}$ triplet of heavy vector bosons, which allows the results to be interpreted in a large class of models. The new heavy vector bosons, W' and Z', collectively denoted by V', couple to the Higgs and gauge bosons via a combination of parameters $g_{\mathrm{V}}c_{\mathrm{H}}$ and to the fermions via the combination $(g^2/g_{\mathrm{V}})\,c_{\mathrm{F}}$, where g is the $\mathrm{SU}(2)_{\mathrm{L}}$ gauge coupling. The parameter g_{V} represents the strength of the new vector-boson interaction, and c_{H} and c_{F} represent corrections to the coupling strength specific to Higgs bosons and fermions, respectively. Two benchmark models are used in this analysis. In the first model, referred to as *Model A*, the branching fractions to fermions and gauge bosons are comparable, as in some models with an extended gauge symmetry [27]. For *Model B*, fermionic couplings are suppressed, as in strong dynamical models such as the minimal composite Higgs model [28]. At low resonance masses and large g_{V} couplings, the HVT models fail to reproduce the SM parameters, thus this search focuses on high masses, from 500 GeV up to 5 TeV.

The results from the $A \to Zh$ search are interpreted as exclusion limits on the ratio of the vacuum expectation values of the two Higgs doublets, $\tan(\beta)$, and on $\cos(\beta-\alpha)$, where α is the mixing angle between the two CP-even Higgs bosons. The exclusion limits are evaluated for the Type I, Type II, Lepton-specific, and Flipped 2HDMs. These differ with respect to which doublets couple to the up-type and down-type quarks as well as to the charged leptons [16]. Both the production via gluon–gluon fusion and the production with associated b-quarks ($b\bar{b}A$) are considered in this search. The $A \to Zh$ decay mode is mostly

relevant below the $t\bar{t}$ production threshold and the cross-section falls steeply with increasing A boson mass. Therefore, this search starts at the Zh threshold of approximately 220 GeV and goes up to 2 TeV.

Previous searches in the same final states have been performed by the ATLAS and the CMS collaborations using data at $\sqrt{s}$ = 8 TeV and 13 TeV. The ATLAS searches for $W' \to Wh$ ($Z' \to Zh$) exclude, at 95% confidence level (CL), W' (Z') resonances with masses below 1.75 (1.49) TeV assuming the HVT benchmark *Model A* ($g_V = 1$) and below 2.22 (1.58) TeV assuming *Model B* ($g_V = 3$) [29, 30]. Searches by the CMS Collaboration exclude resonances with masses less than 2.0 TeV at 95% CL assuming the HVT benchmark *Model B* ($g_V = 3$) [31]. Searches using the fully hadronic final state ($W/Zh \to qq'b\bar{b}$) have also been performed by CMS and ATLAS and exclude W' (Z') resonances below 3.15 TeV (2.6 TeV) assuming the HVT benchmark *Model B* ($g_V = 3$) [32–34]. Previous searches for a CP-odd scalar boson A in the Zh decay mode are reported in Refs. [35–39].

The search presented in this paper is performed by looking for a localised excess in the distribution of the reconstructed mass of the $\nu\bar{\nu}b\bar{b}$, $\ell^{\pm}\nu b\bar{b}$, and $\ell^{+}\ell^{-}b\bar{b}$ systems. The mass range covered by the search, from 220 GeV to 5 TeV, probes a wide range of Higgs boson transverse momenta. Thus, two methods are used to reconstruct Higgs boson candidates. At low transverse momenta, the decay products of the Higgs boson are reconstructed as individual jets. At high transverse momenta, the decay products start to merge and are reconstructed as a single jet. The signal yield and background normalisations are determined from a binned maximum-likelihood fit to the data distribution for each of the V' and A boson models (W', Z', gluon–gluon fusion A, bbA) and are used to set upper limits on the production cross-section times decay branching fraction. A combined fit using all three lepton channels sets bounds on the HVT model in the case where the V' bosons are degenerate in mass.

This paper is structured as follows. Sections 2 and 3 provide a brief description of the ATLAS experiment and the data and simulated event samples. The event reconstruction and selections are discussed in Sections 4 and 5. The background estimation and systematic uncertainties are described in Sections 6 and 7. Finally, Sections 8 and 9 detail the statistical analysis and provide a discussion of the results and concluding remarks.

2 ATLAS detector

The ATLAS detector [40] at the LHC covers nearly the entire solid angle[1] around the collision point. It consists of an inner tracking detector (ID) surrounded by a thin superconducting solenoid, electromagnetic and hadronic calorimeters, and a muon spectrometer incorporating three large superconducting toroid magnets.

The ID is immersed in a 2 T axial magnetic field and provides charged-particle tracking in the range $|\eta| < 2.5$. It consists of silicon pixel, silicon microstrip, and transition radiation tracking detectors. Prior to the data-taking at the increased centre-of-mass energy of 13 TeV, the ID was enhanced by adding a new layer of pixel detectors (the IBL [41]) inside the existing pixel detector layers in the barrel region (at a radius of approximately 33 mm). The upgraded detector typically provides four three-dimensional

[1] ATLAS uses a right-handed coordinate system with its origin at the nominal interaction point (IP) in the centre of the detector and the z-axis along the beam pipe. The x-axis points from the IP to the centre of the LHC ring, and the y-axis points upwards. Cylindrical coordinates (r, ϕ) are used in the transverse plane, ϕ being the azimuthal angle around the z-axis. The pseudorapidity is defined in terms of the polar angle θ as $\eta = -\ln\tan(\theta/2)$. Angular distance is measured in units of $\Delta R \equiv \sqrt{(\Delta\eta)^2 + (\Delta\phi)^2}$.

measurements for tracks originating from the luminous region. The silicon microstrip tracker provides four two-dimensional measurement points per track. The transition radiation tracker enables track reconstruction at large radii up to $|\eta| = 2.0$ and provides electron identification information based on the number of hits above the threshold for transition radiation.

The calorimeter system covers the pseudorapidity range $|\eta| < 4.9$. Within the region $|\eta| < 3.2$, electromagnetic calorimetry is provided by barrel and endcap high-granularity lead/liquid-argon (LAr) electromagnetic calorimeters. An additional thin LAr presampler, covering $|\eta| < 1.8$, is used to correct for energy loss in material upstream of the calorimeters. Hadronic calorimetry is provided by a steel/scintillator-tile calorimeter, segmented into three barrel structures within $|\eta| < 1.7$, and two copper/LAr hadronic endcap calorimeters. The solid-angle coverage is completed with forward copper/LAr and tungsten/LAr calorimeter modules optimised for electromagnetic and hadronic measurements, respectively.

The muon spectrometer is composed of separate trigger and high-precision tracking chambers, measuring the deflection of muons in a magnetic field generated by superconducting air-core toroids. The precision chamber system covers the region $|\eta| < 2.7$ with three layers of monitored drift tubes, complemented by cathode strip chambers in the forward region, where the particle flux is highest. The muon trigger system covers the range $|\eta| < 2.4$ with resistive plate chambers in the barrel, and thin-gap chambers in the endcap regions.

A two-level trigger system is used to select interesting events [42]. The level-1 trigger is implemented in hardware and uses a subset of detector information to reduce the event rate to a design value of at most 100 kHz. This is followed by the software-based trigger level, the high-level trigger, which reduces the event rate further to about 1 kHz.

3 Data and simulated event samples

The data used in this analysis were recorded with the ATLAS detector during the 2015 and 2016 pp-collision runs at $\sqrt{s} = 13$ TeV and correspond to a total integrated luminosity of 36.1 fb^{-1}. The data are required to satisfy a number of criteria that ensure that the ATLAS detector was in good operating condition. A number of Monte Carlo (MC) simulation samples are used to model the background and signal processes for this search.

For the W' and Z' processes, simulated events were generated with MadGraph5_aMC@NLO (MG5_aMC) 2.2.2 [43] at leading-order (LO) accuracy using the NNPDF 2.3 LO parton density function (PDF) set [44]. The parton shower and hadronisation were simulated with Pythia 8.186 [45] using the A14 set [46] of tuned parameters ("tune") together with the NNPDF 2.3 LO PDF set. Events were generated for a range of resonance masses from 500 to 5000 GeV, assuming a zero natural width. Higgs boson decays into $b\bar{b}$ and $c\bar{c}$ pairs were simulated, with a relative branching fraction $B(h \to c\bar{c})/B(h \to b\bar{b}) = 0.05$ fixed to the SM prediction [47].

Events for the gluon–gluon fusion production of A bosons were generated at LO accuracy using the same set-up as for the W' and Z' samples. The b-quark associated production of A bosons was simulated with MG5_aMC 2.2.3 using next-to-leading-order (NLO) matrix elements with massive b-quarks and the CT10F4 NLO PDF set [48]. The parton shower and hadronisation were simulated with Pythia 8.210 [49]. Events were generated for a range of A boson masses from 220 to 2000 GeV assuming a zero natural width. For the A boson signals, only decays of the Higgs boson into a $b\bar{b}$ pair were generated.

For the interpretation of the $A \to Zh$ search in the context of 2HDMs, the masses of the $H^{\pm}$ and H bosons are assumed to be equal to the mass of the A boson. The cross-sections were calculated using up to next-to-next-to-leading-order (NNLO) QCD corrections for gluon–gluon fusion and b-quark associated production in the five-flavour scheme as implemented in SUSHI [50–53]. For the b-quark associated production, a cross-section in the four-flavour scheme was also calculated as described in Refs. [54, 55] and the results were combined with the five-flavour scheme calculation following Ref. [56]. The A boson width and the branching fractions for $A \to Zh$ and $h \to b\bar{b}$ have been calculated using 2HDMC [57, 58]. The procedure for the calculation of the cross-section and branching fractions as well as the choice of the 2HDM parameters follows Ref. [9].

The production of W and Z bosons in association with jets was simulated with SHERPA 2.2.1 [59] using the NNPDF 3.0 NNLO PDF set [60] for both the matrix element calculation and the dedicated parton-shower tuning developed by the SHERPA authors. The event generation utilises COMIX [61] and OPENLOOPS [62], for the matrix element calculation, matched to the SHERPA parton shower using the ME+PS@NLO prescription [63]. The matrix elements were calculated for up to two additional partons at NLO and for three and four partons at LO in QCD. The cross-sections for W/Z+jets were calculated at NNLO accuracy [64].

The $t\bar{t}$ process was simulated with POWHEG-BOX v2 [65–67] interfaced to PYTHIA 6.428 [68]. The CT10 PDF set [48] was used in the calculation of the matrix elements, while the parton shower used the Perugia 2012 tune [69] with the CTEQ6L1 PDF set [70]. The cross-section was calculated at NNLO accuracy including the resummation of next-to-next-to-leading logarithmic (NNLL) soft gluon terms with TOP++2.0 [71–77]. The predicted transverse momentum spectra of top quarks and the $t\bar{t}$ system were reweighted to the corresponding NNLO parton-level spectra [78].

The production of single top quarks (t-channel, s-channel, and Wt) was simulated using the POWHEG-BOX event generator with the CT10 PDF set. The shower and hadronisation was simulated using the same event generator and set-up as for the $t\bar{t}$ process. The cross-section for the t- and s-channel single-top-quark production was calculated at NLO accuracy using HATHOR v2.1 [79, 80], while for the Wt process an approximate NNLO calculation was used [81]. The top mass is set fixed to 172.5 GeV in the $t\bar{t}$ and single-top-quark samples.

Diboson events (WW, WZ, ZZ) were simulated using the SHERPA 2.1.1 event generator using the CT10 PDFs. Matrix elements were calculated for up to one (ZZ) or no (WW, WZ) additional partons at NLO and up to three additional partons at LO, and the cross-sections were calculated at NLO accuracy.

Finally, the SM processes $Vh(h \to b\bar{b})$, $t\bar{t}h$, $t\bar{t}W$, and $t\bar{t}Z$ are included in the total background estimation. The $q\bar{q} \to Zh$ and $q\bar{q} \to Wh$ processes were simulated at LO with PYTHIA 8.186 using the NNPDF 2.3 LO PDF set and the A14 tune. The $gg \to Zh$ process was simulated at NLO using the POWHEG-BOX v2 event generator with the CT10 PDF set. The modelling of the shower, hadronisation and underlying event was provided by PYTHIA 8.186 using the AZNLO tune [82] with the same PDF set as for the matrix element calculation. The cross-sections for the Wh and Zh processes were taken from Ref. [9]. The $t\bar{t}h$ and $t\bar{t}V$ samples were generated at NLO accuracy with MG5_aMC 2.3.2 interfaced to PYTHIA 8.210. The NNPDF 3.0 NLO PDF set was used in the matrix element calculation while for the parton shower the A14 tune was used with the NNPDF 2.3 LO PDF set.

A summary of event generators used for the simulation of signal and background processes is shown in Table 1.

All simulated event samples include the effect of multiple pp interactions in the same and neighbouring bunch crossings (pile-up) by overlaying simulated minimum-bias events on each generated signal or

Table 1: Event generators used for the simulation of the signal and background processes. The acronyms ME and PS are used for matrix element and parton shower, respectively.

Process	ME generator	ME PDF	PS and Hadronisation	MC tune	Cross-section calc. order
Signal					
V'	MG5_aMC 2.2.2	NNPDF 2.3 LO	Pythia 8.186	A14	LO
Gluon–gluon fusion A	MG5_aMC 2.2.2	NNPDF 2.3 LO	Pythia 8.186	A14	NNLO
bbA	MG5_aMC 2.2.3	CT10F4	Pythia 8.210	A14	NLO
Top quark					
$t\bar{t}$	Powheg-Box v2	CT10	Pythia 6.428	Perugia 2012	NNLO+NNLL
s-channel	Powheg-Box	CT10	Pythia 6.428	Perugia 2012	NLO
t-channel	Powheg-Box	CT10	Pythia 6.428	Perugia 2012	NLO
Wt	Powheg-Box	CT10	Pythia 6.428	Perugia 2012	approx. NNLO
Vector boson					
V + jets	Sherpa 2.2.1	NNPDF 3.0 NNLO	Sherpa 2.2.1	Default	NNLO
WW, WZ, ZZ	Sherpa 2.1.1	CT10	Sherpa 2.2.1	Default	NLO
Other					
$t\bar{t}h$, $t\bar{t}W$, $t\bar{t}Z$	MG5_aMC 2.3.2	NNPDF 3.0 NLO	Pythia 8.210	A14	NLO
$q\bar{q} \to Zh$, Wh	Pythia 8.186	NNPDF 2.3 LO	Pythia 8.186	A14	NNLO+NLO
$gg \to Zh$	Powheg-Box v2	CT10	Pythia 8.186	AZNLO	NLO+NLL

background event. The minimum-bias events were simulated with the single-, double- and non-diffractive pp processes of Pythia 8.186 using the A2 tune [83] and the MSTW2008 LO PDF [84]. For all MadGraph and Powheg samples, the EvtGen v1.2.0 program [85] was used for the bottom and charm hadron decays. The generated samples were processed using the Geant-based ATLAS detector simulation [86, 87] and the same event reconstruction algorithms were used as for the data.

4 Event reconstruction

This search makes use of the reconstruction of multi-particle vertices, the identification and the kinematic properties of reconstructed electrons, muons, τ leptons, jets, and the determination of missing transverse momentum.

Collision vertices are reconstructed from at least two ID tracks with transverse momentum $p_{\mathrm{T}} > 400$ MeV. The primary vertex is selected as the one with the highest $\sum p_{\mathrm{T}}^2$, calculated considering all associated tracks.

Electrons are reconstructed from ID tracks that are matched to energy clusters in the electromagnetic calorimeter. The clusters are reconstructed using the standard ATLAS sliding-window algorithm, which clusters calorimeter cells within fixed-size η/ϕ rectangles [88]. Electron candidates are required to satisfy requirements for the electromagnetic shower shape, track quality, and track–cluster matching; these requirements are applied using a likelihood-based approach. The "Loose" and "Tight" working points defined in Ref. [89] are used.

Muons are identified by matching tracks found in the ID to either full tracks or track segments reconstructed in the muon spectrometer ("combined muons"), or by stand-alone tracks in the muon spectrometer [90]. Muons are required to pass identification requirements based on quality requirements applied to the ID and muon spectrometer tracks. The "Loose" and "Medium" identification working points defined in Ref. [90] are used in this analysis. The "Loose" working point includes muons reconstructed with the muon spectrometer alone to extend the acceptance to $|\eta| = 2.7$.

Electron and muon candidates are required to have a minimum p_{T} of 7 GeV and to lie within a region where there is good reconstruction and identification efficiency ($|\eta| < 2.7$ for muons and $|\eta| < 2.47$ for electrons). The "Loose" lepton identification criterion has to be fulfilled and all candidates have to originate from the primary vertex. The last condition is satisfied by requiring that the significance of the transverse impact parameter $|d_0|/\sigma(d_0)$ is less than 5.0 for electrons (< 3.0 for muons) and $|z_0 \sin(\theta)|$ is less than 0.5 mm, where z_0 is the longitudinal impact parameter and θ is the polar angle defined in Section 2. The lepton candidates are required to be isolated using requirements on the sum of the p_{T} of the tracks lying in a cone around the lepton direction whose size, ΔR, decreases as a function of the lepton p_{T} [91]. The efficiency of the isolation selection is tuned to be larger than 99% in a sample of $Z \to \ell^+\ell^-$ decays [88, 90, 92]. The identification and isolation efficiencies of both the electrons and muons are calibrated using a tag-and-probe method in $Z \to \ell^+\ell^-$ data events [88, 90].

Two types of calorimeter-based jets, "small-R" and "large-R" jets, are used to reconstruct Higgs boson candidates over a wide momentum spectrum. Small-R jets are reconstructed from noise-suppressed topological clusters in the calorimeter [93] using the anti-k_t [94] algorithm implemented in the FastJet package [95] with a radius parameter $R = 0.4$ and are required to have a $p_{\mathrm{T}} > 20$ GeV for $|\eta| < 2.5$ (central jets) or $p_{\mathrm{T}} > 30$ GeV for $2.5 < |\eta| < 4.5$ (forward jets). To reduce the number of small-R jets originating from pile-up interactions, these jets are required to pass the jet vertex tagger [96] selection, with an efficiency of about 90%, if they are in the range $p_{\mathrm{T}} < 60$ GeV and $|\eta| < 2.4$.

Large-R jets are used to reconstruct Higgs boson candidates with high momenta for which the b-quarks are emitted close to each other. They are constructed using the anti-k_t algorithm with a radius parameter of $R = 1.0$ and are trimmed [97] to remove the energy of clusters that originate from initial-state radiation, pile-up interactions or the underlying event. This is done by reclustering the constituents of the initial jet, using the k_t algorithm [98, 99], into smaller $R_{\mathrm{sub}} = 0.2$ subjets and then removing any subjet that has a p_{T} less than 5% of the p_{T} of the parent jet [100]. The jet mass resolution is improved at high momentum using tracking in addition to calorimeter information [101]. Large-R jets are required to have $p_{\mathrm{T}} > 250$ GeV and $|\eta| < 2.0$.

The momenta of both the large-R and small-R jets are corrected for energy losses in passive material and for the non-compensating response of the calorimeter. Small-R jets are also corrected for the average additional energy due to pile-up interactions [102, 103].

A third type of jet, built from tracks (hereafter referred to as a track-jet), is used in this analysis for the identification of b-jets from decays of boosted Higgs bosons. The jets are built with the anti-k_t algorithm with $R = 0.2$ from at least two ID tracks with $p_{\mathrm{T}} > 400$ MeV associated with the primary vertex, or with a longitudinal impact parameter $|z_0 \sin(\theta)| < 3$ mm [104]. Track-jets are required to have $p_{\mathrm{T}} > 10$ GeV and $|\eta| < 2.5$, and are matched to the large-R jets via ghost-association [105].

Small-R jets and track-jets containing b-hadrons are identified with the multivariate MV2c10 b-tagging algorithm [106, 107], which makes use of information about the jet kinematics, the properties of tracks within jets, and the presence of displaced secondary vertices. The algorithm is used at the 70% efficiency working point and provides a factor of 380 (120) in rejecting small-R jets (track-jets) from gluons and

light quarks, and a factor of 12 (7) in rejecting small-R jets (track-jets) from c-quarks. Jets satisfying these requirements are referred to as "b-tagged jets".

To improve the mass resolution of the Higgs boson candidate, dedicated energy corrections are applied for b-tagged small-R and large-R jets to account for the semileptonic decays of the b-hadrons. The momentum of the closest muon in ΔR with p_{T} larger than 5 GeV inside the jet cone is added to the jet momentum after removing the energy deposited by the muon in the calorimeter (the muon-in-jet correction) [104]. For this correction, muons are not required to pass the isolation requirements. For small-R jets only, an additional p_{T}-dependent correction, denoted "PtReco", is applied to the jet four-momentum to account for biases in the response of b-jets, improving the resolution of the dijet mass. This correction is determined from $Vh(h \to b\bar{b})$ simulated events by calculating the ratio of the p_{T} of the true b-jets from the Higgs boson decay to the p_{T} of the reconstructed b-tagged jets after the muon-in-jet correction. The resolution of the dijet mass, m_{jj} (m_{J}), in this process is improved by 18% (22%) for the resolved (merged) Higgs boson reconstruction after these corrections, as shown in Figure 1.

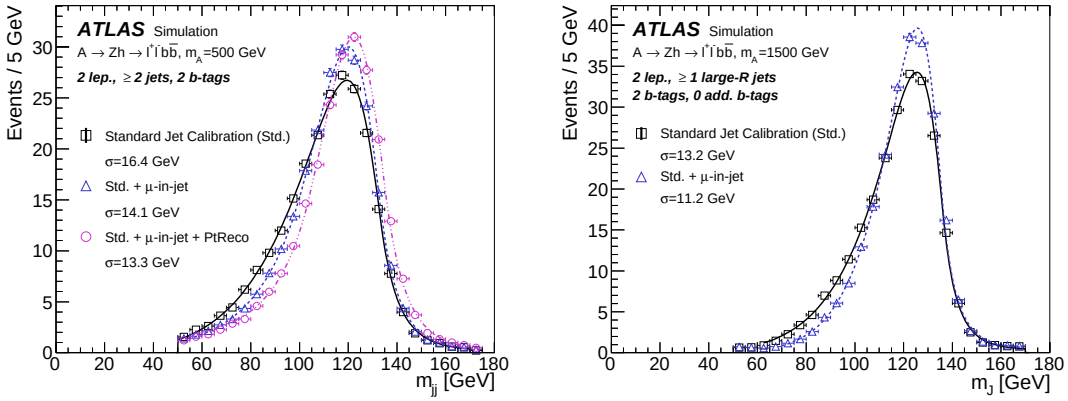

Figure 1: Reconstructed mass of the Higgs boson candidates for the (left) resolved and (right) merged event topologies in a sample of simulated signal events with $m_A = 500$ GeV and $m_A = 1500$ GeV respectively. The different distributions correspond to the different b-jet energy corrections applied in each case as described in the text. The distributions are fit to the asymmetric function described in Ref. [108] and the resolution parameter is shown in the plots.

Hadronically decaying τ-lepton candidates (τ_{had}) are identified using small-R jets with $p_{\mathrm{T}} > 20$ GeV and $|\eta| < 2.5$, outside the transition region between the barrel and endcap calorimeters ($1.37 < |\eta| < 1.52$). These τ_{had} candidates must have either one or three associated tracks and must satisfy the "Medium" identification criterion [109]. They are used in the $\nu\bar{\nu}b\bar{b}$ channel to reject backgrounds with real hadronic τ-leptons.

The presence of neutrinos in the $\nu\bar{\nu}b\bar{b}$ and $\ell^{\pm}\nu b\bar{b}$ final states can be inferred from a momentum imbalance in the transverse plane. The missing transverse momentum ($\vec{E}_{\mathrm{T}}^{\mathrm{miss}}$) is calculated as the negative vectorial sum of the transverse momenta of all the muons, electrons, small-R jets, and ID tracks associated with the primary vertex but not associated with any of those leptons and jets [110, 111]. To suppress non-collision and multijet backgrounds in the $\nu\bar{\nu}b\bar{b}$ channel, an additional track-based missing transverse momentum estimator, $\vec{p}_{\mathrm{T}}^{\,\mathrm{miss}}$, is built independently as the negative vectorial sum of the transverse momenta of all tracks from the primary vertex.

An overlap-removal algorithm is applied to prevent double counting of the leptons and jets used for the

resonance reconstruction. A τ-lepton is removed if the ΔR between the τ-lepton and an electron or a muon is below 0.2. In the case of a muon, the τ-lepton is not removed if the τ-lepton has p_{T} above 50 GeV and the reconstructed muon is not a combined muon. If a reconstructed muon and electron share the same ID track then the electron is removed. Small-R jets are removed if they are within a cone of size $\Delta R = 0.2$ around an electron or muon that has passed the isolation requirements. To account for semi-muonic b-jet decays, the jet is only removed if it has fewer than three associated tracks, or if more than 70% of the sum of the p_{T} of its associated tracks comes from the muon and $p_{\mathrm{T}}^{j}/p_{\mathrm{T}}^{\mu} < 2$, where p_{T}^{j} (p_{T}^{μ}) is the p_{T} of the jet (muon). Next, electrons and muons within a cone of size $\Delta R = 0.4$ around a surviving small-R jet are discarded if their distance from the jet direction is smaller than $\Delta R = (0.04 + 10\,\mathrm{GeV}/p_{\mathrm{T}}^{\ell})$. The shrinking cone size ensures a high efficiency for boosted topologies. Small-R jets are also removed if they are within $\Delta R = 0.2$ of the axis of a τ_{had} candidate. Finally, large-R jets within $\Delta R = 1.2$ of any surviving electron are removed.

5 Analysis strategy and event selection

The search for the Z' and A bosons in the $Zh \to \nu\bar{\nu}b\bar{b}$ and $Zh \to \ell^{+}\ell^{-}b\bar{b}$ decay modes uses event samples wherein the number of reconstructed charged leptons is exactly zero or two (0-lepton and 2-lepton channels). For the W' search in the $Wh \to \ell^{\pm}\nu b\bar{b}$ channel, events with exactly zero or one charged lepton are used (0-lepton or 1-lepton channels). The lepton selection requirements described in the previous section are applied, using the "Loose" identification working point. The selections outlined below define regions sensitive to the different models.

For the 0-lepton channel, an $E_{\mathrm{T}}^{\mathrm{miss}}$ trigger with a threshold of 70 GeV was used to record the data in 2015 runs; the threshold varied between 90 and 110 GeV in 2016 runs due to the increasing instantaneous luminosity. Events are required to have $E_{\mathrm{T}}^{\mathrm{miss}} > 150$ GeV, where $E_{\mathrm{T}}^{\mathrm{miss}}$ is reconstructed with fully calibrated leptons and jets. The efficiency of the trigger selection exceeds 80% above 150 GeV. In the 2-lepton channel, events were recorded using a combination of single-lepton triggers with isolation requirements. In 2015, the lowest p_{T} threshold was 24 GeV; in 2016, it ranged from 24 to 26 GeV. Additional triggers without an isolation requirement are used to recover efficiency for leptons with $p_{\mathrm{T}} > 60$ GeV. In the single-electron channel, the same single-electron triggers as in the 2-lepton channel are applied. In the single-muon channel, the same $E_{\mathrm{T}}^{\mathrm{miss}}$ triggers as in the 0-lepton channel are used because they are more efficient than the single-muon triggers for this analysis. For events selected by the lepton triggers, the lepton that satisfied the trigger is required to match a reconstructed electron (muon) with $p_{\mathrm{T}} > 27$ GeV and $|\eta| < 2.47$ ($|\eta| < 2.5$).

The wide range of resonance masses probed by this search implies that the resonance decay products can be produced with a wide range of transverse momenta. When the Higgs boson has relatively low p_{T}, the b-quarks from its decay can be reconstructed as two small-R jets. As the momentum of the Higgs boson increases, the two b-quarks become more collimated and a selection using a single large-R jet becomes more efficient. Two different methods are used for the reconstruction of the Higgs boson candidate: a "resolved" category in which two small-R jets are used to build the Higgs boson candidate, and a "merged" category where the highest-p_{T} (“leading”) large-R jet is selected as the Higgs boson candidate.

For the resolved signal region, two small-R jets are required to have an invariant mass (m_{jj}) in the range 110 –140 GeV for the 0- and 1-lepton channels and in the range 100 –145 GeV for the 2-lepton channel. The latter selection is relaxed to take advantage of the smaller backgrounds in this channel. This dijet

candidate is defined by the two leading b-tagged small-R jets when two or more b-tagged jets are present in the event. In the case where only one b-tagged jet is present, the dijet pair is defined by the b-tagged jet and the leading small-R jet in the remaining set. The leading jet in the pair must have $p_{\mathrm{T}} > 45$ GeV. For the merged signal region, a large-R jet is required with mass (m_{J}) in the range 75 to 145 GeV and at least one associated b-tagged track-jet.

Events which satisfy the selection requirements of both the resolved and merged categories, are assigned to the resolved one, since its better dijet mass resolution and lower background contamination increases the expected sensitivity. Events failing to satisfy both the resolved and merged signal region requirements are assigned to control regions defined in Section 6, with priority given to the resolved category. This procedure provides a higher sensitivity for resonances of mass near 1 TeV compared to a procedure in which the merged category is prioritised.

Higgs boson candidates with one or two b-tagged jets define the "1 b-tag" or "2 b-tag" categories, respectively. For the merged selection, only one or two leading track-jets associated with the large-R jet are considered in this counting. For the 0- and 2-lepton channels, resolved events with more than two b-tagged jets or merged events with additional b-tagged track-jets not associated with the large-R jet are used to define signal regions sensitive to $b\bar{b}A$ production. These are labeled as "3+ b-tag" in the resolved category, and "1 b-tag additional b-tag" or "2 b-tag additional b-tag" in the merged category. In the 2-lepton channel, the latter two are merged and labeled as "1+2 b-tag additional b-tag".

The calculation of the reconstructed resonance mass depends on the decay channel. In the 0-lepton channel, where it is not possible to reconstruct the Zh system fully due to the presence of two neutrinos from the Z boson decay, the transverse mass defined as

$$m_{\mathrm{T},Vh} = \sqrt{(E_{\mathrm{T}}^{h} + E_{\mathrm{T}}^{\mathrm{miss}})^2 - (\vec{p}_{\mathrm{T}}^{\,h} + \vec{E}_{\mathrm{T}}^{\mathrm{miss}})^2},$$

is used as the final discriminant. In order to reconstruct the invariant mass of the $Wh \to \ell^{\pm}\nu b\bar{b}$ system in the 1-lepton channel, the momentum of the neutrino in the z-direction, p_z, is obtained by imposing a W boson mass constraint on the lepton–$E_{\mathrm{T}}^{\mathrm{miss}}$ system. In the resulting quadratic equation, the neutrino p_z is taken as the real component in the case of complex solutions, or as the smaller of the two solutions if both solutions are real. The mass resolution of the Vh system is improved in the resolved signal regions of all channels by rescaling the four-momentum of the dijet system by 125 GeV/ m_{jj}. In the 2-lepton channel, the four-momentum of the dimuon system is scaled by 91.2 GeV / $m_{\mu\mu}$ as well in all signal regions. This helps to address the worse momentum resolution of high-momentum muons which are measured solely by the tracking detectors.

Additional selections are applied for each lepton channel, as outlined below, to reduce the main backgrounds and enhance the signal sensitivity. These selections are summarised in Table 2.

For the resolved and merged categories in the 0-lepton channel, the following selections are applied to reduce multijet and non-collision backgrounds to a negligible level:

- $p_{\mathrm{T}}^{\mathrm{miss}} > 30$ GeV (not applied in the resolved 2 and 3+ b-tag categories);
- the azimuthal angle between $\vec{E}_{\mathrm{T}}^{\mathrm{miss}}$ and $\vec{p}_{\mathrm{T}}^{\,\mathrm{miss}}$, $\Delta\phi(\vec{E}_{\mathrm{T}}^{\mathrm{miss}}, \vec{p}_{\mathrm{T}}^{\,\mathrm{miss}}) < \pi/2$;
- the azimuthal angle between $\vec{E}_{\mathrm{T}}^{\mathrm{miss}}$ and the Higgs boson candidate momentum direction, $\Delta\phi(\vec{E}_{\mathrm{T}}^{\mathrm{miss}}, h) > 2\pi/3$;

- the azimuthal angle between $\vec{E}_{\mathrm{T}}^{\mathrm{miss}}$ and the nearest small-R jet momentum direction, $\min[\Delta\phi(\vec{E}_{\mathrm{T}}^{\mathrm{miss}}, \text{small-}R\text{ jet})] > \pi/9$ (for the resolved category with four or more jets, $> \pi/6$ is used).

For the resolved category, $\min[\Delta\phi(\vec{E}_{\mathrm{T}}^{\mathrm{miss}}, \text{small-}R\text{ jet})]$ is calculated using the small-R jets that constitute the Higgs boson candidate and an additional small-R jet, which is the third leading b-tagged jet (if the event contains at least three b-tagged jets), the leading central jet which is not b-tagged (if the event contains only two b-tagged jets) and the leading forward jet (if the event contains only two central small-R jets). For the merged category, all central and forward small-R jets are used in the $\min[\Delta\phi(\vec{E}_{\mathrm{T}}^{\mathrm{miss}}, \text{small-}R\text{ jet})]$ calculation. For the Z'/A search, the $t\bar{t}$ and W+jets backgrounds are further reduced by rejecting events with at least one identified τ_{had} candidate. This veto is not applied when searching for the W' boson or in the HVT combined search, because it leads to a loss of signal events in the $Wh \to \tau^{\pm}\nu b\bar{b}$ final state.

For the 0-lepton resolved category, two additional selections are applied:

- the scalar sum of the p_{T} of the three leading central small-R jets, $\sum p_{\mathrm{T}}^{\mathrm{jet}_i}$, is greater than 150 GeV. In the case where there are only two central small-R jets, the sum of the p_{T} of these two jets and of the leading forward small-R jet, if any, is required to be greater than 120 GeV;
- the azimuthal angle between the two jets used to reconstruct the Higgs boson candidate, $\Delta\phi$(j, j), is required to be less than $7\pi/9$.

Finally, for the merged category, the missing transverse momentum must be larger than 200 GeV.

For the 1-lepton channel, a selection on the transverse momentum of the W boson candidate ($p_{\mathrm{T},W}$), which increases as a function of the reconstructed resonance mass, is applied to reduce the contribution of W+jets: $p_{\mathrm{T},W} > \max[150, 710 - 3.3 \times 10^5\ \mathrm{GeV}/m_{Vh}]$ GeV for the resolved category, while $p_{\mathrm{T},W} > \max[150, 394 \cdot \ln(m_{Vh}/(1\ \mathrm{GeV})) - 2350]$ GeV for the merged category. This selection is optimised taking advantage of the larger transverse momentum of W bosons expected to be produced in the decays of high-mass resonances. The $t\bar{t}$ background is reduced in the resolved category by requiring fewer than four central jets in the event and in the merged category by rejecting events with additional b-tagged track-jets not associated with the large-R jet. For all categories, the transverse mass of the W candidate ($m_{\mathrm{T},W}$), calculated from the transverse components of the lepton and $E_{\mathrm{T}}^{\mathrm{miss}}$ momentum vectors, is required to be less than 300 GeV.

In the 1-lepton channel, a significant contribution of multijet events arises mainly from non-prompt leptons from hadron decays and from jets misidentified as electrons. This background is significantly reduced by applying tighter selection requirements on the lepton isolation and identification, as well as on $E_{\mathrm{T}}^{\mathrm{miss}}$. Muons must satisfy the "Medium" identification and electrons must satisfy the "Tight" identification requirements. Stringent lepton isolation requirements are applied: the scalar sum of the p_{T} of tracks within a variable-size cone around the lepton (excluding its own track) must be less than 6% of the lepton p_{T}. In addition, in the case of electrons the sum of the transverse energy of the calorimeter energy clusters in a cone of $\Delta R = 0.2$ around the electron must be less than 6% of the electron p_{T} [90, 92]. Finally, the $E_{\mathrm{T}}^{\mathrm{miss}}$ value is required to be greater than 100 GeV for the merged category and greater than 80 (40) GeV for the resolved category in the electron (muon) channel.

In the 2-lepton channel, same-flavour leptons (ee or $\mu\mu$) are used. For both the resolved and merged categories, three kinematic selections are optimised as a function of the resonance mass to reduce the $t\bar{t}$ and Z+jets backgrounds. Selections on the mass of the dilepton system, $\max[40\ \mathrm{GeV},\ 87\ \mathrm{GeV} - 0.030 \cdot m_{Vh}] < m_{\ell\ell} < 97\ \mathrm{GeV} + 0.013 \cdot m_{Vh}$, and on $E_{\mathrm{T}}^{\mathrm{miss}} / \sqrt{(1\ \mathrm{GeV}) \cdot H_{\mathrm{T}}} < 1.15 + 8 \times 10^{-3} \cdot m_{Vh}\ /\ (1\ \mathrm{GeV})$ are relaxed

Table 2: Topological and kinematic selections for each channel and category as described in the text. $^{(*)}$ Applies in the case of only two central jets. $^{(**)}$ Tau veto only applied for the Z'/A search. $^{(\dagger)}$ Tighter threshold (80 GeV) is used for the single-electron channel. $^{(\dagger\dagger)}$ Applied only for $m_{Zh} > 320$ GeV. $^{(\ddagger)}$ Not applied in the resolved 2 and 3+ b-tag categories.

Variable	Resolved	Merged
Common selection		
Number of jets	≥2 small-R jets (0, 2-lep.) 2 or 3 small-R jets (1-lep.)	≥1 large-R jet
Leading jet p_{T} [GeV]	> 45	> 250
m_{jj}, m_{J} [GeV]	110–140 (0,1-lep.), 100–145 (2-lep.)	75–145
0-lepton selection		
$E_{\mathrm{T}}^{\mathrm{miss}}$ [GeV]	> 150	> 200
$\sum p_{\mathrm{T}}^{\mathrm{jet}_i}$ [GeV]	> 150 (120^{*})	–
$\Delta\phi$(j, j)	$< 7\pi/9$	–
$p_{\mathrm{T}}^{\mathrm{miss}}$ [GeV]	$> 30^{\ddagger}$	
$\Delta\phi(\vec{E}_{\mathrm{T}}^{\mathrm{miss}}, \vec{p}_{\mathrm{T}}^{\mathrm{miss}})$	$< \pi/2$	
$\Delta\phi(\vec{E}_{\mathrm{T}}^{\mathrm{miss}}, h)$	$> 2\pi/3$	
min[$\Delta\phi(\vec{E}_{\mathrm{T}}^{\mathrm{miss}}$, small-$R$ jet)]	$> \pi/9$ (2 or 3 jets), $> \pi/6$ (≥ 4 jets)	
$N_{\tau_{\mathrm{had}}}$	0^{**}	
1-lepton selection		
Leading lepton p_{T} [GeV]	> 27	> 27
$E_{\mathrm{T}}^{\mathrm{miss}}$ [GeV]	> 40 ($80^{\dagger}$)	> 100
$p_{\mathrm{T},W}$ [GeV]	$> \max[150,\ 710 - (3.3 \times 10^5\ \mathrm{GeV})/m_{Vh}]$	$> \max[150,\ 394 \cdot \ln(m_{Vh}/(1\ \mathrm{GeV})) - 2350]$
$m_{\mathrm{T},W}$ [GeV]	< 300	
2-lepton selection		
Leading lepton p_{T} [GeV]	> 27	> 27
Sub-leading lepton p_{T} [GeV]	> 7	> 25
$E_{\mathrm{T}}^{\mathrm{miss}}/\sqrt{H_{\mathrm{T}}}$ [$\sqrt{\mathrm{GeV}}$]	$< 1.15 + 8 \times 10^{-3} \cdot m_{Vh}/(1\ \mathrm{GeV})$	
$p_{\mathrm{T},\ell\ell}$ [GeV]	$> 20 + 9 \cdot \sqrt{m_{Vh}/(1\ \mathrm{GeV}) - 320}^{\dagger\dagger}$	
$m_{\ell\ell}$ [GeV]	$[\max[40\ \mathrm{GeV},\ 87 - 0.030 \cdot m_{Vh}/(1\ \mathrm{GeV})], 97 + 0.013 \cdot m_{Vh}/(1\ \mathrm{GeV})]$	

for higher-mass resonances to account for resolution effects and smaller backgrounds. The variable H_{T} is calculated as the scalar sum of the p_{T} of the leptons and small-R jets in the event. The momentum of the dilepton system ($p_{\mathrm{T},\ell\ell}$) is required to be greater than 20 GeV + 9 GeV $\cdot$ $\sqrt{m_{Vh}/(1\ \mathrm{GeV}) - 320}$ for m_{Vh} greater than 320 GeV. In the resolved dimuon category, an opposite-charge requirement is applied since the probability to mis-reconstruct the charge of individual muons is extremely low. Additionally, in this category the leading muon is required to have $|\eta|$ less than 2.5. Finally, for the merged category, the sub-leading lepton is required to have $p_{\mathrm{T}} > 25$ GeV and for muons $|\eta|$ is restricted to be less than 2.5.

6 Background estimation

The background contamination in the signal regions is different for each of the three channels studied. In the 0-lepton channel, the dominant background sources are Z+jets and $t\bar{t}$ events with a significant

contribution from W+jets. In the 1-lepton channel, the largest backgrounds are $t\bar{t}$, single-top-quark and W+jets production. In the 2-lepton channel, Z+jets production is the predominant background followed by the $t\bar{t}$ background. The contribution from diboson, SM Vh, $t\bar{t}h$, and $t\bar{t}V$ production is small in all three channels. The multijet background, due to semileptonic hadron decays or misidentified jets, is found to be negligible in the 0- and 2-lepton channels after applying the event selections described in Section 5. In the 1-lepton channel, the multijet background remains significant only in the resolved 1 b-tag category. All background distribution shapes except those for multijet are estimated from the samples of simulated events with normalisations of the main backgrounds estimated from the data; the multijet shape and normalisation is determined using data.

The W/Z+jets simulated event samples are split into different components. In the resolved category, the samples are split according to the true flavour of the two small-R jets forming the Higgs boson candidate. In the merged category, they are split according to the true flavour of the one or two leading track-jets associated with the large-R jet. The true jet flavour is determined by counting true heavy-flavour hadrons with $p_{\mathrm{T}} > 5$ GeV within the cone of the reconstructed jet. If a true b-hadron is found, the jet is labelled as a b-jet, otherwise if a true c-hadron is found the jet is labelled as a c-jet. If neither a true b-hadron nor a true c-hadron is associated with the reconstructed jet, it is labelled as a light jet. For large-R jets with only one track-jet, the true hadrons are counted within this track-jet. Based on this association scheme, the W/Z+jets simulated event samples are split into six components: W/Z+bb, W/Z+bc, W/Z+bl, W/Z+cc, W/Z+cl and W/Z+ll; in this notation l refers to a light jet. In the statistical analysis described in Section 8, the components W/Z+bb, W/Z+bc, and W/Z+cc are treated as a single component denoted by W/Z+(bb, bc, cc). The combination of W/Z+bl and W/Z+cl is denoted by W/Z+(bl, cl). For the HVT, Z', and A boson interpretations, the normalisations of the largest components Z+(bb, bc, cc) and Z+(bl, cl) are determined from data. In the A boson interpretation, the Z+(bb, bc, cc) background normalisation in the 3+ b-tag region is determined from this region independently. The normalisations of W+(bb, bc, cc) and W+(bl, cl) are determined from data for the W' and HVT interpretations.

The normalisation of the $t\bar{t}$ background is determined from the fits to data separately for the 0-, 1-, and 2-lepton channels. In the 0-lepton channel, only the signal regions are used in the fit. In the 1- and 2-lepton channels, dedicated control regions enhanced in $t\bar{t}$ events are used in addition to the signal regions. In the 1-lepton channel, resolved events in the sidebands of the m_{jj} distribution between 50 GeV and 200 GeV (excluding the signal region with $110 < m_{\mathrm{jj}} < 140$ GeV) are primarily composed of $t\bar{t}$ and W+jets events. These control regions are included in the fit for the 1 and 2 b-tag categories. In the 2-lepton channel, a $t\bar{t}$ control region is defined using resolved events with different-flavour ($e\mu$), oppositely charged leptons, and without the $E_{\mathrm{T}}^{\mathrm{miss}}/\sqrt{H_{\mathrm{T}}}$ requirement. The $t\bar{t}$ purity of this selection is greater than 90%. This region combining the 1 and 2 b-tag events is used in the A, Z', and HVT interpretations; for the A interpretation, a control region with $e\mu$ events and 3+ b-tags is also included in the fit to provide an independent constraint on $t\bar{t}$ production with associated heavy-flavour jets.

The shape of the multijet background in the 1-lepton channel is estimated from a sample of data events orthogonal to the signal regions, the anti-isolated lepton region. In the muon channel, this region is defined by events where the sum of the transverse momentum of tracks in a cone of $\Delta R = 0.2$ around the muon is between 6% and 15% of the muon p_{T}. In the electron channel, this region is defined by events where the sum of the calorimeter energy deposits in a cone of $\Delta R = 0.2$ around the electron is larger than 6% of the electron p_{T}; this region is defined after applying the track isolation requirement described in Section 4. A template shape for the multijet background is extracted from the anti-isolated lepton region after removing the contribution from the simulated electroweak and top-quark backgrounds. In this subtraction, the normalisation of the simulated electroweak and top-quark backgrounds is estimated

Table 3: Relative systematic uncertainties in the normalisation, cross-region extrapolation, and shape of the signal and background processes included in the fits described in the text. An "S" indicates a shape variation is included for the sources listed, "/" indicates a ratio of two regions, and "norm." is the sum of cross-section and acceptance variations. A range of values means the value depends on the lepton channel. Parentheses indicate when the uncertainty applies only to a given fit or a given region.

Process	Quantity/source	Value
Signal	acceptance	3–7%
SM Vh, $t\bar{t}V$, $t\bar{t}h$	norm.	50%
Diboson	norm.	11%
Multijet (1-lep.)	norm.	50%
	template method	S
Single top quark	norm.	19%
	resolved / merged	24%
	m_{jj} SR / m_{jj} CR (1-lep.)	7%
$t\bar{t}$	resolved / merged	15–46%
	m_{jj} SR / m_{jj} CR (1-lep.)	7%
	SR / $e\mu$ CR (2-lep.)	2%
	PS, ISR/FSR, ME	S
	p_{T} reweight	S
Z+(bb, bc, cc)	resolved / merged	19%
	0-lep. / 2-lep.	15%
	generator, PDF, scale	S
Z+(bl, cl)	resolved / merged	28%
	0-lep. / 2-lep.	12%
	generator, PDF, scale	S

Process	Quantity/source	Value
Z+l	norm.	19%
	resolved / merged	23%
	0-lep. / 2-lep.	8%
	generator, PDF, scale	S
W+(bb, bc, cc)	norm. (A,Z')	26%
	resolved / merged	18–43%
	m_{jj} SR / m_{jj} CR (1-lep.)	6%
	0-lep. / 1-lep.	26%
	generator, PDF, scale	S
W+(bl, cl)	norm. (A,Z')	23%
	resolved / merged	15–35%
	m_{jj} SR / m_{jj} CR (1-lep.)	5%
	0-lep. / 1-lep.	22%
	generator, PDF, scale	S
W+l	norm.	20–30%
	resolved / merged	16–20%
	m_{jj} SR / m_{jj} CR (1-lep.)	2%
	0-lep. / 1-lep.	19%
	generator, PDF, scale	S

by fitting them to data in the region $E_{\mathrm{T}}^{\mathrm{miss}} > 200$ GeV where the contribution from multijet events is negligible. In the signal and control regions used in the statistical analysis, the multijet normalisation is determined by fitting the $E_{\mathrm{T}}^{\mathrm{miss}}$ multijet template and the $E_{\mathrm{T}}^{\mathrm{miss}}$ combined template of the electroweak and top-quark backgrounds to data in the 1 and 2 b-tag categories separately. Using this method, the multijet contribution is estimated to be less than 6% in all signal and control regions and is included in the statistical analysis.

7 Systematic uncertainties

Two types of systematic uncertainties, experimental and modelling, affect the reconstruction of the m_{Vh} and $m_{\mathrm{T},Vh}$ observables. Experimental uncertainties arise due to the trigger selection, the reconstruction, identification, energy/momentum, mass, and resolution for the leptons, jets and missing transverse momentum. Modelling uncertainties result in shape and normalisation uncertainties of the different MC samples used to model the signal and backgrounds. These stem from uncertainties in the matrix element calculation, the choice of parton shower and hadronisation models and their free parameters, the PDF set and the choice of renormalisation and factorisation scales.

The largest experimental systematic uncertainties are associated with the calibration and resolution of the small-R and large-R jet energy, the calibration and resolution of the large-R jet mass, and the determination

of the jet b-tagging efficiency and misidentification rate. The uncertainties in the small-R jet energy scale have contributions from *in situ* calibration studies, from the dependency on the pile-up activity and on the flavour composition of jets [103, 112]. The small-R jet uncertainties are propagated to the $E_{\mathrm{T}}^{\mathrm{miss}}$ measurement. The uncertainty in the scale and resolution of large-R jet energy and mass is estimated by comparing the ratio of calorimeter-based to track-based measurements in dijet data and simulation [100, 101]. The flavour tagging efficiency and its uncertainty for b-jets and c-jets is estimated in $t\bar{t}$ and $W + c$-jet events, respectively, while the light-jet misidentification rate and uncertainty is determined using dijet events [106, 107, 113, 114]. Other experimental systematic uncertainties with a smaller impact are those in the lepton energy and momentum scales, in lepton reconstruction and identification efficiency, and in the efficiency of the triggers. Finally, a global normalisation uncertainty of 3.2% is assigned due to the luminosity measurement from a preliminary calibration of the luminosity scale using x–y beam-separation scans performed in August 2015 and May 2016, following a methodology similar to that detailed in Ref. [115]. Experimental uncertainties have an impact on the shape of the mass distributions and account for possible migration of events across the different regions.

Modelling uncertainties are assigned to each signal and background process and lead to variations in the normalisation and in the case of main backgrounds also in the shape of the templates in the different regions. In addition, for all MC samples, the statistical uncertainty arising from the number of simulated events is considered by introducing shape variations determined from the uncertainty in each bin of the m_{Vh} or $m_{\mathrm{T},Vh}$ distributions. The modelling uncertainties considered are shown in Table 3 and described below.

For the signal processes, the uncertainties in the acceptance were derived by considering the following variations: the renormalisation and factorisation scales were varied by a factor of two, the nominal PDF set was replaced by the MSTW2008 LO PDF set and the tuned parameters were varied according to the variations derived from the eigentune method [46]. For both the A and V' signals, the total variations are less than 3% at resonance masses above 500 GeV. The variations increase to 7% for the A boson masses below 500 GeV.

The modelling uncertainties affecting $t\bar{t}$ and single-top-quark processes are derived as follows [116]. A variation of the parton shower, hadronisation, and the underlying-event model is obtained by replacing Pythia 6.428 by Herwig++ (version 2.7.1) [117] with the UE-EE-5 tune and the CTEQ6L1 PDF set [70]. To assess potential differences in the matrix element calculation, a comparison is made to a sample where Powheg is replaced by MG5_aMC [43]. A comparison is also made to samples with smaller and larger amount of initial- and final-state radiation (ISR/FSR) by changing the renormalisation and factorisation scales by a factor of two and switching to the corresponding low- and high-radiation Perugia 2012 tunes. Finally, the difference between the nominal and corrected distributions due to the top-quark and $t\bar{t}$ p_{T} reweighting described in Section 3 is included as a symmetrised shape uncertainty.

Similarly, for W/Z+jets backgrounds, the following comparisons have been performed. The PDF set in the nominal samples was replaced by the alternative PDF sets: the hundred NNPDF 3.0 NNLO replicas, including the sets resulting from variations of α_{S} [60], the MMHT2014 NNLO set, and the CT14 NNLO PDF set [118]. The scale uncertainties are estimated by comparing samples where the renormalisation and factorisation scales were modified by a factor of two. Finally, a comparison was made to a sample generated using MG5_aMC v2.2.2 interfaced to Pythia 8.186 and using the A14 tune together with the NNPDF 2.3 LO PDF set [49, 119, 120].

For the $t\bar{t}$, single-top-quark, and W/Z+jets backgrounds, the acceptance differences that affect the relative normalisation across regions with a common background normalisation are estimated by summing in

Table 4: A list of the signal and control regions (separated by commas below) included in the statistical analysis of the A and HVT model hypotheses. The notation 1+2 b-tag indicates the 1 and 2 b-tag regions are combined, and add. b-tag indicates the regions with additional b-tags not associated with the large-R jet.

Fit		Channel	Resolved signal regions	Merged signal regions	Resolved control regions
A		0-lepton	1, 2, 3+ b-tag	1, 2 b-tag, and 1, 2 b-tag add. b-tag	–
		2-lepton	1, 2, 3+ b-tag	1, 2 b-tag, and 1+2 b-tag add. b-tag	1+2 b-tag , 3+ b-tag $e\mu$
HVT	Z', W'	0-lepton	1, 2 b-tag	1, 2 b-tag	–
	W'	1-lepton	1, 2 b-tag	1, 2 b-tag	1, 2 b-tag m_{jj} sideband
	Z'	2-lepton	1, 2 b-tag	1, 2 b-tag	1+2 b-tag $e\mu$

quadrature the relative yield variations between the different regions. These uncertainties are assigned to all regions used in the fit as shown in Table 4 and across the different lepton channels as shown in Table 3.

For the multijet background included in the 1-lepton channel, a 50% uncertainty in the normalisation is estimated from the fit to the $E_{\mathrm{T}}^{\mathrm{miss}}$ distribution described in Section 6. Also, a shape variation is included to account for uncertainties in the determination of the template in the anti-isolated lepton region, arising from differences in the trigger scheme between isolated and anti-isolated regions and uncertainties in the normalisation of the top-quark and electroweak backgrounds in this region.

Finally, for the remaining small backgrounds only a normalisation uncertainty is assigned. For the diboson backgrounds a normalisation uncertainty of 11% is applied [121]. For the SM Vh, ttV, and tth production, a 50% uncertainty is assigned which covers the uncertainty in the cross-sections.

8 Results

In order to test for the presence of a massive resonance, the $m_{\mathrm{T},Vh}$ and m_{Vh} templates obtained from the signal and background simulated event samples are fit to data using a binned maximum-likelihood approach based on the RooStats framework [122–124]. A total of five different fits are performed according to the signal interpretation: Z', W', HVT, A in gluon–gluon fusion, and A in b-quark associated production. The list of channels and regions used for the different fits is shown in Table 4.

The fits are performed on the $m_{\mathrm{T},Vh}$ distribution in the 0-lepton channel and the m_{Vh} distribution in the 1- and 2-lepton channels using a binning of the distributions chosen to optimise the search sensitivity while minimising statistical fluctuations. As described in Section 6, the normalisations of the $t\bar{t}$, Z+(bb, bc, cc), and Z+(bl, cl) backgrounds are free parameters in all fits, as are the normalisations of W+(bb, bc, cc) and W+(bl, cl) in the W' and HVT fits. The systematic uncertainties described in Section 7 are incorporated in the fit as nuisance parameters with correlations across regions and processes taken into account. The signal normalisation is a free parameter in the fit. In order to account for migrations of signal events across different channels due to lepton reconstruction and selection inefficiencies, the $Zh \to \ell^+\ell^- b\bar{b}$ ($Wh \to \ell^{\pm}\nu b\bar{b}$) signal samples are included in the 1(0)-lepton categories.

The total uncertainty in the signal yield is dominated by different sources of systematic uncertainty depending on the mass of the resonance used in the fit. The uncertainties in the W/Z+(bb, bc, cc) shape and normalisation, $t\bar{t}$ normalisation, and in the flavour tagging efficiencies constitute the dominant sources of systematic uncertainty for low-mass resonances. For all interpretations, the statistical uncertainty dominates for resonances above 1 TeV. The uncertainties in the large-R jet mass resolution and in the track-jet b-tagging efficiency constitute the dominant systematic uncertainties at high masses.

The expected and observed event yields after the HVT fit are shown in Table 5. The $m_{\mathrm{T},Vh}$ and m_{Vh} distributions after the HVT fit are shown in Figures 2 and 3. Similar distributions are obtained from the W', Z' and A fits with background yields consistent within the uncertainties. The mass distributions for the resolved 3+ b-tag category and the merged categories with additional b-tagged jets, used in the A boson fits, are shown in Figure 4.

As no significant excess over the background prediction is observed, upper limits at the 95% CL are set on the production cross-section times the branching fraction for each model. The limits are evaluated using a modified frequentist method known as $\mathrm{CL_s}$ [125] and the profile-likelihood-ratio test statistic [126] using the asymptotic approximation.

The 95% CL upper limits on the production cross-section multiplied by the branching fraction for $W' \to Wh$ and $Z' \to Zh$ and the sum of branching fractions $B(h \to b\bar{b}) + B(h \to c\bar{c})$, which is fixed to 60.6% [47], are shown in Figure 5(a) and Figure 5(b) as a function of the resonance mass. The existence of W' and Z' bosons with masses $m_{W'} < 2.67$ TeV and $m_{Z'} < 2.65$ TeV, respectively, are excluded for the HVT benchmark *Model A* with coupling constant $g_{\mathrm{V}} = 1$ [25]. For *Model B* with coupling constant $g_{\mathrm{V}} = 3$ [25], the corresponding excluded masses are $m_{W'} < 2.82$ TeV and $m_{Z'} < 2.83$ TeV.

To study the scenario in which the masses of charged and neutral resonances are degenerate, a likelihood fit over all the signal regions and control regions is performed. The 95% CL upper limit on the combined signal strength for the processes $W' \to Wh$ and $Z' \to Zh$, assuming $m_{W'} = m_{Z'}$, relative to the HVT model predictions, is shown in Figure 5(c). For *Model A* (*Model B*), $m_{V'} < 2.80$ TeV (2.93 TeV) is excluded.

The exclusion contours in the HVT parameter space $\{g_{\mathrm{V}} c_{\mathrm{H}}, (g^2/g_{\mathrm{V}}) c_{\mathrm{F}}\}$ for resonances of mass 1.2 TeV, 2.0 TeV and 3.0 TeV are shown in Figure 5(d) where all three lepton channels are combined, taking into account the branching fractions to Wh and Zh from the HVT model prediction. Here, the parameter c_{F} is assumed to be the same for quarks and leptons, including third-generation fermions, and other parameters involving more than one heavy vector boson, $g_{\mathrm{V}} c_{\mathrm{VVV}}$, $g_{\mathrm{V}}^2 c_{\mathrm{VVhh}}$ and c_{VVW}, are assumed to have negligible contributions to the overall cross-sections for the processes of interest.

Figures 6(a) and 6(b) show the 95% CL upper limits on the production cross-section of the A boson times its branching fraction to Zh and the branching fraction of $h \to b\bar{b}$ as a function of the resonance mass. Upper limits are placed separately for a signal arising from pure gluon–gluon fusion production (Figure 6(a)) and from pure b-quark associated production (Figure 6(b)). In the search for the A boson with b-quark associated production, a mild excess of events is observed around 440 GeV, mainly driven by the dimuon channel in the resolved category with 3+ b-tags. The local significance of this excess with respect to the background-only hypothesis is estimated to be 3.6 σ, and the global significance, accounting for the look-elsewhere effect [127] is estimated to be 2.4 σ.

The data are also interpreted in terms of limits at 95% CL on the 2HDM parameters $\tan(\beta)$ and $\cos(\beta - \alpha)$. The admixture of gluon–gluon fusion and b-quark associated production, and the variation of the A and h boson widths and branching fractions are taken into account according to the predictions of the different models. In this interpretation, the $m_{\mathrm{T},Vh}$ and m_{Vh} distributions of the simulated signal events are

smeared according to a Breit–Wigner function with a width predicted by the parameters of the model. This procedure has been verified to produce the same line-shape as the one including non-resonant and interference effects for widths $\Gamma_A/m_A < 10\%$.

Figure 7 shows the excluded parameter space for a resonance mass of $m_A = 300$ GeV in four 2HDM types: I, II, Lepton-Specific, and Flipped. Greater sensitivity is observed at high $\tan(\beta)$ for the Type-II and Flipped models, due to an increased cross-section for b-quark associated production. The narrow regions with no exclusion power in Type-I and Type-II at low $\tan(\beta)$ that are far from $\cos(\beta - \alpha)$=0 are caused by the vanishing branching fraction of $h \to b\bar{b}$.

Figure 8 shows the parameter exclusion for the four models in the $\tan(\beta)$–m_A plane for $\cos(\beta - \alpha) = 0.1$. For the interpretation in Type-II and Flipped 2HDMs, the b-quark associated production is included in addition to the gluon–gluon fusion production. The shape of the expected exclusions is determined by the interplay of the expected cross-section limit, which decreases as a function of m_A, and the signal production cross-section times the $A \to Zh$ branching fraction at a given m_A and $\tan(\beta)$. This branching fraction decreases significantly at $m_A = 350$ GeV due to the opening of the $A \to t\bar{t}$ channel, but increases again at higher m_A, maintaining similar sensitivity into this m_A region. The variable $\tan(\beta)$ controls the admixture of the gluon–gluon fusion and b-quark associated production thereby affecting the rate at which the signal cross-section falls as a function of m_A, which leads to a varying sensitivity as a function of $\tan(\beta)$. The excesses or deficits in the data visible in Figure 6 are also reflected in Figure 8.

Table 5: The predicted and observed event yields in the signal regions defined in the text. The yields in the 1 and 2 b-tag regions correspond to the HVT fit for a signal of mass 1.5 TeV. In the 3+ b-tag and 1 and 2 b-tag with additional b-tags regions, the yields are from the fit using the A boson produced in association with b-quarks as signal with a mass of 1.5 TeV. The quoted uncertainties are the statistical and systematic uncertainties combined in quadrature after the fit. The uncertainties in the individual background predictions are larger than the total background uncertainty due to correlations in the normalisation parameters in the fit.

0-lepton	Resolved			Merged			
	1 b-tag	2 b-tag	3+ b-tag	1 b-tag	2 b-tag	1 b-tag add. b-tag	2 b-tag add. b-tag
$t\bar{t}$	22900 ± 890	6640 ± 180	1000 ± 34	1650 ± 160	68 ± 12	2110 ± 70	105 ± 11
Single top quark	2440 ± 330	552 ± 76	25.8 ± 5.6	217 ± 52	15.4 ± 4.1	136 ± 50	5.6 ± 2.4
Diboson	317 ± 41	41.2 ± 5.8	4.5 ± 1.1	188 ± 30	34.8 ± 4.8	12.9 ± 2.3	1.6 ± 0.4
Z+l	580 ± 210	1.3 ± 1.3	–	310 ± 130	0.38 ± 0.29	11.8 ± 8.2	0.1 ± 0.1
Z+(bl, cl)	8240 ± 840	50 ± 17	5.4 ± 1.8	910 ± 160	10.1 ± 3.7	118 ± 27	0.6 ± 0.4
Z+(bb, bc, cc)	1280 ± 170	1270 ± 150	41 ± 8	238 ± 45	101 ± 16	16.8 ± 4.2	8.6 ± 2.3
W+l	960 ± 300	3 ± 2	–	227 ± 95	1.0 ± 0.6	5.4 ± 3.9	0.02 ± 0.02
W+(bl, cl)	5960 ± 1100	56 ± 17	3.7 ± 2.3	770 ± 230	6.6 ± 3.2	65 ± 21	0.1 ± 0.1
W+(bb, bc, cc)	530 ± 150	470 ± 130	16.5 ± 4.7	112 ± 44	40 ± 16	10.2 ± 5.1	3 ± 2
SM Vh	55 ± 21	102 ± 39	1.04 ± 0.57	7.4 ± 2.9	4.7 ± 1.8	0.4 ± 0.2	0.06 ± 0.04
$t\bar{t}h$	10.4 ± 5.3	7.8 ± 3.9	6 ± 3	1.4 ± 0.7	0.2 ± 0.1	4 ± 2	0.6 ± 0.3
$t\bar{t}V$	102 ± 54	41 ± 22	8.7 ± 4.5	17.7 ± 9.5	1.4 ± 0.8	24 ± 12	1.8 ± 1.0
Total	43400 ± 200	9240 ± 95	1110 ± 30	4650 ± 79	282 ± 14	2510 ± 50	127 ± 11
Data	43387	9236	1125	4657	283	2516	127

1-lepton	1 b-tag	2 b-tag	1 b-tag	2 b-tag
$t\bar{t}$	16300 ± 600	3900 ± 120	8100 ± 300	400 ± 50
Single top quark	4100 ± 600	860 ± 130	1100 ± 300	120 ± 30
Diboson	110 ± 20	12 ± 2	220 ± 30	34 ± 5
Z+l	40 ± 10	0.09 ± 0.05	14 ± 6	0.2 ± 0.1
Z+(bl, cl)	170 ± 10	0.7 ± 0.5	38 ± 6	0.4 ± 0.2
Z+(bb, bc, cc)	27 ± 4	17 ± 2	11 ± 2	4.5 ± 0.6
W+l	550 ± 180	3 ± 3	590 ± 230	0.2 ± 0.2
W+(bl, cl)	5700 ± 440	24 ± 8	1800 ± 300	30 ± 10
W+(bb, bc, cc)	820 ± 140	420 ± 70	350 ± 80	180 ± 40
SM Vh	60 ± 20	90 ± 30	14 ± 6	11 ± 4
Multijet	200 ± 100	1.7 ± 0.9	–	–
Total	28100 ± 170	5320 ± 70	12200 ± 120	780 ± 30
Data	28073	5348	12224	775

2-lepton	1 b-tag	2 b-tag	3+ b-tag	1 b-tag	2 b-tag	1+2 b-tag add. b-tag
$t\bar{t}$	2570 ± 80	1940 ± 110	58 ± 9	5.3 ± 2.6	0.4 ± 0.2	11 ± 5
Single top quark	185 ± 25	58 ± 9	1.5 ± 0.4	0.7 ± 0.1	0.2 ± 0.2	0.5 ± 0.3
Diboson	570 ± 80	159 ± 24	5.2 ± 1.3	35 ± 5	8.5 ± 1.3	4.6 ± 0.8
Z+l	2210 ± 950	2 ± 3	–	85 ± 34	1.0 ± 0.5	6 ± 4
Z+(bl, cl)	37200 ± 1100	130 ± 50	12 ± 5	240 ± 40	2.3 ± 0.8	55 ± 11
Z+(bb, bc, cc)	7840 ± 690	6320 ± 170	150 ± 20	74 ± 12	34 ± 5	12 ± 3
W+l	1.9 ± 0.7	–	–	0.03 ± 0.01	–	0.01 ± 0.01
W+(bl, cl)	37 ± 9	0.9 ± 0.7	–	0.4 ± 0.1	–	0.01 ± 0.01
W+(bb, bc, cc)	5.4 ± 1.4	1.9 ± 0.3	0.03 ± 0.01	0.17 ± 0.06	0.02 ± 0.01	0.06 ± 0.05
SM Vh	105 ± 40	140 ± 60	1.3 ± 0.7	1.6 ± 0.6	0.8 ± 0.3	0.2 ± 0.1
$t\bar{t}h$	0.9 ± 0.5	1.6 ± 0.8	1.1 ± 0.5	0.05 ± 0.02	0.01 ± 0.01	0.15 ± 0.07
$t\bar{t}V$	140 ± 80	60 ± 30	6 ± 3	10 ± 5	0.6 ± 0.3	12 ± 6
Total	50900 ± 230	8810 ± 90	240 ± 20	450 ± 20	47 ± 5	101 ± 9
Data	50876	8798	235	439	50	101

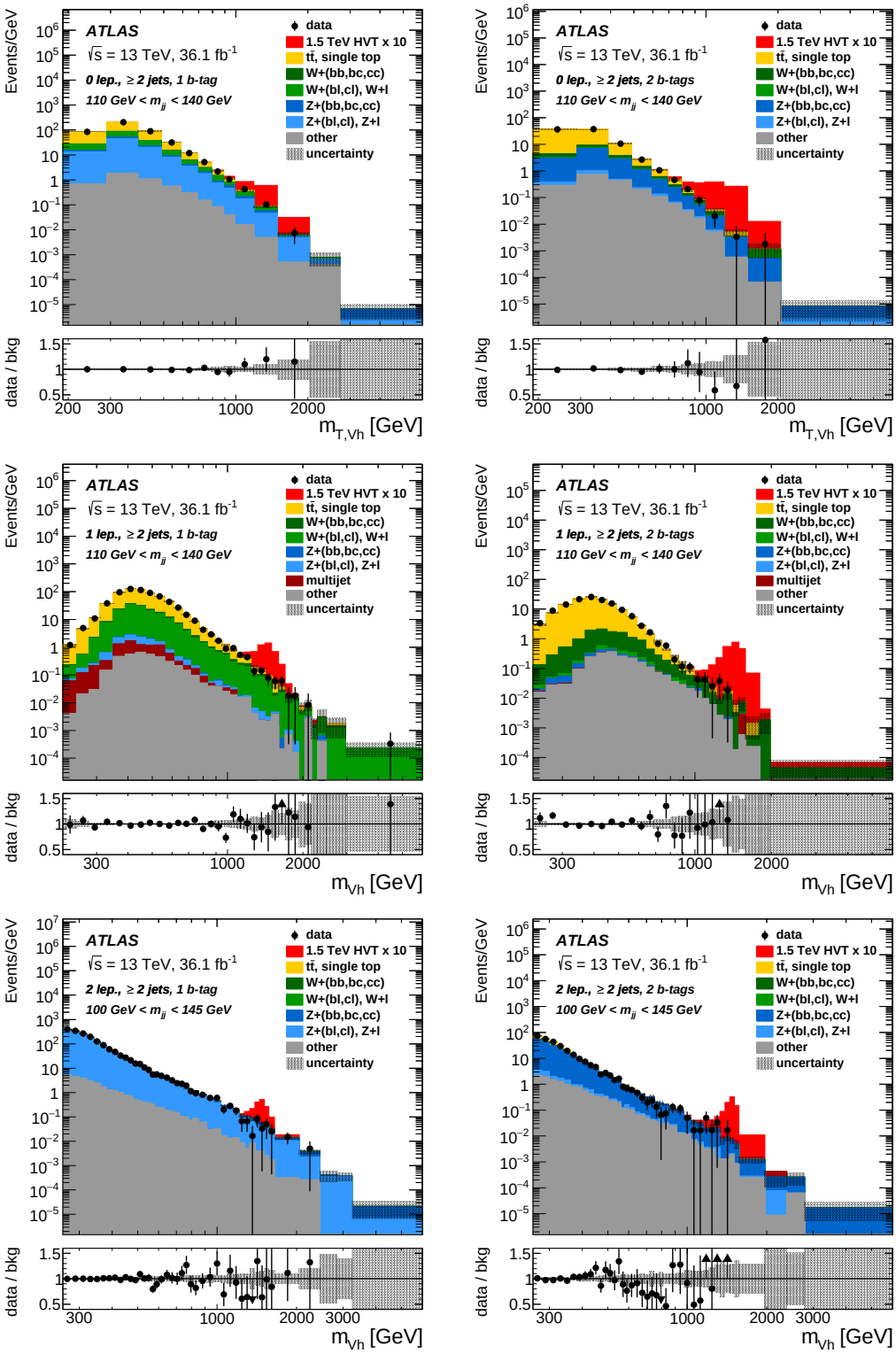

Figure 2: Event distributions of $m_{\mathrm{T},Vh}$ for the 0-lepton channel, and m_{Vh} for the 1-lepton and 2-lepton channels in the resolved categories. The quantity on the vertical axis is the number of data events divided by the bin width in GeV. The background prediction is shown after a background-only maximum-likelihood fit to the data. The signal for the benchmark HVT *Model A* with $m_{V'} = 1.5$ TeV is normalised to 10 times the theoretical cross-section. The background uncertainty band shown includes both the statistical and systematic uncertainties after the fit added in quadrature. The lower panels show the ratio of the observed data to the estimated SM background.

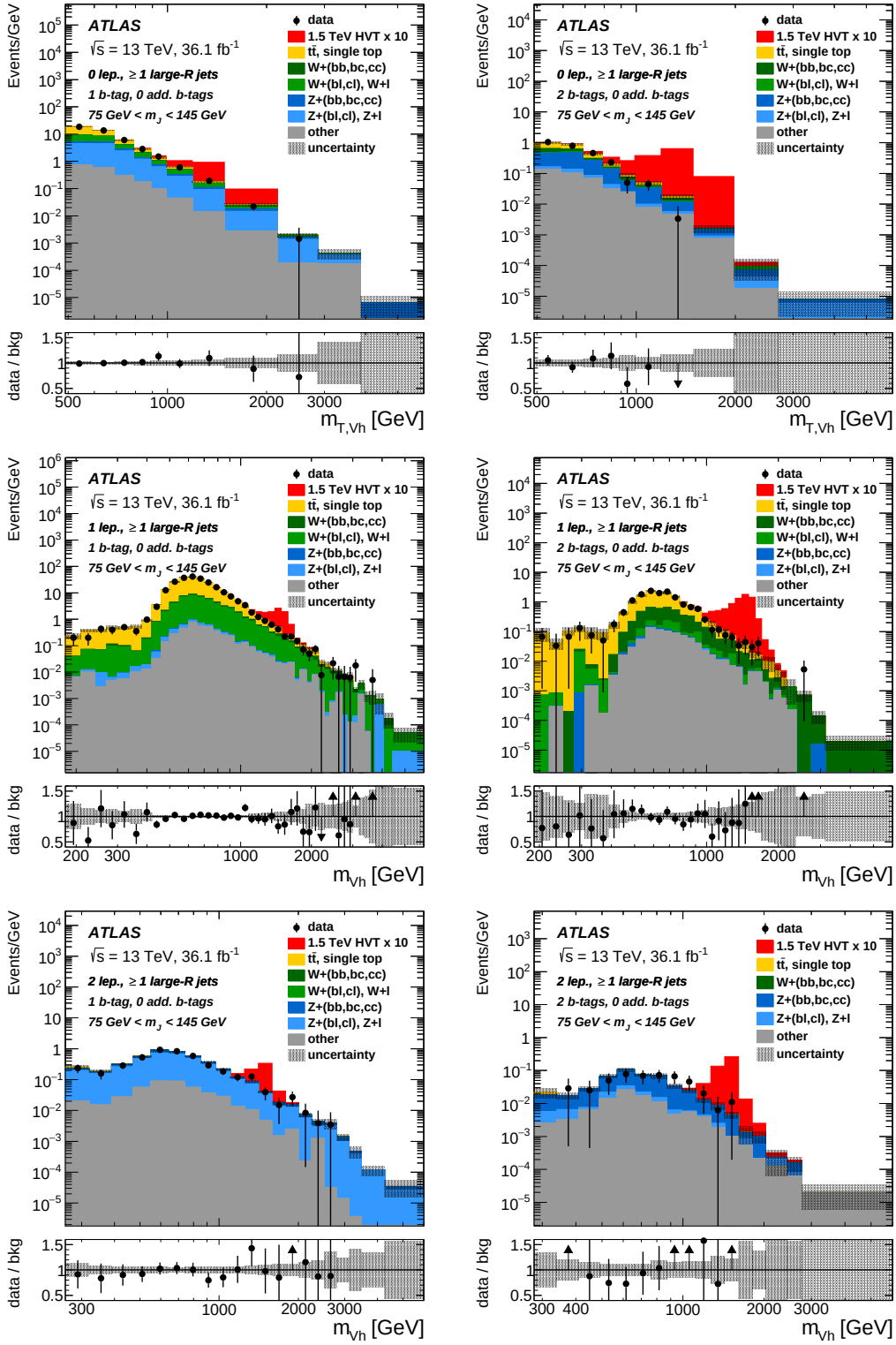

Figure 3: Event distributions of $m_{\mathrm{T},Vh}$ for the 0-lepton channel, and m_{Vh} for the 1-lepton and 2-lepton channels in the merged categories. The quantity on the vertical axis is the number of data events divided by the bin width in GeV. The background prediction is shown after a background-only maximum-likelihood fit to the data. The signal for the benchmark HVT *Model A* with $m_{V'} = 1.5$ TeV is normalised to 10 times the theoretical cross-section. The background uncertainty band shown includes both the statistical and systematic uncertainties after the fit added in quadrature. The lower panels show the ratio of the observed data to the estimated SM background.

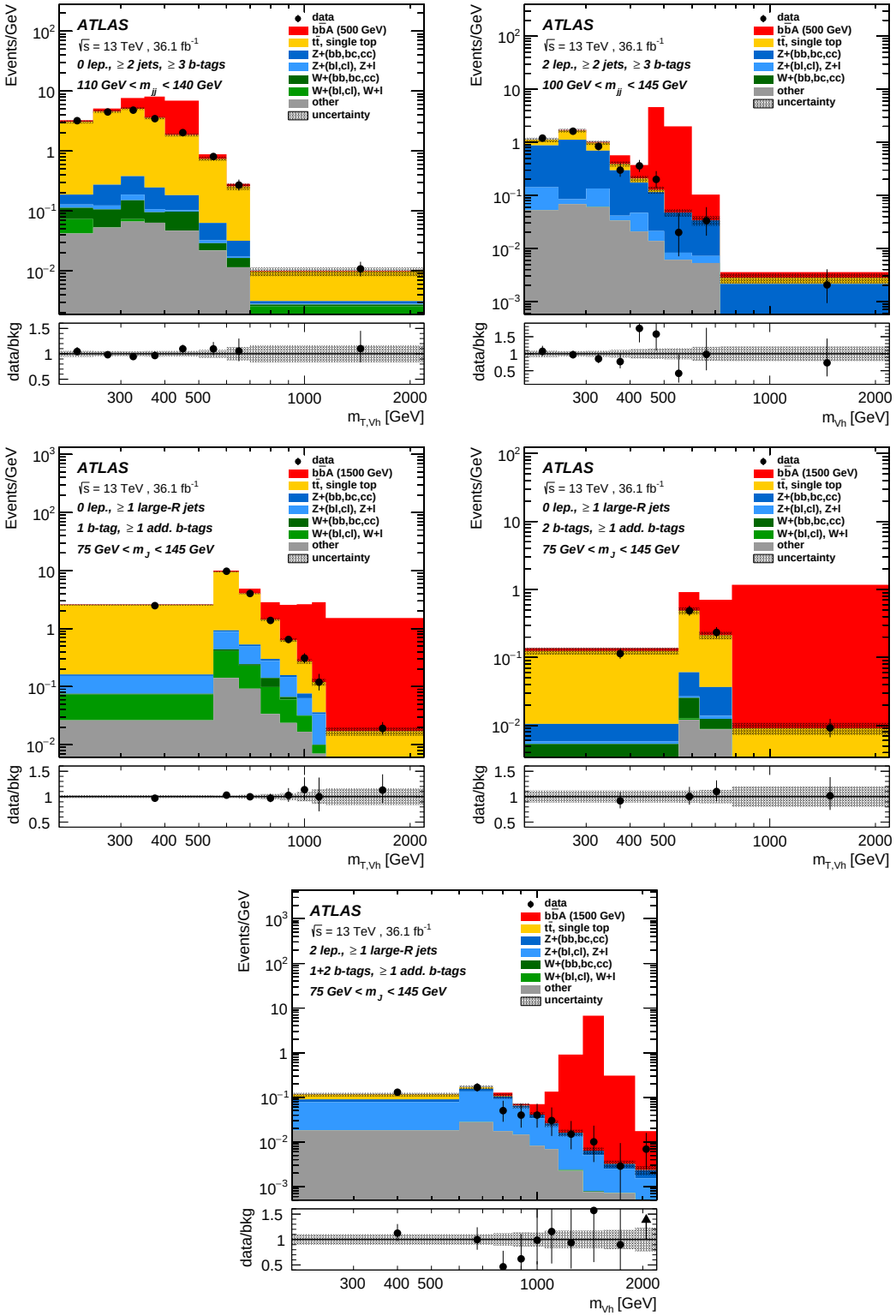

Figure 4: Event distributions of $m_{\mathrm{T},Vh}$ for the 0-lepton channel and m_{Vh} for the 2-lepton channel after a background-only fit to the categories used in the search for the A boson produced in association with b-quarks. The quantity on the vertical axis is the number of data events divided by the bin width in GeV. The distribution for an A boson with mass of 500 GeV (1.5 TeV) is shown for illustration in the resolved (merged) regions normalised using a cross-section of 5 pb. The background uncertainty band shown includes both the statistical and systematic uncertainties after the fit added in quadrature. The lower panels show the ratio of the observed data to the estimated SM background.

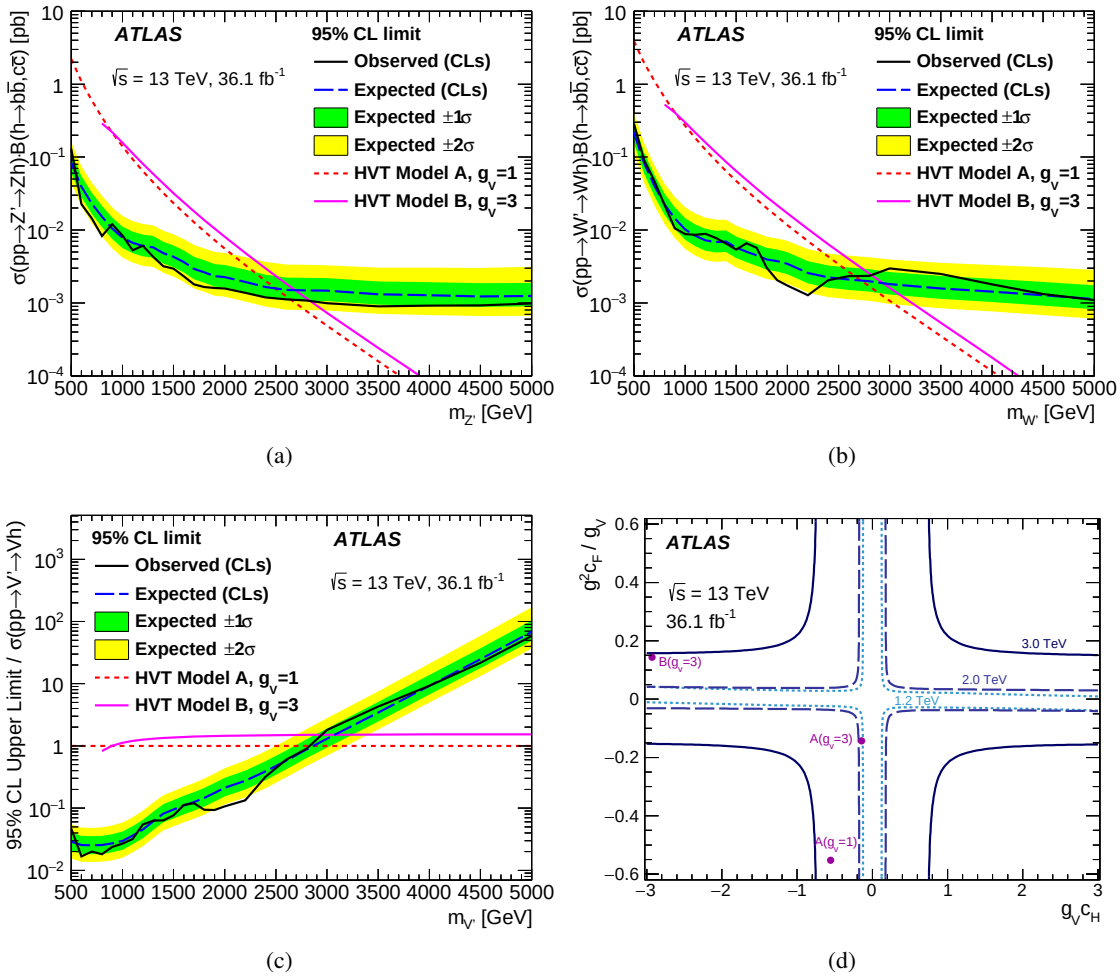

Figure 5: Upper limits as a function of the resonance mass at the 95% CL for (a) the production cross-section of Z' times its branching fraction to Zh and the branching fraction $B(h \to b\bar{b}, c\bar{c})$ and (b) the production cross-section of W' times its branching fraction to Wh and the branching fraction $B(h \to b\bar{b}, c\bar{c})$. (c) Upper limits at the 95% CL for the scaling factor of the production cross-section for V' times its branching fraction to Wh/Zh in *Model A*. The production cross-sections predicted by *Model A* and *Model B* are shown for comparison in (a)–(c). (d) Observed 95% CL exclusion contours in the HVT parameter space $\{g_V c_H, (g^2/g_V)c_F\}$ for resonances of mass 1.2 TeV, 2.0 TeV and 3.0 TeV. The areas outside the curves are excluded. Also shown are the benchmark model parameters A($g_V = 1$), A($g_V = 3$) and B($g_V = 3$).

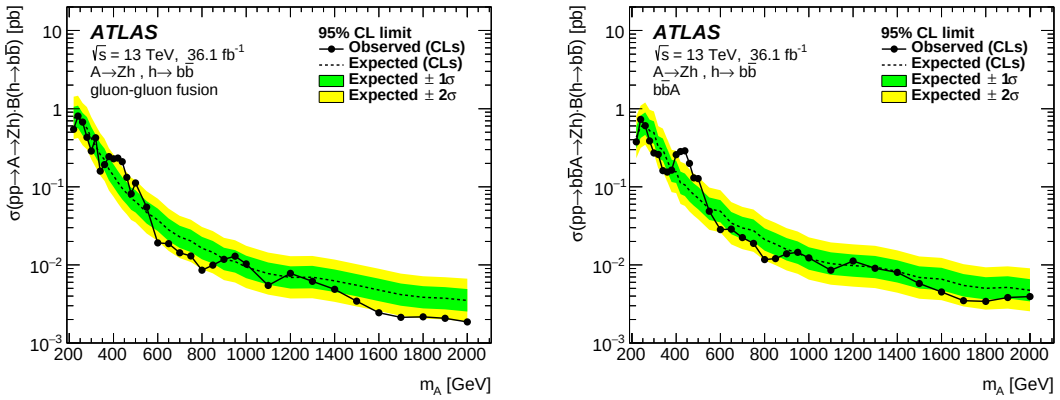

(a) Pure gluon–gluon fusion production

(b) Pure b-quark associated production

Figure 6: Upper limits at the 95% CL on the product of the production cross-section for $pp \to A$ and the branching fractions for $A \to Zh$ and $h \to b\bar{b}$ evaluated by combining the 0-lepton and 2-lepton channels. The possible signal components of the data are interpreted assuming (a) pure gluon–gluon fusion production, and (b) pure b-quark associated production.

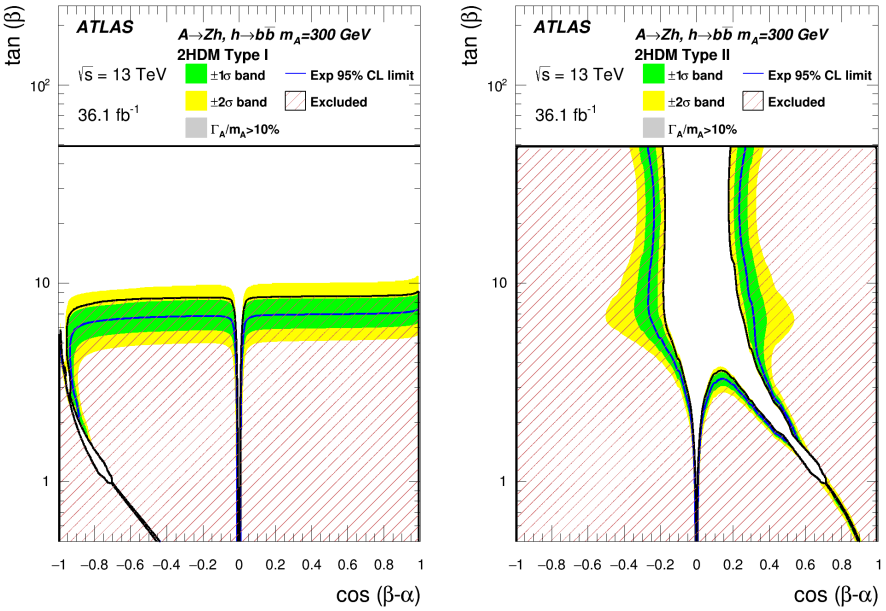

(a) 2HDM Type-I

(b) 2HDM Type-II

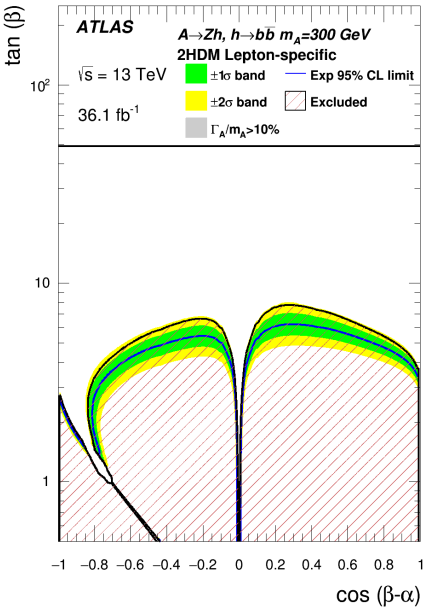

(c) 2HDM Lepton-specific

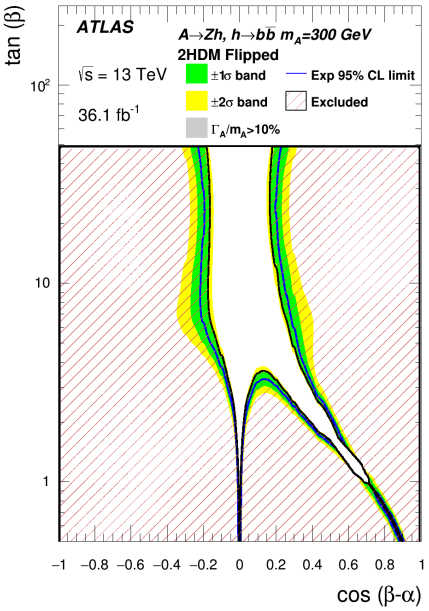

(d) 2HDM Flipped

Figure 7: The interpretation of the cross-section limits in the context of the various 2HDM types as a function of the parameters tan(β) and cos($\beta - \alpha$) for m_A = 300 GeV: (a) Type-I , (b) Type-II, (c) Lepton-specific, and (d) Flipped. Variations of the natural width up to Γ_A/m_A=10% have been taken into account. For the interpretation in Type-II and Flipped 2HDM, the b-quark associated production is included in addition to the gluon–gluon fusion production.

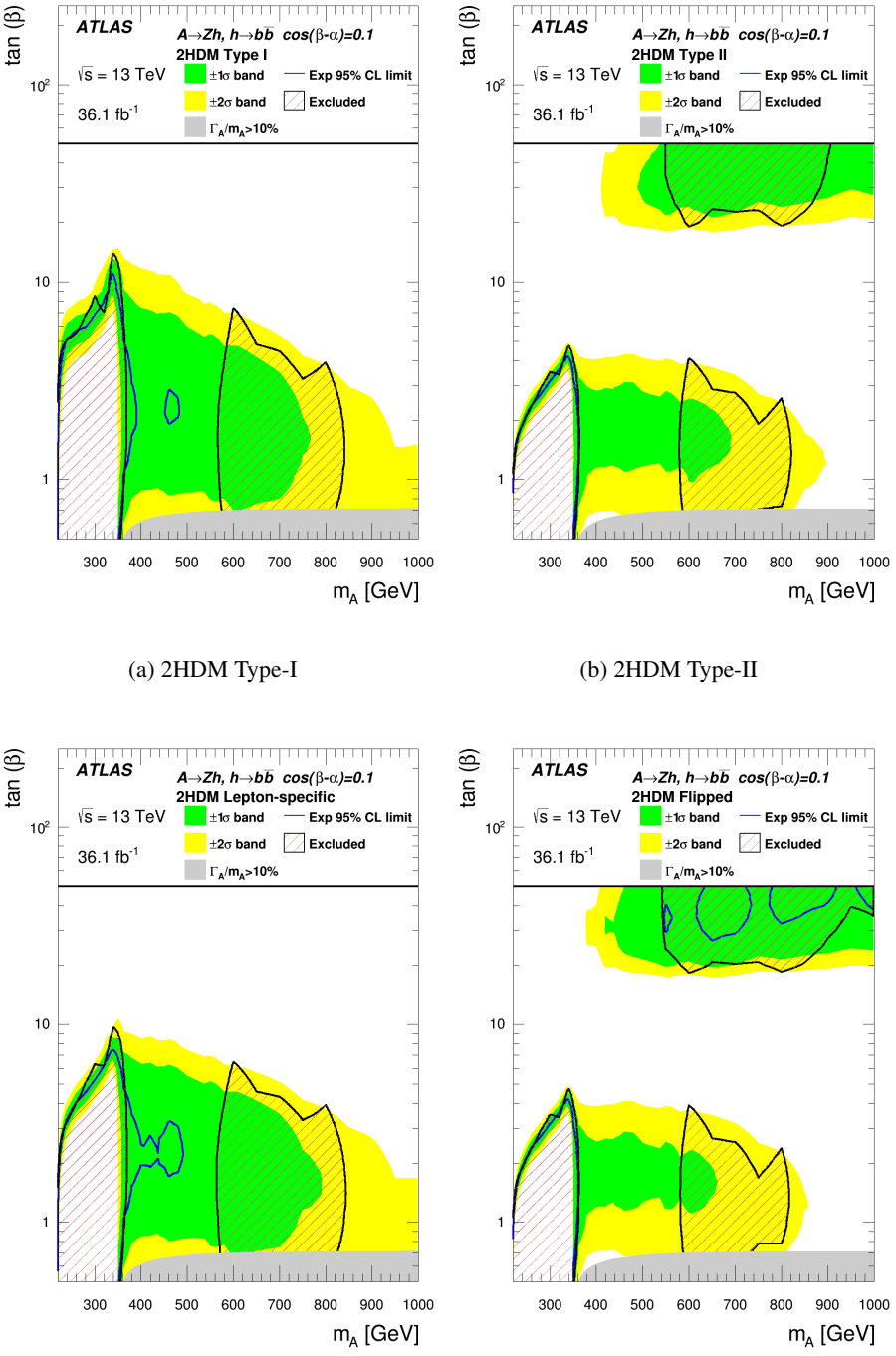

(a) 2HDM Type-I

(b) 2HDM Type-II

(c) 2HDM Lepton-specific

(d) 2HDM Flipped

Figure 8: The interpretation of the cross-section limits in the context of 2HDMs of Type (a) I , (b) II, (c) Lepton-specific, and (d) Flipped, as a function of the parameters tan(β) and m_A for cos($\beta-\alpha$)= 0.1. Variations of the natural width up to Γ_A/m_A=10% have been taken into account.

9 Conclusion

A search for W' and Z' bosons and for a CP-odd Higgs boson A in the $\nu\bar{\nu}b\bar{b}$, $\ell^{\pm}\nu b\bar{b}$ and $\ell^{+}\ell^{-}b\bar{b}$ final states is performed using 36.1 fb^{-1} of 13 TeV pp collision data collected with the ATLAS detector at the LHC. No significant excess of events is observed above the SM predictions in all three channels.

Upper limits are placed at the 95% CL on the cross-section times branching fraction, $\sigma(pp \to V' \to Vh) \times B(h \to b\bar{b}, c\bar{c})$, ranging between 1.1×10^{-3} and 2.8×10^{-1} pb for the W' boson and between 9.0×10^{-4} and 1.3×10^{-1} pb for the Z' boson in the mass range of 500 GeV to 5 TeV. The W' and Z' bosons with masses $m_{W'} < 2.67$ TeV (2.82 TeV) and $m_{Z'} < 2.65$ TeV (2.83 TeV) are excluded for the benchmark HVT *Model A (Model B)*, while for the combined HVT search masses up to 2.80 TeV (2.93 TeV) are excluded.

For an A boson, upper limits are placed on $\sigma(pp \to A \to Zh) \times B(h \to b\bar{b})$ between 5.5×10^{-3} and 2.4×10^{-1} pb for gluon–gluon fusion production and between 3.4×10^{-3} and 7.3×10^{-1} pb for production with associated b-quarks in the mass range 220 GeV to 2 TeV.

Acknowledgements

We thank CERN for the very successful operation of the LHC, as well as the support staff from our institutions without whom ATLAS could not be operated efficiently.

We acknowledge the support of ANPCyT, Argentina; YerPhI, Armenia; ARC, Australia; BMWFW and FWF, Austria; ANAS, Azerbaijan; SSTC, Belarus; CNPq and FAPESP, Brazil; NSERC, NRC and CFI, Canada; CERN; CONICYT, Chile; CAS, MOST and NSFC, China; COLCIENCIAS, Colombia; MSMT CR, MPO CR and VSC CR, Czech Republic; DNRF and DNSRC, Denmark; IN2P3-CNRS, CEA-DRF/IRFU, France; SRNSFG, Georgia; BMBF, HGF, and MPG, Germany; GSRT, Greece; RGC, Hong Kong SAR, China; ISF, I-CORE and Benoziyo Center, Israel; INFN, Italy; MEXT and JSPS, Japan; CNRST, Morocco; NWO, Netherlands; RCN, Norway; MNiSW and NCN, Poland; FCT, Portugal; MNE/IFA, Romania; MES of Russia and NRC KI, Russian Federation; JINR; MESTD, Serbia; MSSR, Slovakia; ARRS and MIZŠ, Slovenia; DST/NRF, South Africa; MINECO, Spain; SRC and Wallenberg Foundation, Sweden; SERI, SNSF and Cantons of Bern and Geneva, Switzerland; MOST, Taiwan; TAEK, Turkey; STFC, United Kingdom; DOE and NSF, United States of America. In addition, individual groups and members have received support from BCKDF, the Canada Council, CANARIE, CRC, Compute Canada, FQRNT, and the Ontario Innovation Trust, Canada; EPLANET, ERC, ERDF, FP7, Horizon 2020 and Marie Skłodowska-Curie Actions, European Union; Investissements d'Avenir Labex and Idex, ANR, Région Auvergne and Fondation Partager le Savoir, France; DFG and AvH Foundation, Germany; Herakleitos, Thales and Aristeia programmes co-financed by EU-ESF and the Greek NSRF; BSF, GIF and Minerva, Israel; BRF, Norway; CERCA Programme Generalitat de Catalunya, Generalitat Valenciana, Spain; the Royal Society and Leverhulme Trust, United Kingdom.

The crucial computing support from all WLCG partners is acknowledged gratefully, in particular from CERN, the ATLAS Tier-1 facilities at TRIUMF (Canada), NDGF (Denmark, Norway, Sweden), CC-IN2P3 (France), KIT/GridKA (Germany), INFN-CNAF (Italy), NL-T1 (Netherlands), PIC (Spain), ASGC (Taiwan), RAL (UK) and BNL (USA), the Tier-2 facilities worldwide and large non-WLCG resource providers. Major contributors of computing resources are listed in Ref. [128].

References

[1] ATLAS Collaboration, *Observation of a new particle in the search for the Standard Model Higgs boson with the ATLAS detector at the LHC*, Phys. Lett. B **716** (2012) 1, arXiv: 1207.7214 [hep-ex].

[2] CMS Collaboration, *Observation of a new boson at a mass of 125 GeV with the CMS experiment at the LHC*, Phys. Lett. B **716** (2012) 30, arXiv: 1207.7235 [hep-ex].

[3] ATLAS Collaboration, *Study of the spin and parity of the Higgs boson in diboson decays with the ATLAS detector*, Eur. Phys. J. C **75** (2015) 476, arXiv: 1506.05669 [hep-ex], Erratum: Eur. Phys. J. C **76** (2016) 152.

[4] CMS Collaboration, *Constraints on the spin-parity and anomalous HVV couplings of the Higgs boson in proton collisions at* 7 *and* 8 *TeV*, Phys. Rev. D **92** (2015) 012004, arXiv: 1411.3441 [hep-ex].

[5] ATLAS and CMS Collaborations, *Combined measurement of the Higgs boson mass in pp collisions at* $\sqrt{s} = 7$ *and* 8 *TeV with the ATLAS and CMS experiments*, Phys. Rev. Lett. **114** (2015) 191803, arXiv: 1503.07589 [hep-ex].

[6] S. Weinberg, *Gauge hierarchies*, Phys. Lett. B **82** (1979) 387.

[7] M. J. G. Veltman, *The infrared - ultraviolet connection*, Acta Phys. Polon. B **12** (1981) 437.

[8] C. H. Llewellyn Smith and G. G. Ross, *The real gauge hierarchy problem*, Phys. Lett. B **105** (1981) 38.

[9] LHC Higgs Cross Section Working Group, *Handbook of LHC Higgs cross sections: 4. Deciphering the nature of the Higgs sector*, (2016), arXiv: 1610.07922 [hep-ph].

[10] F. Sannino and K. Tuominen, *Orientifold theory dynamics and symmetry breaking*, Phys. Rev. D **71** (2005) 051901, arXiv: 0405209 [hep-ph].

[11] R. Foadi, M. T. Frandsen, T. A. Ryttov and F. Sannino, *Minimal walking technicolor: set up for collider physics*, Phys. Rev. D **76** (2007) 055005, arXiv: 0706.1696 [hep-ph].

[12] A. Belyaev, R. Foadi, M. T. Frandsen, M. Jarvinen, F. Sannino et al., *Technicolor walks at the LHC*, Phys. Rev. D **79** (2009) 035006, arXiv: 0809.0793 [hep-ph].

[13] M. Schmaltz and D. Tucker-Smith, *Little Higgs review*, Ann. Rev. Nucl. Part. Sci. **55** (2005) 229, arXiv: 0502182 [hep-ph].

[14] M. J. Dugan, H. Georgi and D. B. Kaplan, *Anatomy of a composite Higgs model*, Nucl. Phys. B **254** (1985) 299.

[15] K. Agashe, R. Contino and A. Pomarol, *The minimal composite Higgs model*, Nucl. Phys. B **719** (2005) 165, arXiv: 0412089 [hep-ph].

[16] G. C. Branco et al., *Theory and phenomenology of two-Higgs-doublet models*, Phys. Rept. **516** (2012) 1, arXiv: 1106.0034 [hep-ph].

[17] P. Fayet, *Supersymmetry and weak, electromagnetic and strong interactions*, Phys. Lett. B **64** (1976) 159.

[18] P. Fayet,
Spontaneously broken supersymmetric theories of weak, electromagnetic and strong interactions,
Phys. Lett. B **69** (1977) 489.

[19] G. R. Farrar and P. Fayet, *Phenomenology of the production, decay, and detection of new hadronic states associated with supersymmetry*, Phys. Lett. B **76** (1978) 575.

[20] P. Fayet, *Relations between the masses of the superpartners of leptons and quarks, the goldstino couplings and the neutral currents*, Phys. Lett. B **84** (1979) 416.

[21] S. Dimopoulos and H. Georgi, *Softly broken supersymmetry and SU(5)*,
Nucl. Phys. B **193** (1981) 150.

[22] J. E. Kim, *Light pseudoscalars, particle physics and cosmology*, Phys. Rept. **150** (1987) 1.

[23] M. Joyce, T. Prokopec and N. Turok,
Nonlocal electroweak baryogenesis. Part 2: The classical regime, Phys. Rev. D **53** (1996) 2958,
arXiv: hep-ph/9410282.

[24] D. Alves et al., *Simplified models for LHC new physics searches*, J. Phys. G **39** (2012) 105005,
arXiv: 1105.2838 [hep-ph].

[25] D. Pappadopulo, A. Thamm, R. Torre and A. Wulzer,
Heavy vector triplets: bridging theory and data, JHEP **09** (2014) 060,
arXiv: 1402.4431 [hep-ph].

[26] J. de Blas, J. M. Lizana and M. Perez-Victoria, *Combining searches of Z' and W' bosons*,
JHEP **01** (2013) 166, arXiv: 1211.2229 [hep-ph].

[27] V. D. Barger, W.-Y. Keung and E. Ma, *A gauge model with light W and Z bosons*,
Phys. Rev. D **22** (1980) 727.

[28] R. Contino, D. Marzocca, D. Pappadopulo and R. Rattazzi,
On the effect of resonances in composite Higgs phenomenology, JHEP **10** (2011) 081,
arXiv: 1109.1570 [hep-ph].

[29] ATLAS Collaboration, *Search for a new resonance decaying to a W or Z boson and a Higgs boson in the $\ell\ell/\ell\nu/\nu\nu + b\bar{b}$ final states with the ATLAS detector*, Eur. Phys. J. C **75** (2015) 263,
arXiv: 1503.08089 [hep-ex].

[30] ATLAS Collaboration,
Search for new resonances decaying to a W or Z boson and a Higgs boson in the $\ell^+\ell^- b\bar{b}$, $\ell\nu b\bar{b}$, and $\nu\bar{\nu}b\bar{b}$ channels with pp collisions at $\sqrt{s} = 13$ TeV with the ATLAS detector,
Phys. Lett. B **765** (2017) 32, arXiv: 1607.05621 [hep-ex].

[31] CMS Collaboration, *Search for heavy resonances decaying into a vector boson and a Higgs boson in final states with charged leptons, neutrinos, and b quarks*,
Phys. Lett. B **768** (2017) 137, arXiv: 1610.08066 [hep-ex].

[32] CMS Collaboration, *Search for a massive resonance decaying into a Higgs boson and a W or Z boson in hadronic final states in proton–proton collisions at $\sqrt{s} = 8$ TeV*, JHEP **02** (2016) 145,
arXiv: 1506.01443 [hep-ex].

[33] CMS Collaboration, *Search for heavy resonances that decay into a vector boson and a Higgs boson in hadronic final states at $\sqrt{s} = 13$ TeV*, Eur. Phys. J. C **77** (2017) 636,
arXiv: 1707.01303 [hep-ex].

[34] ATLAS Collaboration, *Search for heavy resonances decaying to a W or Z boson and a Higgs boson in the $q\bar{q}^{(\prime)}b\bar{b}$ final state in pp collisions at $\sqrt{s} = 13$ TeV with the ATLAS detector*, (2017), arXiv: 1707.06958 [hep-ex].

[35] ALEPH, DELPHI, L3, OPAL Collaborations, *Search for neutral MSSM Higgs bosons at LEP*, Eur. Phys. J. C **47** (2006) 547, arXiv: hep-ex/0602042.

[36] ATLAS Collaboration, *Search for neutral Higgs bosons of the minimal supersymmetric standard model in pp collisions at $\sqrt{s} = 8$ TeV with the ATLAS detector*, JHEP **11** (2014) 056, arXiv: 1409.6064 [hep-ex].

[37] CMS Collaboration, *Search for neutral MSSM Higgs bosons decaying to a pair of tau leptons in pp collisions*, JHEP **10** (2014) 160, arXiv: 1408.3316 [hep-ex].

[38] ATLAS Collaboration, *Search for a CP-odd Higgs boson decaying to Zh in pp collisions at $\sqrt{s} = 8$ TeV with the ATLAS detector*, Phys. Lett. B **744** (2015) 163, arXiv: 1502.04478 [hep-ex].

[39] CMS Collaboration, *Search for a pseudoscalar boson decaying into a Z boson and the 125 GeV Higgs boson in $\ell^+\ell^- b\bar{b}$ final states*, Phys. Lett. B **748** (2015) 221, arXiv: 1504.04710 [hep-ex].

[40] ATLAS Collaboration, *The ATLAS experiment at the CERN Large Hadron Collider*, JINST **3** (2008) S08003.

[41] ATLAS Collaboration, *ATLAS insertable B-layer technical design report*, ATLAS-TDR-19, 2010, URL: https://cds.cern.ch/record/1291633, *ATLAS insertable B-layer technical design report addendum*, ATLAS-TDR-19-ADD-1, 2012, URL: https://cds.cern.ch/record/1451888.

[42] ATLAS Collaboration, *Performance of the ATLAS trigger system in 2015*, Eur. Phys. J. C **77** (2017) 317, arXiv: 1611.09661 [hep-ex].

[43] J. Alwall et al., *The automated computation of tree-level and next-to-leading order differential cross sections, and their matching to parton shower simulations*, JHEP **07** (2014) 079, arXiv: 1405.0301 [hep-ph].

[44] R. D. Ball et al., *Impact of heavy quark masses on parton distributions and LHC phenomenology*, Nucl. Phys. B **849** (2011) 296, arXiv: 1101.1300 [hep-ph].

[45] T. Sjöstrand, S. Mrenna and P. Z. Skands, *A brief introduction to PYTHIA 8.1*, Comput. Phys. Commun. **178** (2008) 852, arXiv: 0710.3820 [hep-ph].

[46] ATLAS Collaboration, *ATLAS Pythia 8 tunes to 7 TeV data*, ATL-PHYS-PUB-2014-021, 2014, URL: https://cds.cern.ch/record/1966419.

[47] LHC Higgs Cross Section Working Group, *Handbook of LHC Higgs cross sections: 3. Higgs properties*, (2013), arXiv: 1307.1347 [hep-ph].

[48] H.-L. Lai, M. Guzzi, J. Huston, Z. Li, P. M. Nadolsky et al., *New parton distributions for collider physics*, Phys. Rev. D **82** (2010) 074024, arXiv: 1007.2241 [hep-ph].

[49] T. Sjöstrand et al., *An introduction to PYTHIA 8.2*, Comput. Phys. Commun. **191** (2015) 159, arXiv: 1410.3012 [hep-ph].

[50] R. Harlander, S. Liebler and H. Mantler, *SusHi: A program for the calculation of Higgs production in gluon fusion and bottom-quark annihilation in the Standard Model and the MSSM*, Comput. Phys. Commun. **184** (2013) 1605, arXiv: 1212.3249 [hep-ph].

[51] R. Harlander and P. Kant, *Higgs production and decay: analytic results at next-to-leading order QCD*, JHEP **12** (2005) 015, arXiv: hep-ph/0509189.

[52] R. Harlander and W. B. Kilgore, *Higgs boson production in bottom quark fusion at next-to-next-to leading order*, Phys. Rev. D **68** (2003) 013001, arXiv: hep-ph/0304035.

[53] R. Harlander and W. B. Kilgore, *Next-to-next-to-leading order Higgs production at hadron colliders*, Phys. Rev. Lett. **88** (2002) 201801, arXiv: hep-ph/0201206.

[54] S. Dawson, C. B. Jackson, L. Reina and D. Wackeroth, *Exclusive Higgs boson production with bottom quarks at hadron colliders*, Phys. Rev. D **69** (2004) hep, arXiv: hep-ph/0311067.

[55] S. Dittmaier, M. Kramer and M. Spira, *Higgs radiation off bottom quarks at the Tevatron and the CERN LHC*, Phys. Rev. D **70** (2004) hep, arXiv: hep-ph/0309204.

[56] R. Harlander, M. Kramer and M. Schumacher, *Bottom-quark associated Higgs-boson production: reconciling the four- and five-flavour scheme approach*, (2011), arXiv: 1112.3478 [hep-ph].

[57] D. Eriksson, J. Rathsman and O. Stal, *2HDMC: two-Higgs-doublet model calculator physics and manual*, Comput. Phys. Commun. **181** (2010) 189, arXiv: 0902.0851 [hep-ph].

[58] H. E. Haber and O. Stal, *New LHC benchmarks for the $\mathcal{CP}$ -conserving two-Higgs-doublet model*, Eur. Phys. J. C **75** (2015) 491, Erratum: Eur. Phys. J. C 76 (2016) 312, arXiv: 1507.04281 [hep-ph].

[59] T. Gleisberg, S. Höche, F. Krauss, M. Schönherr, S. Schumann et al., *Event generation with SHERPA 1.1*, JHEP **02** (2009) 007, arXiv: 0811.4622 [hep-ph].

[60] NNPDF Collaboration: R. D. Ball et al., *Parton distributions for the LHC run 2*, JHEP **04** (2015) 040, arXiv: 1410.8849 [hep-ph].

[61] T. Gleisberg and S. Höche, *Comix, a new matrix element generator*, JHEP **12** (2008) 039, arXiv: 0808.3674 [hep-ph].

[62] F. Cascioli, P. Maierhofer and S. Pozzorini, *Scattering amplitudes with Open Loops*, Phys. Rev. Lett. **108** (2012) 111601, arXiv: 1111.5206 [hep-ph].

[63] S. Höche, F. Krauss, M. Schönherr and F. Siegert, *QCD matrix elements + parton showers: the NLO case*, JHEP **04** (2013) 027, arXiv: 1207.5030 [hep-ph].

[64] K. Melnikov and F. Petriello,
Electroweak gauge boson production at hadron colliders through $O(\alpha_s^2)$,
Phys. Rev. D **74** (2006) 114017, arXiv: 0609070 [hep-ph].

[65] P. Nason, *A new method for combining NLO QCD with shower Monte Carlo algorithms*,
JHEP **11** (2004) 040, arXiv: 0409146 [hep-ph].

[66] S. Frixione, P. Nason and C. Oleari,
Matching NLO QCD computations with parton shower simulations: the POWHEG method,
JHEP **11** (2007) 070, arXiv: 0709.2092 [hep-ph].

[67] S. Alioli, P. Nason, C. Oleari and E. Re, *A general framework for implementing NLO calculations in shower Monte Carlo programs: the POWHEG BOX*, JHEP **06** (2010) 043,
arXiv: 1002.2581 [hep-ph].

[68] T. Sjöstrand, S. Mrenna and P. Z. Skands, *PYTHIA 6.4 physics and manual*,
JHEP **05** (2006) 026, arXiv: hep-ph/0603175.

[69] P. Z. Skands, *Tuning Monte Carlo generators: the Perugia tunes*,
Phys. Rev. D **82** (2010) 074018, arXiv: 1005.3457 [hep-ph].

[70] J. Pumplin et al.,
New generation of parton distributions with uncertainties from global QCD analysis,
JHEP **07** (2002) 012, arXiv: hep-ph/0201195.

[71] M. Beneke, P. Falgari, S. Klein and C. Schwinn,
Hadronic top-quark pair production with NNLL threshold resummation,
Nucl. Phys. B **855** (2012) 695, arXiv: 1109.1536 [hep-ph].

[72] M. Cacciari, M. Czakon, M. Mangano, A. Mitov and P. Nason, *Top-pair production at hadron colliders with next-to-next-to-leading logarithmic soft-gluon resummation*,
Phys. Lett. B **710** (2012) 612, arXiv: 1111.5869 [hep-ph].

[73] P. Bärnreuther, M. Czakon and A. Mitov, *Percent level precision physics at the Tevatron: First genuine NNLO QCD corrections to $q\bar{q} \to t\bar{t} + X$*, Phys. Rev. Lett. **109** (2012) 132001,
arXiv: 1204.5201 [hep-ph].

[74] M. Czakon and A. Mitov, *NNLO corrections to top-pair production at hadron colliders: the all-fermionic scattering channels*, JHEP **12** (2012) 054, arXiv: 1207.0236 [hep-ph].

[75] M. Czakon and A. Mitov,
NNLO corrections to top pair production at hadron colliders: the quark-gluon reaction,
JHEP **01** (2013) 080, arXiv: 1210.6832 [hep-ph].

[76] M. Czakon, P. Fiedler and A. Mitov,
Total top-quark-pair-production cross section at hadron colliders through $O(\alpha_S^4)$,
Phys. Rev. Lett. **110** (2013) 252004, arXiv: 1303.6254 [hep-ph].

[77] M. Czakon and A. Mitov,
Top++: A Program for the Calculation of the Top-Pair Cross-Section at Hadron Colliders,
Comput. Phys. Commun. **185** (2014) 2930, arXiv: 1112.5675 [hep-ph].

[78] M. Czakon, D. Heymes and A. Mitov,
Dynamical scales for multi-TeV top-pair production at the LHC, JHEP **04** (2017) 071,
arXiv: 1606.03350 [hep-ph].

[79] M. Aliev et al., *HATHOR: HAdronic Top and Heavy quarks crOss section calculatoR*, Comput. Phys. Commun. **182** (2011) 1034, arXiv: 1007.1327 [hep-ph].

[80] P. Kant et al., *HatHor for single top-quark production: Updated predictions and uncertainty estimates for single top-quark production in hadronic collisions*, Comput. Phys. Commun. **191** (2015) 74, arXiv: 1406.4403 [hep-ph].

[81] N. Kidonakis, *Two-loop soft anomalous dimensions for single top quark associated production with a W^- or H^-*, Phys. Rev. D **82** (2010) 054018, arXiv: 1005.4451 [hep-ph].

[82] ATLAS Collaboration, *Measurement of the Z/γ^* boson transverse momentum distribution in pp collisions at $\sqrt{s} = 7$ TeV with the ATLAS detector*, JHEP **09** (2014) 145, arXiv: 1406.3660 [hep-ex].

[83] ATLAS Collaboration, *Summary of ATLAS Pythia 8 tunes*, ATL-PHYS-PUB-2012-003, 2012, URL: https://cds.cern.ch/record/1474107.

[84] A. D. Martin, W. J. Stirling, R. S. Thorne and G. Watt, *Parton distributions for the LHC*, Eur. Phys. J. C **63** (2009) 189, arXiv: 0901.0002 [hep-ph].

[85] D. J. Lange, *The EvtGen particle decay simulation package*, Nucl. Instrum. Meth. A **462** (2001) 152.

[86] S. Agostinelli et al., *GEANT4 - a simulation toolkit*, Nucl. Instrum. Meth. A **506** (2003) 250.

[87] ATLAS Collaboration, *The ATLAS Simulation Infrastructure*, Eur. Phys. J. C **70** (2010) 823, arXiv: 1005.4568 [hep-ex].

[88] ATLAS Collaboration, *Electron and photon energy calibration with the ATLAS detector using LHC Run 1 data*, Eur. Phys. J. C **74** (2014) 3071, arXiv: 1407.5063 [hep-ex].

[89] ATLAS Collaboration, *Electron reconstruction and identification efficiency measurements with the ATLAS detector using the 2011 LHC proton–proton collision data*, Eur. Phys. J. C **74** (2014) 2941, arXiv: 1404.2240 [hep-ex].

[90] ATLAS Collaboration, *Muon reconstruction performance of the ATLAS detector in proton–proton collision data at $\sqrt{s} = 13$ TeV*, Eur. Phys. J. C **76** (2016) 292, arXiv: 1603.05598 [hep-ex].

[91] K. Rehermann and B. Tweedie, *Efficient identification of boosted semileptonic top quarks at the LHC*, JHEP **03** (2011) 059, arXiv: 1007.2221 [hep-ph].

[92] ATLAS Collaboration, *Electron efficiency measurements with the ATLAS detector using the 2015 LHC proton–proton collision data*, ATLAS-CONF-2016-024, 2016, URL: https://cds.cern.ch/record/2157687.

[93] W. Lampl et al., *Calorimeter Clustering Algorithms: Description and Performance*, ATL-LARG-PUB-2008-002, 2008, URL: https://cds.cern.ch/record/1099735.

[94] M. Cacciari, G. P. Salam and G. Soyez, *The anti-k_t jet clustering algorithm*, JHEP **04** (2008) 063, arXiv: 0802.1189 [hep-ph].

[95] M. Cacciari, G. P. Salam and G. Soyez, *FastJet User Manual*, Eur. Phys. J. C **72** (2012) 1896, arXiv: 1111.6097 [hep-ph].

[96] ATLAS Collaboration, *Performance of pile-up mitigation techniques for jets in pp collisions at $\sqrt{s}$ = 8 TeV using the ATLAS detector*, Eur. Phys. J. C **76** (2016) 581, arXiv: 1510.03823 [hep-ex].

[97] D. Krohn, J. Thaler and L.-T. Wang, *Jet trimming*, JHEP **02** (2010) 084, arXiv: 0912.1342 [hep-ph].

[98] S. Catani, Y. L. Dokshitzer, M. H. Seymour and B. R. Webber, *Longitudinally invariant $k_\perp$ clustering algorithms for hadron hadron collisions*, Nucl. Phys. B **406** (1993) 187.

[99] S. D. Ellis and D. E. Soper, *Successive combination jet algorithm for hadron collisions*, Phys. Rev. D **48** (1993) 3160, arXiv: hep-ph/9305266.

[100] ATLAS Collaboration, *Identification of Boosted, Hadronically-Decaying W and Z Bosons in $\sqrt{s}$ = 13 TeV Monte Carlo Simulations for ATLAS*, ATL-PHYS-PUB-2015-033, 2015, URL: https://cds.cern.ch/record/2041461.

[101] ATLAS Collaboration, *Jet mass reconstruction with the ATLAS Detector in early Run 2 data*, ATLAS-CONF-2016-035, 2016, URL: https://cds.cern.ch/record/2200211.

[102] ATLAS Collaboration, *Jet energy measurement with the ATLAS detector in proton–proton collisions at $\sqrt{s}$ = 7 TeV*, Eur. Phys. J. C **73** (2013) 2304, arXiv: 1112.6426 [hep-ex].

[103] ATLAS Collaboration, *Jet Calibration and Systematic Uncertainties for Jets Reconstructed in the ATLAS Detector at $\sqrt{s}$ = 13 TeV*, ATL-PHYS-PUB-2015-015, 2015, URL: https://cds.cern.ch/record/2037613.

[104] ATLAS Collaboration, *Boosted Higgs ($\to b\bar{b}$) boson identification with the ATLAS detector at $\sqrt{s}$ = 13 TeV*, ATLAS-CONF-2016-039, 2016, URL: https://cds.cern.ch/record/2206038.

[105] M. Cacciari, G. P. Salam and G. Soyez, *The catchment area of jets*, JHEP **04** (2008) 005, arXiv: 0802.1188 [hep-ph].

[106] ATLAS Collaboration, *Performance of b-jet identification in the ATLAS experiment*, JINST **11** (2016) P04008, arXiv: 1512.01094 [hep-ex].

[107] ATLAS Collaboration, *Optimisation of the ATLAS b-tagging performance for the 2016 LHC Run*, ATL-PHYS-PUB-2016-012, 2016, URL: https://cds.cern.ch/record/2160731.

[108] A. D. Bukin, *Fitting function for asymmetric peaks*, (2007), arXiv: 0711.4449 [physics.data-an].

[109] ATLAS Collaboration, *Identification and energy calibration of hadronically decaying tau leptons with the ATLAS experiment in pp collisions at $\sqrt{s}$ = 8 TeV*, Eur. Phys. J. C **75** (2015) 303, arXiv: 1412.7086 [hep-ex].

[110] ATLAS Collaboration, *Performance of algorithms that reconstruct missing transverse momentum in $\sqrt{s}$ = 8 TeV proton–proton collisions in the ATLAS detector*, Eur. Phys. J. C **77** (2017) 241, arXiv: 1609.09324 [hep-ex].

[111] ATLAS Collaboration, *Expected performance of missing transverse momentum reconstruction for the ATLAS detector at $\sqrt{s}$ = 13 TeV*, ATL-PHYS-PUB-2015-023, 2015, URL: https://cds.cern.ch/record/2037700.

[112] ATLAS Collaboration, *Jet global sequential corrections with the ATLAS detector in proton–proton collisions at* $\sqrt{s} = 8$ *TeV*, ATLAS-CONF-2015-002, 2015, URL: https://cds.cern.ch/record/2001682.

[113] ATLAS Collaboration, *Calibration of b-tagging using dileptonic top pair events in a combinatorial likelihood approach with the ATLAS experiment*, ATLAS-CONF-2014-004, 2014, URL: https://cds.cern.ch/record/1664335.

[114] ATLAS Collaboration, *Calibration of the performance of b-tagging for c and light-flavour jets in the 2012 ATLAS data*, ATLAS-CONF-2014-046, 2014, URL: https://cds.cern.ch/record/1741020.

[115] ATLAS Collaboration, *Luminosity determination in pp collisions at* $\sqrt{s} = 8$ *TeV using the ATLAS detector at the LHC*, Eur. Phys. J. C **76** (2016) 653, arXiv: 1608.03953 [hep-ex].

[116] ATLAS Collaboration, *Simulation of top-quark production for the ATLAS experiment at* $\sqrt{s} = 13$ *TeV*, ATL-PHYS-PUB-2016-004, 2016, URL: https://cds.cern.ch/record/2120417.

[117] M. Bahr, S. Gieseke, M. Gigg, D. Grellscheid, K. Hamilton et al., *Herwig++ physics and manual*, Eur. Phys. J. C **58** (2008) 639, arXiv: 0803.0883 [hep-ph].

[118] J. Butterworth et al., *PDF4LHC recommendations for LHC run 2*, J. Phys. G **43** (2016) 023001, arXiv: 1510.03865 [hep-ph].

[119] J. Alwall et al., *The automated computation of tree-level and next-to-leading order differential cross sections, and their matching to parton shower simulations*, JHEP **07** (2014) 158, arXiv: 1405.0301 [hep-ph].

[120] R. D. Ball, V. Bertone, S. Carrazza, C. S. Deans, L. Del Debbio et al., *Parton distributions with LHC data*, Nucl. Phys. B **867** (2013) 244, arXiv: 1207.1303 [hep-ph].

[121] J. M. Campbell and R. Ellis, *MCFM for the Tevatron and the LHC*, Nucl. Phys. Proc. Suppl. (2010) 205, arXiv: 1007.3492 [hep-ph].

[122] L. Moneta et al., *The RooStats project*, 2010, arXiv: 1009.1003 [hep-ph].

[123] W. Verkerke and D. Kirkby, *The RooFit toolkit for data modeling*, 2003, arXiv: physics/0306116 [physics.data-an].

[124] M. Baak et al., *HistFitter software framework for statistical data analysis*, Eur. Phys. J. C **75** (2015) 153, arXiv: 1410.1280 [hep-ex].

[125] A. L. Read, *Presentation of search results: The* CL_s *technique*, J. Phys. G **28** (2002) 2693.

[126] G. Cowan, K. Cranmer, E. Gross and O. Vitells, *Asymptotic formulae for likelihood-based tests of new physics*, Eur. Phys. J. C **71** (2011) 1554, arXiv: 1007.1727 [physics.data-an], Erratum: Eur. Phys. J. C **73** (2013) 2501.

[127] E. Gross and O. Vitells, *Trial factors or the look elsewhere effect in high energy physics*, Eur. Phys. J. C **70** (2010) 525, arXiv: 1005.1891 [physics.data-an].

[128] ATLAS Collaboration, *ATLAS Computing Acknowledgements 2016–2017*, ATL-GEN-PUB-2016-002, URL: https://cds.cern.ch/record/2202407.

The ATLAS Collaboration

M. Aaboud[137d], G. Aad[88], B. Abbott[115], O. Abdinov[12,*], B. Abeloos[119], S.H. Abidi[161], O.S. AbouZeid[139], N.L. Abraham[151], H. Abramowicz[155], H. Abreu[154], R. Abreu[118], Y. Abulaiti[148a,148b], B.S. Acharya[167a,167b,a], S. Adachi[157], L. Adamczyk[41a], J. Adelman[110], M. Adersberger[102], T. Adye[133], A.A. Affolder[139], Y. Afik[154], T. Agatonovic-Jovin[14], C. Agheorghiesei[28c], J.A. Aguilar-Saavedra[128a,128f], S.P. Ahlen[24], F. Ahmadov[68,b], G. Aielli[135a,135b], S. Akatsuka[71], H. Akerstedt[148a,148b], T.P.A. Åkesson[84], E. Akilli[52], A.V. Akimov[98], G.L. Alberghi[22a,22b], J. Albert[172], P. Albicocco[50], M.J. Alconada Verzini[74], S.C. Alderweireldt[108], M. Aleksa[32], I.N. Aleksandrov[68], C. Alexa[28b], G. Alexander[155], T. Alexopoulos[10], M. Alhroob[115], B. Ali[130], M. Aliev[76a,76b], G. Alimonti[94a], J. Alison[33], S.P. Alkire[38], B.M.M. Allbrooke[151], B.W. Allen[118], P.P. Allport[19], A. Aloisio[106a,106b], A. Alonso[39], F. Alonso[74], C. Alpigiani[140], A.A. Alshehri[56], M.I. Alstaty[88], B. Alvarez Gonzalez[32], D. Álvarez Piqueras[170], M.G. Alviggi[106a,106b], B.T. Amadio[16], Y. Amaral Coutinho[26a], C. Amelung[25], D. Amidei[92], S.P. Amor Dos Santos[128a,128c], S. Amoroso[32], G. Amundsen[25], C. Anastopoulos[141], L.S. Ancu[52], N. Andari[19], T. Andeen[11], C.F. Anders[60b], J.K. Anders[77], K.J. Anderson[33], A. Andreazza[94a,94b], V. Andrei[60a], S. Angelidakis[37], I. Angelozzi[109], A. Angerami[38], A.V. Anisenkov[111,c], N. Anjos[13], A. Annovi[126a], C. Antel[60a], M. Antonelli[50], A. Antonov[100,*], D.J. Antrim[166], F. Anulli[134a], M. Aoki[69], L. Aperio Bella[32], G. Arabidze[93], Y. Arai[69], J.P. Araque[128a], V. Araujo Ferraz[26a], A.T.H. Arce[48], R.E. Ardell[80], F.A. Arduh[74], J-F. Arguin[97], S. Argyropoulos[66], M. Arik[20a], A.J. Armbruster[32], L.J. Armitage[79], O. Arnaez[161], H. Arnold[51], M. Arratia[30], O. Arslan[23], A. Artamonov[99,*], G. Artoni[122], S. Artz[86], S. Asai[157], N. Asbah[45], A. Ashkenazi[155], L. Asquith[151], K. Assamagan[27], R. Astalos[146a], M. Atkinson[169], N.B. Atlay[143], K. Augsten[130], G. Avolio[32], B. Axen[16], M.K. Ayoub[35a], G. Azuelos[97,d], A.E. Baas[60a], M.J. Baca[19], H. Bachacou[138], K. Bachas[76a,76b], M. Backes[122], P. Bagnaia[134a,134b], M. Bahmani[42], H. Bahrasemani[144], J.T. Baines[133], M. Bajic[39], O.K. Baker[179], P.J. Bakker[109], E.M. Baldin[111,c], P. Balek[175], F. Balli[138], W.K. Balunas[124], E. Banas[42], A. Bandyopadhyay[23], Sw. Banerjee[176,e], A.A.E. Bannoura[178], L. Barak[155], E.L. Barberio[91], D. Barberis[53a,53b], M. Barbero[88], T. Barillari[103], M-S Barisits[32], J.T. Barkeloo[118], T. Barklow[145], N. Barlow[30], S.L. Barnes[36c], B.M. Barnett[133], R.M. Barnett[16], Z. Barnovska-Blenessy[36a], A. Baroncelli[136a], G. Barone[25], A.J. Barr[122], L. Barranco Navarro[170], F. Barreiro[85], J. Barreiro Guimarães da Costa[35a], R. Bartoldus[145], A.E. Barton[75], P. Bartos[146a], A. Basalaev[125], A. Bassalat[119,f], R.L. Bates[56], S.J. Batista[161], J.R. Batley[30], M. Battaglia[139], M. Bauce[134a,134b], F. Bauer[138], H.S. Bawa[145,g], J.B. Beacham[113], M.D. Beattie[75], T. Beau[83], P.H. Beauchemin[165], P. Bechtle[23], H.P. Beck[18,h], H.C. Beck[57], K. Becker[122], M. Becker[86], C. Becot[112], A.J. Beddall[20e], A. Beddall[20b], V.A. Bednyakov[68], M. Bedognetti[109], C.P. Bee[150], T.A. Beermann[32], M. Begalli[26a], M. Begel[27], J.K. Behr[45], A.S. Bell[81], G. Bella[155], L. Bellagamba[22a], A. Bellerive[31], M. Bellomo[154], K. Belotskiy[100], O. Beltramello[32], N.L. Belyaev[100], O. Benary[155,*], D. Benchekroun[137a], M. Bender[102], N. Benekos[10], Y. Benhammou[155], E. Benhar Noccioli[179], J. Benitez[66], D.P. Benjamin[48], M. Benoit[52], J.R. Bensinger[25], S. Bentvelsen[109], L. Beresford[122], M. Beretta[50], D. Berge[109], E. Bergeaas Kuutmann[168], N. Berger[5], L.J. Bergsten[25], J. Beringer[16], S. Berlendis[58], N.R. Bernard[89], G. Bernardi[83], C. Bernius[145], F.U. Bernlochner[23], T. Berry[80], P. Berta[86], C. Bertella[35a], G. Bertoli[148a,148b], I.A. Bertram[75], C. Bertsche[45], G.J. Besjes[39], O. Bessidskaia Bylund[148a,148b], M. Bessner[45], N. Besson[138], A. Bethani[87], S. Bethke[103], A. Betti[23], A.J. Bevan[79], J. Beyer[103], R.M. Bianchi[127], O. Biebel[102], D. Biedermann[17], R. Bielski[87], K. Bierwagen[86], N.V. Biesuz[126a,126b], M. Biglietti[136a], T.R.V. Billoud[97], H. Bilokon[50], M. Bindi[57], A. Bingul[20b], C. Bini[134a,134b], S. Biondi[22a,22b], T. Bisanz[57], C. Bittrich[47], D.M. Bjergaard[48], J.E. Black[145], K.M. Black[24], R.E. Blair[6], T. Blazek[146a], I. Bloch[45], C. Blocker[25], A. Blue[56], U. Blumenschein[79], Dr. Blunier[34a], G.J. Bobbink[109], V.S. Bobrovnikov[111,c], S.S. Bocchetta[84],

A. Bocci[48], C. Bock[102], M. Boehler[51], D. Boerner[178], D. Bogavac[102], A.G. Bogdanchikov[111], C. Bohm[148a], V. Boisvert[80], P. Bokan[168,i], T. Bold[41a], A.S. Boldyrev[101], A.E. Bolz[60b], M. Bomben[83], M. Bona[79], M. Boonekamp[138], A. Borisov[132], G. Borissov[75], J. Bortfeldt[32], D. Bortoletto[122], V. Bortolotto[62a], D. Boscherini[22a], M. Bosman[13], J.D. Bossio Sola[29], J. Boudreau[127], E.V. Bouhova-Thacker[75], D. Boumediene[37], C. Bourdarios[119], S.K. Boutle[56], A. Boveia[113], J. Boyd[32], I.R. Boyko[68], A.J. Bozson[80], J. Bracinik[19], A. Brandt[8], G. Brandt[57], O. Brandt[60a], F. Braren[45], U. Bratzler[158], B. Brau[89], J.E. Brau[118], W.D. Breaden Madden[56], K. Brendlinger[45], A.J. Brennan[91], L. Brenner[109], R. Brenner[168], S. Bressler[175], D.L. Briglin[19], T.M. Bristow[49], D. Britton[56], D. Britzger[45], F.M. Brochu[30], I. Brock[23], R. Brock[93], G. Brooijmans[38], T. Brooks[80], W.K. Brooks[34b], J. Brosamer[16], E. Brost[110], J.H Broughton[19], P.A. Bruckman de Renstrom[42], D. Bruncko[146b], A. Bruni[22a], G. Bruni[22a], L.S. Bruni[109], S. Bruno[135a,135b], BH Brunt[30], M. Bruschi[22a], N. Bruscino[127], P. Bryant[33], L. Bryngemark[45], T. Buanes[15], Q. Buat[144], P. Buchholz[143], A.G. Buckley[56], I.A. Budagov[68], F. Buehrer[51], M.K. Bugge[121], O. Bulekov[100], D. Bullock[8], T.J. Burch[110], S. Burdin[77], C.D. Burgard[109], A.M. Burger[5], B. Burghgrave[110], K. Burka[42], S. Burke[133], I. Burmeister[46], J.T.P. Burr[122], D. Büscher[51], V. Büscher[86], P. Bussey[56], J.M. Butler[24], C.M. Buttar[56], J.M. Butterworth[81], P. Butti[32], W. Buttinger[27], A. Buzatu[153], A.R. Buzykaev[111,c], Changqiao C.-Q.[36a], S. Cabrera Urbán[170], D. Caforio[130], H. Cai[169], V.M. Cairo[40a,40b], O. Cakir[4a], N. Calace[52], P. Calafiura[16], A. Calandri[88], G. Calderini[83], P. Calfayan[64], G. Callea[40a,40b], L.P. Caloba[26a], S. Calvente Lopez[85], D. Calvet[37], S. Calvet[37], T.P. Calvet[88], R. Camacho Toro[33], S. Camarda[32], P. Camarri[135a,135b], D. Cameron[121], R. Caminal Armadans[169], C. Camincher[58], S. Campana[32], M. Campanelli[81], A. Camplani[94a,94b], A. Campoverde[143], V. Canale[106a,106b], M. Cano Bret[36c], J. Cantero[116], T. Cao[155], M.D.M. Capeans Garrido[32], I. Caprini[28b], M. Caprini[28b], M. Capua[40a,40b], R.M. Carbone[38], R. Cardarelli[135a], F. Cardillo[51], I. Carli[131], T. Carli[32], G. Carlino[106a], B.T. Carlson[127], L. Carminati[94a,94b], R.M.D. Carney[148a,148b], S. Caron[108], E. Carquin[34b], S. Carrá[94a,94b], G.D. Carrillo-Montoya[32], D. Casadei[19], M.P. Casado[13,j], A.F. Casha[161], M. Casolino[13], D.W. Casper[166], R. Castelijn[109], V. Castillo Gimenez[170], N.F. Castro[128a,k], A. Catinaccio[32], J.R. Catmore[121], A. Cattai[32], J. Caudron[23], V. Cavaliere[169], E. Cavallaro[13], D. Cavalli[94a], M. Cavalli-Sforza[13], V. Cavasinni[126a,126b], E. Celebi[20d], F. Ceradini[136a,136b], L. Cerda Alberich[170], A.S. Cerqueira[26b], A. Cerri[151], L. Cerrito[135a,135b], F. Cerutti[16], A. Cervelli[22a,22b], S.A. Cetin[20d], A. Chafaq[137a], D. Chakraborty[110], S.K. Chan[59], W.S. Chan[109], Y.L. Chan[62a], P. Chang[169], J.D. Chapman[30], D.G. Charlton[19], C.C. Chau[31], C.A. Chavez Barajas[151], S. Che[113], S. Cheatham[167a,167c], A. Chegwidden[93], S. Chekanov[6], S.V. Chekulaev[163a], G.A. Chelkov[68,l], M.A. Chelstowska[32], C. Chen[36a], C. Chen[67], H. Chen[27], J. Chen[36a], S. Chen[35b], S. Chen[157], X. Chen[35c,m], Y. Chen[70], H.C. Cheng[92], H.J. Cheng[35a,35d], A. Cheplakov[68], E. Cheremushkina[132], R. Cherkaoui El Moursli[137e], E. Cheu[7], K. Cheung[63], L. Chevalier[138], V. Chiarella[50], G. Chiarelli[126a], G. Chiodini[76a], A.S. Chisholm[32], A. Chitan[28b], Y.H. Chiu[172], M.V. Chizhov[68], K. Choi[64], A.R. Chomont[37], S. Chouridou[156], Y.S. Chow[62a], V. Christodoulou[81], M.C. Chu[62a], J. Chudoba[129], A.J. Chuinard[90], J.J. Chwastowski[42], L. Chytka[117], A.K. Ciftci[4a], D. Cinca[46], V. Cindro[78], I.A. Cioara[23], A. Ciocio[16], F. Cirotto[106a,106b], Z.H. Citron[175], M. Citterio[94a], M. Ciubancan[28b], A. Clark[52], B.L. Clark[59], M.R. Clark[38], P.J. Clark[49], R.N. Clarke[16], C. Clement[148a,148b], Y. Coadou[88], M. Cobal[167a,167c], A. Coccaro[52], J. Cochran[67], L. Colasurdo[108], B. Cole[38], A.P. Colijn[109], J. Collot[58], T. Colombo[166], P. Conde Muiño[128a,128b], E. Coniavitis[51], S.H. Connell[147b], I.A. Connelly[87], S. Constantinescu[28b], G. Conti[32], F. Conventi[106a,n], M. Cooke[16], A.M. Cooper-Sarkar[122], F. Cormier[171], K.J.R. Cormier[161], M. Corradi[134a,134b], F. Corriveau[90,o], A. Cortes-Gonzalez[32], G. Costa[94a], M.J. Costa[170], D. Costanzo[141], G. Cottin[30], G. Cowan[80], B.E. Cox[87], K. Cranmer[112], S.J. Crawley[56], R.A. Creager[124], G. Cree[31], S. Crépé-Renaudin[58], F. Crescioli[83], W.A. Cribbs[148a,148b], M. Cristinziani[23], V. Croft[112], G. Crosetti[40a,40b], A. Cueto[85], T. Cuhadar Donszelmann[141], A.R. Cukierman[145], J. Cummings[179], M. Curatolo[50], J. Cúth[86], S. Czekierda[42], P. Czodrowski[32], G. D'amen[22a,22b],

S. D'Auria[56], L. D'eramo[83], M. D'Onofrio[77], M.J. Da Cunha Sargedas De Sousa[128a,128b], C. Da Via[87], W. Dabrowski[41a], T. Dado[146a], T. Dai[92], O. Dale[15], F. Dallaire[97], C. Dallapiccola[89], M. Dam[39], J.R. Dandoy[124], M.F. Daneri[29], N.P. Dang[176], A.C. Daniells[19], N.S. Dann[87], M. Danninger[171], M. Dano Hoffmann[138], V. Dao[150], G. Darbo[53a], S. Darmora[8], J. Dassoulas[3], A. Dattagupta[118], T. Daubney[45], W. Davey[23], C. David[45], T. Davidek[131], D.R. Davis[48], P. Davison[81], E. Dawe[91], I. Dawson[141], K. De[8], R. de Asmundis[106a], A. De Benedetti[115], S. De Castro[22a,22b], S. De Cecco[83], N. De Groot[108], P. de Jong[109], H. De la Torre[93], F. De Lorenzi[67], A. De Maria[57], D. De Pedis[134a], A. De Salvo[134a], U. De Sanctis[135a,135b], A. De Santo[151], K. De Vasconcelos Corga[88], J.B. De Vivie De Regie[119], R. Debbe[27], C. Debenedetti[139], D.V. Dedovich[68], N. Dehghanian[3], I. Deigaard[109], M. Del Gaudio[40a,40b], J. Del Peso[85], D. Delgove[119], F. Deliot[138], C.M. Delitzsch[7], A. Dell'Acqua[32], L. Dell'Asta[24], M. Dell'Orso[126a,126b], M. Della Pietra[106a,106b], D. della Volpe[52], M. Delmastro[5], C. Delporte[119], P.A. Delsart[58], D.A. DeMarco[161], S. Demers[179], M. Demichev[68], A. Demilly[83], S.P. Denisov[132], D. Denysiuk[138], D. Derendarz[42], J.E. Derkaoui[137d], F. Derue[83], P. Dervan[77], K. Desch[23], C. Deterre[45], K. Dette[161], M.R. Devesa[29], P.O. Deviveiros[32], A. Dewhurst[133], S. Dhaliwal[25], F.A. Di Bello[52], A. Di Ciaccio[135a,135b], L. Di Ciaccio[5], W.K. Di Clemente[124], C. Di Donato[106a,106b], A. Di Girolamo[32], B. Di Girolamo[32], B. Di Micco[136a,136b], R. Di Nardo[32], K.F. Di Petrillo[59], A. Di Simone[51], R. Di Sipio[161], D. Di Valentino[31], C. Diaconu[88], M. Diamond[161], F.A. Dias[39], M.A. Diaz[34a], J. Dickinson[16], E.B. Diehl[92], J. Dietrich[17], S. Díez Cornell[45], A. Dimitrievska[14], J. Dingfelder[23], P. Dita[28b], S. Dita[28b], F. Dittus[32], F. Djama[88], T. Djobava[54b], J.I. Djuvsland[60a], M.A.B. do Vale[26c], D. Dobos[32], M. Dobre[28b], D. Dodsworth[25], C. Doglioni[84], J. Dolejsi[131], Z. Dolezal[131], M. Donadelli[26d], S. Donati[126a,126b], P. Dondero[123a,123b], J. Donini[37], J. Dopke[133], A. Doria[106a], M.T. Dova[74], A.T. Doyle[56], E. Drechsler[57], M. Dris[10], Y. Du[36b], J. Duarte-Campderros[155], F. Dubinin[98], A. Dubreuil[52], E. Duchovni[175], G. Duckeck[102], A. Ducourthial[83], O.A. Ducu[97,p], D. Duda[109], A. Dudarev[32], A.Chr. Dudder[86], E.M. Duffield[16], L. Duflot[119], M. Dührssen[32], C. Dulsen[178], M. Dumancic[175], A.E. Dumitriu[28b], A.K. Duncan[56], M. Dunford[60a], A. Duperrin[88], H. Duran Yildiz[4a], M. Düren[55], A. Durglishvili[54b], D. Duschinger[47], B. Dutta[45], D. Duvnjak[1], M. Dyndal[45], B.S. Dziedzic[42], C. Eckardt[45], K.M. Ecker[103], R.C. Edgar[92], T. Eifert[32], G. Eigen[15], K. Einsweiler[16], T. Ekelof[168], M. El Kacimi[137c], R. El Kosseifi[88], V. Ellajosyula[88], M. Ellert[168], S. Elles[5], F. Ellinghaus[178], A.A. Elliot[172], N. Ellis[32], J. Elmsheuser[27], M. Elsing[32], D. Emeliyanov[133], Y. Enari[157], J.S. Ennis[173], M.B. Epland[48], J. Erdmann[46], A. Ereditato[18], M. Ernst[27], S. Errede[169], M. Escalier[119], C. Escobar[170], B. Esposito[50], O. Estrada Pastor[170], A.I. Etienvre[138], E. Etzion[155], H. Evans[64], A. Ezhilov[125], M. Ezzi[137e], F. Fabbri[22a,22b], L. Fabbri[22a,22b], V. Fabiani[108], G. Facini[81], R.M. Fakhrutdinov[132], S. Falciano[134a], R.J. Falla[81], J. Faltova[32], Y. Fang[35a], M. Fanti[94a,94b], A. Farbin[8], A. Farilla[136a], C. Farina[127], E.M. Farina[123a,123b], T. Farooque[93], S. Farrell[16], S.M. Farrington[173], P. Farthouat[32], F. Fassi[137e], P. Fassnacht[32], D. Fassouliotis[9], M. Faucci Giannelli[49], A. Favareto[53a,53b], W.J. Fawcett[122], L. Fayard[119], O.L. Fedin[125,q], W. Fedorko[171], S. Feigl[121], L. Feligioni[88], C. Feng[36b], E.J. Feng[32], M.J. Fenton[56], A.B. Fenyuk[132], L. Feremenga[8], P. Fernandez Martinez[170], J. Ferrando[45], A. Ferrari[168], P. Ferrari[109], R. Ferrari[123a], D.E. Ferreira de Lima[60b], A. Ferrer[170], D. Ferrere[52], C. Ferretti[92], F. Fiedler[86], A. Filipčič[78], M. Filipuzzi[45], F. Filthaut[108], M. Fincke-Keeler[172], K.D. Finelli[24], M.C.N. Fiolhais[128a,128c,r], L. Fiorini[170], A. Fischer[2], C. Fischer[13], J. Fischer[178], W.C. Fisher[93], N. Flaschel[45], I. Fleck[143], P. Fleischmann[92], R.R.M. Fletcher[124], T. Flick[178], B.M. Flierl[102], L.R. Flores Castillo[62a], M.J. Flowerdew[103], G.T. Forcolin[87], A. Formica[138], F.A. Förster[13], A. Forti[87], A.G. Foster[19], D. Fournier[119], H. Fox[75], S. Fracchia[141], P. Francavilla[126a,126b], M. Franchini[22a,22b], S. Franchino[60a], D. Francis[32], L. Franconi[121], M. Franklin[59], M. Frate[166], M. Fraternali[123a,123b], D. Freeborn[81], S.M. Fressard-Batraneanu[32], B. Freund[97], D. Froidevaux[32], J.A. Frost[122], C. Fukunaga[158], T. Fusayasu[104], J. Fuster[170], O. Gabizon[154], A. Gabrielli[22a,22b], A. Gabrielli[16], G.P. Gach[41a],

S. Gadatsch[32], S. Gadomski[80], G. Gagliardi[53a,53b], L.G. Gagnon[97], C. Galea[108], B. Galhardo[128a,128c], E.J. Gallas[122], B.J. Gallop[133], P. Gallus[130], G. Galster[39], K.K. Gan[113], S. Ganguly[37], Y. Gao[77], Y.S. Gao[145,g], F.M. Garay Walls[34a], C. García[170], J.E. García Navarro[170], J.A. García Pascual[35a], M. Garcia-Sciveres[16], R.W. Gardner[33], N. Garelli[145], V. Garonne[121], A. Gascon Bravo[45], K. Gasnikova[45], C. Gatti[50], A. Gaudiello[53a,53b], G. Gaudio[123a], I.L. Gavrilenko[98], C. Gay[171], G. Gaycken[23], E.N. Gazis[10], C.N.P. Gee[133], J. Geisen[57], M. Geisen[86], M.P. Geisler[60a], K. Gellerstedt[148a,148b], C. Gemme[53a], M.H. Genest[58], C. Geng[92], S. Gentile[134a,134b], C. Gentsos[156], S. George[80], D. Gerbaudo[13], G. Geßner[46], S. Ghasemi[143], M. Ghneimat[23], B. Giacobbe[22a], S. Giagu[134a,134b], N. Giangiacomi[22a,22b], P. Giannetti[126a], S.M. Gibson[80], M. Gignac[171], M. Gilchriese[16], D. Gillberg[31], G. Gilles[178], D.M. Gingrich[3,d], M.P. Giordani[167a,167c], F.M. Giorgi[22a], P.F. Giraud[138], P. Giromini[59], G. Giugliarelli[167a,167c], D. Giugni[94a], F. Giuli[122], C. Giuliani[103], M. Giulini[60b], B.K. Gjelsten[121], S. Gkaitatzis[156], I. Gkialas[9,s], E.L. Gkougkousis[13], P. Gkountoumis[10], L.K. Gladilin[101], C. Glasman[85], J. Glatzer[13], P.C.F. Glaysher[45], A. Glazov[45], M. Goblirsch-Kolb[25], J. Godlewski[42], S. Goldfarb[91], T. Golling[52], D. Golubkov[132], A. Gomes[128a,128b,128d], R. Gonçalo[128a], R. Goncalves Gama[26a], J. Goncalves Pinto Firmino Da Costa[138], G. Gonella[51], L. Gonella[19], A. Gongadze[68], J.L. Gonski[59], S. González de la Hoz[170], S. Gonzalez-Sevilla[52], L. Goossens[32], P.A. Gorbounov[99], H.A. Gordon[27], I. Gorelov[107], B. Gorini[32], E. Gorini[76a,76b], A. Gorišek[78], A.T. Goshaw[48], C. Gössling[46], M.I. Gostkin[68], C.A. Gottardo[23], C.R. Goudet[119], D. Goujdami[137c], A.G. Goussiou[140], N. Govender[147b,t], E. Gozani[154], I. Grabowska-Bold[41a], P.O.J. Gradin[168], J. Gramling[166], E. Gramstad[121], S. Grancagnolo[17], V. Gratchev[125], P.M. Gravila[28f], C. Gray[56], H.M. Gray[16], Z.D. Greenwood[82,u], C. Grefe[23], K. Gregersen[81], I.M. Gregor[45], P. Grenier[145], K. Grevtsov[5], J. Griffiths[8], A.A. Grillo[139], K. Grimm[75], S. Grinstein[13,v], Ph. Gris[37], J.-F. Grivaz[119], S. Groh[86], E. Gross[175], J. Grosse-Knetter[57], G.C. Grossi[82], Z.J. Grout[81], A. Grummer[107], L. Guan[92], W. Guan[176], J. Guenther[32], F. Guescini[163a], D. Guest[166], O. Gueta[155], B. Gui[113], E. Guido[53a,53b], T. Guillemin[5], S. Guindon[32], U. Gul[56], C. Gumpert[32], J. Guo[36c], W. Guo[92], Y. Guo[36a,w], R. Gupta[43], S. Gurbuz[20a], G. Gustavino[115], B.J. Gutelman[154], P. Gutierrez[115], N.G. Gutierrez Ortiz[81], C. Gutschow[81], C. Guyot[138], M.P. Guzik[41a], C. Gwenlan[122], C.B. Gwilliam[77], A. Hönle[103], A. Haas[112], C. Haber[16], H.K. Hadavand[8], N. Haddad[137e], A. Hadef[88], S. Hageböck[23], M. Hagihara[164], H. Hakobyan[180,*], M. Haleem[45], J. Haley[116], G. Halladjian[93], G.D. Hallewell[88], K. Hamacher[178], P. Hamal[117], K. Hamano[172], A. Hamilton[147a], G.N. Hamity[141], P.G. Hamnett[45], L. Han[36a], S. Han[35a,35d], K. Hanagaki[69,x], K. Hanawa[157], M. Hance[139], D.M. Handl[102], B. Haney[124], P. Hanke[60a], J.B. Hansen[39], J.D. Hansen[39], M.C. Hansen[23], P.H. Hansen[39], K. Hara[164], A.S. Hard[176], T. Harenberg[178], F. Hariri[119], S. Harkusha[95], P.F. Harrison[173], N.M. Hartmann[102], Y. Hasegawa[142], A. Hasib[49], S. Hassani[138], S. Haug[18], R. Hauser[93], L. Hauswald[47], L.B. Havener[38], M. Havranek[130], C.M. Hawkes[19], R.J. Hawkings[32], D. Hayakawa[159], D. Hayden[93], C.P. Hays[122], J.M. Hays[79], H.S. Hayward[77], S.J. Haywood[133], S.J. Head[19], T. Heck[86], V. Hedberg[84], L. Heelan[8], S. Heer[23], K.K. Heidegger[51], S. Heim[45], T. Heim[16], B. Heinemann[45,y], J.J. Heinrich[102], L. Heinrich[112], C. Heinz[55], J. Hejbal[129], L. Helary[32], A. Held[171], S. Hellman[148a,148b], C. Helsens[32], R.C.W. Henderson[75], Y. Heng[176], S. Henkelmann[171], A.M. Henriques Correia[32], S. Henrot-Versille[119], G.H. Herbert[17], H. Herde[25], V. Herget[177], Y. Hernández Jiménez[147c], H. Herr[86], G. Herten[51], R. Hertenberger[102], L. Hervas[32], T.C. Herwig[124], G.G. Hesketh[81], N.P. Hessey[163a], J.W. Hetherly[43], S. Higashino[69], E. Higón-Rodriguez[170], K. Hildebrand[33], E. Hill[172], J.C. Hill[30], K.H. Hiller[45], S.J. Hillier[19], M. Hils[47], I. Hinchliffe[16], M. Hirose[51], D. Hirschbuehl[178], B. Hiti[78], O. Hladik[129], D.R. Hlaluku[147c], X. Hoad[49], J. Hobbs[150], N. Hod[163a], M.C. Hodgkinson[141], P. Hodgson[141], A. Hoecker[32], M.R. Hoeferkamp[107], F. Hoenig[102], D. Hohn[23], T.R. Holmes[33], M. Holzbock[102], M. Homann[46], S. Honda[164], T. Honda[69], T.M. Hong[127], B.H. Hooberman[169], W.H. Hopkins[118], Y. Horii[105], A.J. Horton[144], J-Y. Hostachy[58], A. Hostiuc[140], S. Hou[153], A. Hoummada[137a], J. Howarth[87], J. Hoya[74], M. Hrabovsky[117], J. Hrdinka[32],

I. Hristova[17], J. Hrivnac[119], T. Hryn'ova[5], A. Hrynevich[96], P.J. Hsu[63], S.-C. Hsu[140], Q. Hu[27], S. Hu[36c], Y. Huang[35a], Z. Hubacek[130], F. Hubaut[88], F. Huegging[23], T.B. Huffman[122], E.W. Hughes[38], M. Huhtinen[32], R.F.H. Hunter[31], P. Huo[150], N. Huseynov[68,b], J. Huston[93], J. Huth[59], R. Hyneman[92], G. Iacobucci[52], G. Iakovidis[27], I. Ibragimov[143], L. Iconomidou-Fayard[119], Z. Idrissi[137e], P. Iengo[32], O. Igonkina[109,z], T. Iizawa[174], Y. Ikegami[69], M. Ikeno[69], Y. Ilchenko[11,aa], D. Iliadis[156], N. Ilic[145], F. Iltzsche[47], G. Introzzi[123a,123b], P. Ioannou[9,*], M. Iodice[136a], K. Iordanidou[38], V. Ippolito[59], M.F. Isacson[168], N. Ishijima[120], M. Ishino[157], M. Ishitsuka[159], C. Issever[122], S. Istin[20a], F. Ito[164], J.M. Iturbe Ponce[62a], R. Iuppa[162a,162b], H. Iwasaki[69], J.M. Izen[44], V. Izzo[106a], S. Jabbar[3], P. Jackson[1], R.M. Jacobs[23], V. Jain[2], K.B. Jakobi[86], K. Jakobs[51], S. Jakobsen[65], T. Jakoubek[129], D.O. Jamin[116], D.K. Jana[82], R. Jansky[52], J. Janssen[23], M. Janus[57], P.A. Janus[41a], G. Jarlskog[84], N. Javadov[68,b], T. Javůrek[51], M. Javurkova[51], F. Jeanneau[138], L. Jeanty[16], J. Jejelava[54a,ab], A. Jelinskas[173], P. Jenni[51,ac], C. Jeske[173], S. Jézéquel[5], H. Ji[176], J. Jia[150], H. Jiang[67], Y. Jiang[36a], Z. Jiang[145], S. Jiggins[81], J. Jimenez Pena[170], S. Jin[35b], A. Jinaru[28b], O. Jinnouchi[159], H. Jivan[147c], P. Johansson[141], K.A. Johns[7], C.A. Johnson[64], W.J. Johnson[140], K. Jon-And[148a,148b], R.W.L. Jones[75], S.D. Jones[151], S. Jones[7], T.J. Jones[77], J. Jongmanns[60a], P.M. Jorge[128a,128b], J. Jovicevic[163a], X. Ju[176], A. Juste Rozas[13,v], M.K. Köhler[175], A. Kaczmarska[42], M. Kado[119], H. Kagan[113], M. Kagan[145], S.J. Kahn[88], T. Kaji[174], E. Kajomovitz[154], C.W. Kalderon[84], A. Kaluza[86], S. Kama[43], A. Kamenshchikov[132], N. Kanaya[157], L. Kanjir[78], V.A. Kantserov[100], J. Kanzaki[69], B. Kaplan[112], L.S. Kaplan[176], D. Kar[147c], K. Karakostas[10], N. Karastathis[10], M.J. Kareem[163b], E. Karentzos[10], S.N. Karpov[68], Z.M. Karpova[68], K. Karthik[112], V. Kartvelishvili[75], A.N. Karyukhin[132], K. Kasahara[164], L. Kashif[176], R.D. Kass[113], A. Kastanas[149], Y. Kataoka[157], C. Kato[157], A. Katre[52], J. Katzy[45], K. Kawade[70], K. Kawagoe[73], T. Kawamoto[157], G. Kawamura[57], E.F. Kay[77], V.F. Kazanin[111,c], R. Keeler[172], R. Kehoe[43], J.S. Keller[31], E. Kellermann[84], J.J. Kempster[80], J Kendrick[19], H. Keoshkerian[161], O. Kepka[129], B.P. Kerševan[78], S. Kersten[178], R.A. Keyes[90], M. Khader[169], F. Khalil-zada[12], A. Khanov[116], A.G. Kharlamov[111,c], T. Kharlamova[111,c], A. Khodinov[160], T.J. Khoo[52], V. Khovanskiy[99,*], E. Khramov[68], J. Khubua[54b,ad], S. Kido[70], C.R. Kilby[80], H.Y. Kim[8], S.H. Kim[164], Y.K. Kim[33], N. Kimura[156], O.M. Kind[17], B.T. King[77], D. Kirchmeier[47], J. Kirk[133], A.E. Kiryunin[103], T. Kishimoto[157], D. Kisielewska[41a], V. Kitali[45], O. Kivernyk[5], E. Kladiva[146b], T. Klapdor-Kleingrothaus[51], M.H. Klein[92], M. Klein[77], U. Klein[77], K. Kleinknecht[86], P. Klimek[110], A. Klimentov[27], R. Klingenberg[46,*], T. Klingl[23], T. Klioutchnikova[32], F.F. Klitzner[102], E.-E. Kluge[60a], P. Kluit[109], S. Kluth[103], E. Kneringer[65], E.B.F.G. Knoops[88], A. Knue[103], A. Kobayashi[157], D. Kobayashi[73], T. Kobayashi[157], M. Kobel[47], M. Kocian[145], P. Kodys[131], T. Koffas[31], E. Koffeman[109], N.M. Köhler[103], T. Koi[145], M. Kolb[60b], I. Koletsou[5], A.A. Komar[98,*], T. Kondo[69], N. Kondrashova[36c], K. Köneke[51], A.C. König[108], T. Kono[69,ae], R. Konoplich[112,af], N. Konstantinidis[81], B. Konya[84], R. Kopeliansky[64], S. Koperny[41a], A.K. Kopp[51], K. Korcyl[42], K. Kordas[156], A. Korn[81], A.A. Korol[111,c], I. Korolkov[13], E.V. Korolkova[141], O. Kortner[103], S. Kortner[103], T. Kosek[131], V.V. Kostyukhin[23], A. Kotwal[48], A. Koulouris[10], A. Kourkoumeli-Charalampidi[123a,123b], C. Kourkoumelis[9], E. Kourlitis[141], V. Kouskoura[27], A.B. Kowalewska[42], R. Kowalewski[172], T.Z. Kowalski[41a], C. Kozakai[157], W. Kozanecki[138], A.S. Kozhin[132], V.A. Kramarenko[101], G. Kramberger[78], D. Krasnopevtsev[100], M.W. Krasny[83], A. Krasznahorkay[32], D. Krauss[103], J.A. Kremer[41a], J. Kretzschmar[77], K. Kreutzfeldt[55], P. Krieger[161], K. Krizka[16], K. Kroeninger[46], H. Kroha[103], J. Kroll[129], J. Kroll[124], J. Kroseberg[23], J. Krstic[14], U. Kruchonak[68], H. Krüger[23], N. Krumnack[67], M.C. Kruse[48], T. Kubota[91], H. Kucuk[81], S. Kuday[4b], J.T. Kuechler[178], S. Kuehn[32], A. Kugel[60a], F. Kuger[177], T. Kuhl[45], V. Kukhtin[68], R. Kukla[88], Y. Kulchitsky[95], S. Kuleshov[34b], Y.P. Kulinich[169], M. Kuna[134a,134b], T. Kunigo[71], A. Kupco[129], T. Kupfer[46], O. Kuprash[155], H. Kurashige[70], L.L. Kurchaninov[163a], Y.A. Kurochkin[95], M.G. Kurth[35a,35d], E.S. Kuwertz[172], M. Kuze[159], J. Kvita[117], T. Kwan[172], D. Kyriazopoulos[141], A. La Rosa[103], J.L. La Rosa Navarro[26d], L. La Rotonda[40a,40b], F. La Ruffa[40a,40b], C. Lacasta[170], F. Lacava[134a,134b], J. Lacey[45], D.P.J. Lack[87],

H. Lacker[17], D. Lacour[83], E. Ladygin[68], R. Lafaye[5], B. Laforge[83], T. Lagouri[179], S. Lai[57], S. Lammers[64], W. Lampl[7], E. Lançon[27], U. Landgraf[51], M.P.J. Landon[79], M.C. Lanfermann[52], V.S. Lang[45], J.C. Lange[13], R.J. Langenberg[32], A.J. Lankford[166], F. Lanni[27], K. Lantzsch[23], A. Lanza[123a], A. Lapertosa[53a,53b], S. Laplace[83], J.F. Laporte[138], T. Lari[94a], F. Lasagni Manghi[22a,22b], M. Lassnig[32], T.S. Lau[62a], P. Laurelli[50], W. Lavrijsen[16], A.T. Law[139], P. Laycock[77], T. Lazovich[59], M. Lazzaroni[94a,94b], B. Le[91], O. Le Dortz[83], E. Le Guirriec[88], E.P. Le Quilleuc[138], M. LeBlanc[172], T. LeCompte[6], F. Ledroit-Guillon[58], C.A. Lee[27], G.R. Lee[34a], S.C. Lee[153], L. Lee[59], B. Lefebvre[90], G. Lefebvre[83], M. Lefebvre[172], F. Legger[102], C. Leggett[16], G. Lehmann Miotto[32], X. Lei[7], W.A. Leight[45], M.A.L. Leite[26d], R. Leitner[131], D. Lellouch[175], B. Lemmer[57], K.J.C. Leney[81], T. Lenz[23], B. Lenzi[32], R. Leone[7], S. Leone[126a], C. Leonidopoulos[49], G. Lerner[151], C. Leroy[97], R. Les[161], A.A.J. Lesage[138], C.G. Lester[30], M. Levchenko[125], J. Levêque[5], D. Levin[92], L.J. Levinson[175], M. Levy[19], D. Lewis[79], B. Li[36a,w], H. Li[150], L. Li[36c], Q. Li[35a,35d], Q. Li[36a], S. Li[48], X. Li[36c], Y. Li[143], Z. Liang[35a], B. Liberti[135a], A. Liblong[161], K. Lie[62c], J. Liebal[23], W. Liebig[15], A. Limosani[152], C.Y. Lin[30], K. Lin[93], S.C. Lin[182], T.H. Lin[86], R.A. Linck[64], B.E. Lindquist[150], A.E. Lionti[52], E. Lipeles[124], A. Lipniacka[15], M. Lisovyi[60b], T.M. Liss[169,ag], A. Lister[171], A.M. Litke[139], B. Liu[67], H. Liu[92], H. Liu[27], J.K.K. Liu[122], J. Liu[36b], J.B. Liu[36a], K. Liu[88], L. Liu[169], M. Liu[36a], Y.L. Liu[36a], Y. Liu[36a], M. Livan[123a,123b], A. Lleres[58], J. Llorente Merino[35a], S.L. Lloyd[79], C.Y. Lo[62b], F. Lo Sterzo[43], E.M. Lobodzinska[45], P. Loch[7], F.K. Loebinger[87], A. Loesle[51], K.M. Loew[25], T. Lohse[17], K. Lohwasser[141], M. Lokajicek[129], B.A. Long[24], J.D. Long[169], R.E. Long[75], L. Longo[76a,76b], K.A. Looper[113], J.A. Lopez[34b], I. Lopez Paz[13], A. Lopez Solis[83], J. Lorenz[102], N. Lorenzo Martinez[5], M. Losada[21], P.J. Lösel[102], X. Lou[35a], A. Lounis[119], J. Love[6], P.A. Love[75], H. Lu[62a], N. Lu[92], Y.J. Lu[63], H.J. Lubatti[140], C. Luci[134a,134b], A. Lucotte[58], C. Luedtke[51], F. Luehring[64], W. Lukas[65], L. Luminari[134a], O. Lundberg[148a,148b], B. Lund-Jensen[149], M.S. Lutz[89], P.M. Luzi[83], D. Lynn[27], R. Lysak[129], E. Lytken[84], F. Lyu[35a], V. Lyubushkin[68], H. Ma[27], L.L. Ma[36b], Y. Ma[36b], G. Maccarrone[50], A. Macchiolo[103], C.M. Macdonald[141], B. Maček[78], J. Machado Miguens[124,128b], D. Madaffari[170], R. Madar[37], W.F. Mader[47], A. Madsen[45], N. Madysa[47], J. Maeda[70], S. Maeland[15], T. Maeno[27], A.S. Maevskiy[101], V. Magerl[51], C. Maiani[119], C. Maidantchik[26a], T. Maier[102], A. Maio[128a,128b,128d], O. Majersky[146a], S. Majewski[118], Y. Makida[69], N. Makovec[119], B. Malaescu[83], Pa. Malecki[42], V.P. Maleev[125], F. Malek[58], U. Mallik[66], D. Malon[6], C. Malone[30], S. Maltezos[10], S. Malyukov[32], J. Mamuzic[170], G. Mancini[50], I. Mandić[78], J. Maneira[128a,128b], L. Manhaes de Andrade Filho[26b], J. Manjarres Ramos[47], K.H. Mankinen[84], A. Mann[102], A. Manousos[32], B. Mansoulie[138], J.D. Mansour[35a], R. Mantifel[90], M. Mantoani[57], S. Manzoni[94a,94b], L. Mapelli[32], G. Marceca[29], L. March[52], L. Marchese[122], G. Marchiori[83], M. Marcisovsky[129], C.A. Marin Tobon[32], M. Marjanovic[37], D.E. Marley[92], F. Marroquim[26a], S.P. Marsden[87], Z. Marshall[16], M.U.F Martensson[168], S. Marti-Garcia[170], C.B. Martin[113], T.A. Martin[173], V.J. Martin[49], B. Martin dit Latour[15], M. Martinez[13,v], V.I. Martinez Outschoorn[169], S. Martin-Haugh[133], V.S. Martoiu[28b], A.C. Martyniuk[81], A. Marzin[32], L. Masetti[86], T. Mashimo[157], R. Mashinistov[98], J. Masik[87], A.L. Maslennikov[111,c], L.H. Mason[91], L. Massa[135a,135b], P. Mastrandrea[5], A. Mastroberardino[40a,40b], T. Masubuchi[157], P. Mättig[178], J. Maurer[28b], S.J. Maxfield[77], D.A. Maximov[111,c], R. Mazini[153], I. Maznas[156], S.M. Mazza[94a,94b], N.C. Mc Fadden[107], G. Mc Goldrick[161], S.P. Mc Kee[92], A. McCarn[92], R.L. McCarthy[150], T.G. McCarthy[103], L.I. McClymont[81], E.F. McDonald[91], J.A. Mcfayden[32], G. Mchedlidze[57], S.J. McMahon[133], P.C. McNamara[91], C.J. McNicol[173], R.A. McPherson[172,o], S. Meehan[140], T.J. Megy[51], S. Mehlhase[102], A. Mehta[77], T. Meideck[58], K. Meier[60a], B. Meirose[44], D. Melini[170,ah], B.R. Mellado Garcia[147c], J.D. Mellenthin[57], M. Melo[146a], F. Meloni[18], A. Melzer[23], S.B. Menary[87], L. Meng[77], X.T. Meng[92], A. Mengarelli[22a,22b], S. Menke[103], E. Meoni[40a,40b], S. Mergelmeyer[17], C. Merlassino[18], P. Mermod[52], L. Merola[106a,106b], C. Meroni[94a], F.S. Merritt[33], A. Messina[134a,134b], J. Metcalfe[6], A.S. Mete[166], C. Meyer[124], J-P. Meyer[138], J. Meyer[109], H. Meyer Zu Theenhausen[60a],

F. Miano[151], R.P. Middleton[133], S. Miglioranzi[53a,53b], L. Mijović[49], G. Mikenberg[175], M. Mikestikova[129], M. Mikuž[78], M. Milesi[91], A. Milic[161], D.A. Millar[79], D.W. Miller[33], C. Mills[49], A. Milov[175], D.A. Milstead[148a,148b], A.A. Minaenko[132], Y. Minami[157], I.A. Minashvili[54b], A.I. Mincer[112], B. Mindur[41a], M. Mineev[68], Y. Minegishi[157], Y. Ming[176], L.M. Mir[13], A. Mirto[76a,76b], K.P. Mistry[124], T. Mitani[174], J. Mitrevski[102], V.A. Mitsou[170], A. Miucci[18], P.S. Miyagawa[141], A. Mizukami[69], J.U. Mjörnmark[84], T. Mkrtchyan[180], M. Mlynarikova[131], T. Moa[148a,148b], K. Mochizuki[97], P. Mogg[51], S. Mohapatra[38], S. Molander[148a,148b], R. Moles-Valls[23], M.C. Mondragon[93], K. Mönig[45], J. Monk[39], E. Monnier[88], A. Montalbano[150], J. Montejo Berlingen[32], F. Monticelli[74], S. Monzani[94a], R.W. Moore[3], N. Morange[119], D. Moreno[21], M. Moreno Llácer[32], P. Morettini[53a], S. Morgenstern[32], D. Mori[144], T. Mori[157], M. Morii[59], M. Morinaga[174], V. Morisbak[121], A.K. Morley[32], G. Mornacchi[32], J.D. Morris[79], L. Morvaj[150], P. Moschovakos[10], M. Mosidze[54b], H.J. Moss[141], J. Moss[145,ai], K. Motohashi[159], R. Mount[145], E. Mountricha[27], E.J.W. Moyse[89], S. Muanza[88], F. Mueller[103], J. Mueller[127], R.S.P. Mueller[102], D. Muenstermann[75], P. Mullen[56], G.A. Mullier[18], F.J. Munoz Sanchez[87], W.J. Murray[173,133], H. Musheghyan[32], M. Muškinja[78], A.G. Myagkov[132,aj], M. Myska[130], B.P. Nachman[16], O. Nackenhorst[52], K. Nagai[122], R. Nagai[69,ae], K. Nagano[69], Y. Nagasaka[61], K. Nagata[164], M. Nagel[51], E. Nagy[88], A.M. Nairz[32], Y. Nakahama[105], K. Nakamura[69], T. Nakamura[157], I. Nakano[114], R.F. Naranjo Garcia[45], R. Narayan[11], D.I. Narrias Villar[60a], I. Naryshkin[125], T. Naumann[45], G. Navarro[21], R. Nayyar[7], H.A. Neal[92], P.Yu. Nechaeva[98], T.J. Neep[138], A. Negri[123a,123b], M. Negrini[22a], S. Nektarijevic[108], C. Nellist[57], A. Nelson[166], M.E. Nelson[122], S. Nemecek[129], P. Nemethy[112], M. Nessi[32,ak], M.S. Neubauer[169], M. Neumann[178], P.R. Newman[19], T.Y. Ng[62c], Y.S. Ng[17], T. Nguyen Manh[97], R.B. Nickerson[122], R. Nicolaidou[138], J. Nielsen[139], N. Nikiforou[11], V. Nikolaenko[132,aj], I. Nikolic-Audit[83], K. Nikolopoulos[19], P. Nilsson[27], Y. Ninomiya[69], A. Nisati[134a], N. Nishu[36c], R. Nisius[103], I. Nitsche[46], T. Nitta[174], T. Nobe[157], Y. Noguchi[71], M. Nomachi[120], I. Nomidis[31], M.A. Nomura[27], T. Nooney[79], M. Nordberg[32], N. Norjoharuddeen[122], O. Novgorodova[47], M. Nozaki[69], L. Nozka[117], K. Ntekas[166], E. Nurse[81], F. Nuti[91], K. O'connor[25], D.C. O'Neil[144], A.A. O'Rourke[45], V. O'Shea[56], F.G. Oakham[31,d], H. Oberlack[103], T. Obermann[23], J. Ocariz[83], A. Ochi[70], I. Ochoa[38], J.P. Ochoa-Ricoux[34a], S. Oda[73], S. Odaka[69], A. Oh[87], S.H. Oh[48], C.C. Ohm[149], H. Ohman[168], H. Oide[53a,53b], H. Okawa[164], Y. Okumura[157], T. Okuyama[69], A. Olariu[28b], L.F. Oleiro Seabra[128a], S.A. Olivares Pino[34a], D. Oliveira Damazio[27], M.J.R. Olsson[33], A. Olszewski[42], J. Olszowska[42], A. Onofre[128a,128e], K. Onogi[105], P.U.E. Onyisi[11,aa], H. Oppen[121], M.J. Oreglia[33], Y. Oren[155], D. Orestano[136a,136b], N. Orlando[62b], R.S. Orr[161], B. Osculati[53a,53b,*], R. Ospanov[36a], G. Otero y Garzon[29], H. Otono[73], M. Ouchrif[137d], F. Ould-Saada[121], A. Ouraou[138], K.P. Oussoren[109], Q. Ouyang[35a], M. Owen[56], R.E. Owen[19], V.E. Ozcan[20a], N. Ozturk[8], K. Pachal[144], A. Pacheco Pages[13], L. Pacheco Rodriguez[138], C. Padilla Aranda[13], S. Pagan Griso[16], M. Paganini[179], F. Paige[27], G. Palacino[64], S. Palazzo[40a,40b], S. Palestini[32], M. Palka[41b], D. Pallin[37], E.St. Panagiotopoulou[10], I. Panagoulias[10], C.E. Pandini[52], J.G. Panduro Vazquez[80], P. Pani[32], S. Panitkin[27], D. Pantea[28b], L. Paolozzi[52], Th.D. Papadopoulou[10], K. Papageorgiou[9,s], A. Paramonov[6], D. Paredes Hernandez[179], A.J. Parker[75], M.A. Parker[30], K.A. Parker[45], F. Parodi[53a,53b], J.A. Parsons[38], U. Parzefall[51], V.R. Pascuzzi[161], J.M. Pasner[139], E. Pasqualucci[134a], S. Passaggio[53a], Fr. Pastore[80], S. Pataraia[86], J.R. Pater[87], T. Pauly[32], B. Pearson[103], S. Pedraza Lopez[170], R. Pedro[128a,128b], S.V. Peleganchuk[111,c], O. Penc[129], C. Peng[35a,35d], H. Peng[36a], J. Penwell[64], B.S. Peralva[26b], M.M. Perego[138], D.V. Perepelitsa[27], F. Peri[17], L. Perini[94a,94b], H. Pernegger[32], S. Perrella[106a,106b], R. Peschke[45], V.D. Peshekhonov[68,*], K. Peters[45], R.F.Y. Peters[87], B.A. Petersen[32], T.C. Petersen[39], E. Petit[58], A. Petridis[1], C. Petridou[156], P. Petroff[119], E. Petrolo[134a], M. Petrov[122], F. Petrucci[136a,136b], N.E. Pettersson[89], A. Peyaud[138], R. Pezoa[34b], F.H. Phillips[93], P.W. Phillips[133], G. Piacquadio[150], E. Pianori[173], A. Picazio[89], M.A. Pickering[122], R. Piegaia[29], J.E. Pilcher[33], A.D. Pilkington[87], M. Pinamonti[135a,135b], J.L. Pinfold[3], H. Pirumov[45], M. Pitt[175], L. Plazak[146a], M.-A. Pleier[27],

V. Pleskot[86], E. Plotnikova[68], D. Pluth[67], P. Podberezko[111], R. Poettgen[84], R. Poggi[123a,123b], L. Poggioli[119], I. Pogrebnyak[93], D. Pohl[23], I. Pokharel[57], G. Polesello[123a], A. Poley[45], A. Policicchio[40a,40b], R. Polifka[32], A. Polini[22a], C.S. Pollard[56], V. Polychronakos[27], K. Pommès[32], D. Ponomarenko[100], L. Pontecorvo[134a], G.A. Popeneciu[28d], D.M. Portillo Quintero[83], S. Pospisil[130], K. Potamianos[45], I.N. Potrap[68], C.J. Potter[30], H. Potti[11], T. Poulsen[84], J. Poveda[32], M.E. Pozo Astigarraga[32], P. Pralavorio[88], A. Pranko[16], S. Prell[67], D. Price[87], M. Primavera[76a], S. Prince[90], N. Proklova[100], K. Prokofiev[62c], F. Prokoshin[34b], S. Protopopescu[27], J. Proudfoot[6], M. Przybycien[41a], A. Puri[169], P. Puzo[119], J. Qian[92], G. Qin[56], Y. Qin[87], A. Quadt[57], M. Queitsch-Maitland[45], D. Quilty[56], S. Raddum[121], V. Radeka[27], V. Radescu[122], S.K. Radhakrishnan[150], P. Radloff[118], P. Rados[91], F. Ragusa[94a,94b], G. Rahal[181], J.A. Raine[87], S. Rajagopalan[27], C. Rangel-Smith[168], T. Rashid[119], S. Raspopov[5], M.G. Ratti[94a,94b], D.M. Rauch[45], F. Rauscher[102], S. Rave[86], I. Ravinovich[175], J.H. Rawling[87], M. Raymond[32], A.L. Read[121], N.P. Readioff[58], M. Reale[76a,76b], D.M. Rebuzzi[123a,123b], A. Redelbach[177], G. Redlinger[27], R. Reece[139], R.G. Reed[147c], K. Reeves[44], L. Rehnisch[17], J. Reichert[124], A. Reiss[86], C. Rembser[32], H. Ren[35a,35d], M. Rescigno[134a], S. Resconi[94a], E.D. Resseguie[124], S. Rettie[171], E. Reynolds[19], O.L. Rezanova[111,c], P. Reznicek[131], R. Rezvani[97], R. Richter[103], S. Richter[81], E. Richter-Was[41b], O. Ricken[23], M. Ridel[83], P. Rieck[103], C.J. Riegel[178], J. Rieger[57], O. Rifki[115], M. Rijssenbeek[150], A. Rimoldi[123a,123b], M. Rimoldi[18], L. Rinaldi[22a], G. Ripellino[149], B. Ristić[32], E. Ritsch[32], I. Riu[13], F. Rizatdinova[116], E. Rizvi[79], C. Rizzi[13], R.T. Roberts[87], S.H. Robertson[90,o], A. Robichaud-Veronneau[90], D. Robinson[30], J.E.M. Robinson[45], A. Robson[56], E. Rocco[86], C. Roda[126a,126b], Y. Rodina[88,al], S. Rodriguez Bosca[170], A. Rodriguez Perez[13], D. Rodriguez Rodriguez[170], S. Roe[32], C.S. Rogan[59], O. Røhne[121], J. Roloff[59], A. Romaniouk[100], M. Romano[22a,22b], S.M. Romano Saez[37], E. Romero Adam[170], N. Rompotis[77], M. Ronzani[51], L. Roos[83], S. Rosati[134a], K. Rosbach[51], P. Rose[139], N.-A. Rosien[57], E. Rossi[106a,106b], L.P. Rossi[53a], J.H.N. Rosten[30], R. Rosten[140], M. Rotaru[28b], J. Rothberg[140], D. Rousseau[119], D. Roy[147c], A. Rozanov[88], Y. Rozen[154], X. Ruan[147c], F. Rubbo[145], F. Rühr[51], A. Ruiz-Martinez[31], Z. Rurikova[51], N.A. Rusakovich[68], H.L. Russell[90], J.P. Rutherfoord[7], N. Ruthmann[32], E.M. Rüttinger[45], Y.F. Ryabov[125], M. Rybar[169], G. Rybkin[119], S. Ryu[6], A. Ryzhov[132], G.F. Rzehorz[57], A.F. Saavedra[152], G. Sabato[109], S. Sacerdoti[29], H.F-W. Sadrozinski[139], R. Sadykov[68], F. Safai Tehrani[134a], P. Saha[110], M. Sahinsoy[60a], M. Saimpert[45], M. Saito[157], T. Saito[157], H. Sakamoto[157], Y. Sakurai[174], G. Salamanna[136a,136b], J.E. Salazar Loyola[34b], D. Salek[109], P.H. Sales De Bruin[168], D. Salihagic[103], A. Salnikov[145], J. Salt[170], D. Salvatore[40a,40b], F. Salvatore[151], A. Salvucci[62a,62b,62c], A. Salzburger[32], D. Sammel[51], D. Sampsonidis[156], D. Sampsonidou[156], J. Sánchez[170], V. Sanchez Martinez[170], A. Sanchez Pineda[167a,167c], H. Sandaker[121], R.L. Sandbach[79], C.O. Sander[45], M. Sandhoff[178], C. Sandoval[21], D.P.C. Sankey[133], M. Sannino[53a,53b], Y. Sano[105], A. Sansoni[50], C. Santoni[37], H. Santos[128a], I. Santoyo Castillo[151], A. Sapronov[68], J.G. Saraiva[128a,128d], B. Sarrazin[23], O. Sasaki[69], K. Sato[164], E. Sauvan[5], G. Savage[80], P. Savard[161,d], N. Savic[103], C. Sawyer[133], L. Sawyer[82,u], J. Saxon[33], C. Sbarra[22a], A. Sbrizzi[22a,22b], T. Scanlon[81], D.A. Scannicchio[166], J. Schaarschmidt[140], P. Schacht[103], B.M. Schachtner[102], D. Schaefer[33], L. Schaefer[124], R. Schaefer[45], J. Schaeffer[86], S. Schaepe[32], S. Schaetzel[60b], U. Schäfer[86], A.C. Schaffer[119], D. Schaile[102], R.D. Schamberger[150], V.A. Schegelsky[125], D. Scheirich[131], F. Schenck[17], M. Schernau[166], C. Schiavi[53a,53b], S. Schier[139], L.K. Schildgen[23], C. Schillo[51], M. Schioppa[40a,40b], S. Schlenker[32], K.R. Schmidt-Sommerfeld[103], K. Schmieden[32], C. Schmitt[86], S. Schmitt[45], S. Schmitz[86], U. Schnoor[51], L. Schoeffel[138], A. Schoening[60b], B.D. Schoenrock[93], E. Schopf[23], M. Schott[86], J.F.P. Schouwenberg[108], J. Schovancova[32], S. Schramm[52], N. Schuh[86], A. Schulte[86], M.J. Schultens[23], H.-C. Schultz-Coulon[60a], H. Schulz[17], M. Schumacher[51], B.A. Schumm[139], Ph. Schune[138], A. Schwartzman[145], T.A. Schwarz[92], H. Schweiger[87], Ph. Schwemling[138], R. Schwienhorst[93], J. Schwindling[138], A. Sciandra[23], G. Sciolla[25], M. Scornajenghi[40a,40b], F. Scuri[126a], F. Scutti[91], J. Searcy[92], P. Seema[23], S.C. Seidel[107], A. Seiden[139],

J.M. Seixas[26a], G. Sekhniaidze[106a], K. Sekhon[92], S.J. Sekula[43], N. Semprini-Cesari[22a,22b], S. Senkin[37], C. Serfon[121], L. Serin[119], L. Serkin[167a,167b], M. Sessa[136a,136b], R. Seuster[172], H. Severini[115], T. Šfiligoj[78], F. Sforza[165], A. Sfyrla[52], E. Shabalina[57], N.W. Shaikh[148a,148b], L.Y. Shan[35a], R. Shang[169], J.T. Shank[24], M. Shapiro[16], P.B. Shatalov[99], K. Shaw[167a,167b], S.M. Shaw[87], A. Shcherbakova[148a,148b], C.Y. Shehu[151], Y. Shen[115], N. Sherafati[31], A.D. Sherman[24], P. Sherwood[81], L. Shi[153,am], S. Shimizu[70], C.O. Shimmin[179], M. Shimojima[104], I.P.J. Shipsey[122], S. Shirabe[73], M. Shiyakova[68,an], J. Shlomi[175], A. Shmeleva[98], D. Shoaleh Saadi[97], M.J. Shochet[33], S. Shojaii[94a,94b], D.R. Shope[115], S. Shrestha[113], E. Shulga[100], M.A. Shupe[7], P. Sicho[129], A.M. Sickles[169], P.E. Sidebo[149], E. Sideras Haddad[147c], O. Sidiropoulou[177], A. Sidoti[22a,22b], F. Siegert[47], Dj. Sijacki[14], J. Silva[128a,128d], S.B. Silverstein[148a], V. Simak[130], L. Simic[68], S. Simion[119], E. Simioni[86], B. Simmons[81], M. Simon[86], P. Sinervo[161], N.B. Sinev[118], M. Sioli[22a,22b], G. Siragusa[177], I. Siral[92], S.Yu. Sivoklokov[101], J. Sjölin[148a,148b], M.B. Skinner[75], P. Skubic[115], M. Slater[19], T. Slavicek[130], M. Slawinska[42], K. Sliwa[165], R. Slovak[131], V. Smakhtin[175], B.H. Smart[5], J. Smiesko[146a], N. Smirnov[100], S.Yu. Smirnov[100], Y. Smirnov[100], L.N. Smirnova[101,ao], O. Smirnova[84], J.W. Smith[57], M.N.K. Smith[38], R.W. Smith[38], M. Smizanska[75], K. Smolek[130], A.A. Snesarev[98], I.M. Snyder[118], S. Snyder[27], R. Sobie[172,o], F. Socher[47], A. Soffer[155], A. Søgaard[49], D.A. Soh[153], G. Sokhrannyi[78], C.A. Solans Sanchez[32], M. Solar[130], E.Yu. Soldatov[100], U. Soldevila[170], A.A. Solodkov[132], A. Soloshenko[68], O.V. Solovyanov[132], V. Solovyev[125], P. Sommer[141], H. Son[165], A. Sopczak[130], D. Sosa[60b], C.L. Sotiropoulou[126a,126b], S. Sottocornola[123a,123b], R. Soualah[167a,167c], A.M. Soukharev[111,c], D. South[45], B.C. Sowden[80], S. Spagnolo[76a,76b], M. Spalla[126a,126b], M. Spangenberg[173], F. Spanò[80], D. Sperlich[17], F. Spettel[103], T.M. Spieker[60a], R. Spighi[22a], G. Spigo[32], L.A. Spiller[91], M. Spousta[131], R.D. St. Denis[56,*], A. Stabile[94a,94b], R. Stamen[60a], S. Stamm[17], E. Stanecka[42], R.W. Stanek[6], C. Stanescu[136a], M.M. Stanitzki[45], B.S. Stapf[109], S. Stapnes[121], E.A. Starchenko[132], G.H. Stark[33], J. Stark[58], S.H Stark[39], P. Staroba[129], P. Starovoitov[60a], S. Stärz[32], R. Staszewski[42], M. Stegler[45], P. Steinberg[27], B. Stelzer[144], H.J. Stelzer[32], O. Stelzer-Chilton[163a], H. Stenzel[55], T.J. Stevenson[79], G.A. Stewart[56], M.C. Stockton[118], M. Stoebe[90], G. Stoicea[28b], P. Stolte[57], S. Stonjek[103], A.R. Stradling[8], A. Straessner[47], M.E. Stramaglia[18], J. Strandberg[149], S. Strandberg[148a,148b], M. Strauss[115], P. Strizenec[146b], R. Ströhmer[177], D.M. Strom[118], R. Stroynowski[43], A. Strubig[49], S.A. Stucci[27], B. Stugu[15], N.A. Styles[45], D. Su[145], J. Su[127], S. Suchek[60a], Y. Sugaya[120], M. Suk[130], V.V. Sulin[98], DMS Sultan[162a,162b], S. Sultansoy[4c], T. Sumida[71], S. Sun[59], X. Sun[3], K. Suruliz[151], C.J.E. Suster[152], M.R. Sutton[151], S. Suzuki[69], M. Svatos[129], M. Swiatlowski[33], S.P. Swift[2], I. Sykora[146a], T. Sykora[131], D. Ta[51], K. Tackmann[45], J. Taenzer[155], A. Taffard[166], R. Tafirout[163a], E. Tahirovic[79], N. Taiblum[155], H. Takai[27], R. Takashima[72], E.H. Takasugi[103], K. Takeda[70], T. Takeshita[142], Y. Takubo[69], M. Talby[88], A.A. Talyshev[111,c], J. Tanaka[157], M. Tanaka[159], R. Tanaka[119], S. Tanaka[69], R. Tanioka[70], B.B. Tannenwald[113], S. Tapia Araya[34b], S. Tapprogge[86], S. Tarem[154], G.F. Tartarelli[94a], P. Tas[131], M. Tasevsky[129], T. Tashiro[71], E. Tassi[40a,40b], A. Tavares Delgado[128a,128b], Y. Tayalati[137e], A.C. Taylor[107], A.J. Taylor[49], G.N. Taylor[91], P.T.E. Taylor[91], W. Taylor[163b], P. Teixeira-Dias[80], D. Temple[144], H. Ten Kate[32], P.K. Teng[153], J.J. Teoh[120], F. Tepel[178], S. Terada[69], K. Terashi[157], J. Terron[85], S. Terzo[13], M. Testa[50], R.J. Teuscher[161,o], S.J. Thais[179], T. Theveneaux-Pelzer[88], F. Thiele[39], J.P. Thomas[19], J. Thomas-Wilsker[80], P.D. Thompson[19], A.S. Thompson[56], L.A. Thomsen[179], E. Thomson[124], Y. Tian[38], M.J. Tibbetts[16], R.E. Ticse Torres[57], V.O. Tikhomirov[98,ap], Yu.A. Tikhonov[111,c], S. Timoshenko[100], P. Tipton[179], S. Tisserant[88], K. Todome[159], S. Todorova-Nova[5], S. Todt[47], J. Tojo[73], S. Tokár[146a], K. Tokushuku[69], E. Tolley[113], L. Tomlinson[87], M. Tomoto[105], L. Tompkins[145,aq], K. Toms[107], B. Tong[59], P. Tornambe[51], E. Torrence[118], H. Torres[47], E. Torró Pastor[140], J. Toth[88,ar], F. Touchard[88], D.R. Tovey[141], C.J. Treado[112], T. Trefzger[177], F. Tresoldi[151], A. Tricoli[27], I.M. Trigger[163a], S. Trincaz-Duvoid[83], M.F. Tripiana[13], W. Trischuk[161], B. Trocmé[58], A. Trofymov[45], C. Troncon[94a], M. Trottier-McDonald[16], M. Trovatelli[172], L. Truong[147b], M. Trzebinski[42], A. Trzupek[42],

K.W. Tsang[62a], J.C-L. Tseng[122], P.V. Tsiareshka[95], G. Tsipolitis[10], N. Tsirintanis[9], S. Tsiskaridze[13], V. Tsiskaridze[51], E.G. Tskhadadze[54a], I.I. Tsukerman[99], V. Tsulaia[16], S. Tsuno[69], D. Tsybychev[150], Y. Tu[62b], A. Tudorache[28b], V. Tudorache[28b], T.T. Tulbure[28a], A.N. Tuna[59], S. Turchikhin[68], D. Turgeman[175], I. Turk Cakir[4b,as], R. Turra[94a], P.M. Tuts[38], G. Ucchielli[22a,22b], I. Ueda[69], M. Ughetto[148a,148b], F. Ukegawa[164], G. Unal[32], A. Undrus[27], G. Unel[166], F.C. Ungaro[91], Y. Unno[69], K. Uno[157], C. Unverdorben[102], J. Urban[146b], P. Urquijo[91], P. Urrejola[86], G. Usai[8], J. Usui[69], L. Vacavant[88], V. Vacek[130], B. Vachon[90], K.O.H. Vadla[121], A. Vaidya[81], C. Valderanis[102], E. Valdes Santurio[148a,148b], M. Valente[52], S. Valentinetti[22a,22b], A. Valero[170], L. Valéry[13], S. Valkar[131], A. Vallier[5], J.A. Valls Ferrer[170], W. Van Den Wollenberg[109], H. van der Graaf[109], P. van Gemmeren[6], J. Van Nieuwkoop[144], I. van Vulpen[109], M.C. van Woerden[109], M. Vanadia[135a,135b], W. Vandelli[32], A. Vaniachine[160], P. Vankov[109], G. Vardanyan[180], R. Vari[134a], E.W. Varnes[7], C. Varni[53a,53b], T. Varol[43], D. Varouchas[119], A. Vartapetian[8], K.E. Varvell[152], J.G. Vasquez[179], G.A. Vasquez[34b], F. Vazeille[37], D. Vazquez Furelos[13], T. Vazquez Schroeder[90], J. Veatch[57], V. Veeraraghavan[7], L.M. Veloce[161], F. Veloso[128a,128c], S. Veneziano[134a], A. Ventura[76a,76b], M. Venturi[172], N. Venturi[32], A. Venturini[25], V. Vercesi[123a], M. Verducci[136a,136b], W. Verkerke[109], A.T. Vermeulen[109], J.C. Vermeulen[109], M.C. Vetterli[144,d], N. Viaux Maira[34b], O. Viazlo[84], I. Vichou[169,*], T. Vickey[141], O.E. Vickey Boeriu[141], G.H.A. Viehhauser[122], S. Viel[16], L. Vigani[122], M. Villa[22a,22b], M. Villaplana Perez[94a,94b], E. Vilucchi[50], M.G. Vincter[31], V.B. Vinogradov[68], A. Vishwakarma[45], C. Vittori[22a,22b], I. Vivarelli[151], S. Vlachos[10], M. Vogel[178], P. Vokac[130], G. Volpi[13], H. von der Schmitt[103], E. von Toerne[23], V. Vorobel[131], K. Vorobev[100], M. Vos[170], R. Voss[32], J.H. Vossebeld[77], N. Vranjes[14], M. Vranjes Milosavljevic[14], V. Vrba[130], M. Vreeswijk[109], R. Vuillermet[32], I. Vukotic[33], P. Wagner[23], W. Wagner[178], J. Wagner-Kuhr[102], H. Wahlberg[74], S. Wahrmund[47], K. Wakamiya[70], J. Walder[75], R. Walker[102], W. Walkowiak[143], V. Wallangen[148a,148b], C. Wang[35b], C. Wang[36b,at], F. Wang[176], H. Wang[16], H. Wang[3], J. Wang[45], J. Wang[152], Q. Wang[115], R.-J. Wang[83], R. Wang[6], S.M. Wang[153], T. Wang[38], W. Wang[153,au], W. Wang[36a,av], Z. Wang[36c], C. Wanotayaroj[45], A. Warburton[90], C.P. Ward[30], D.R. Wardrope[81], A. Washbrook[49], P.M. Watkins[19], A.T. Watson[19], M.F. Watson[19], G. Watts[140], S. Watts[87], B.M. Waugh[81], A.F. Webb[11], S. Webb[86], M.S. Weber[18], S.M. Weber[60a], S.W. Weber[177], S.A. Weber[31], J.S. Webster[6], A.R. Weidberg[122], B. Weinert[64], J. Weingarten[57], M. Weirich[86], C. Weiser[51], H. Weits[109], P.S. Wells[32], T. Wenaus[27], T. Wengler[32], S. Wenig[32], N. Wermes[23], M.D. Werner[67], P. Werner[32], M. Wessels[60a], T.D. Weston[18], K. Whalen[118], N.L. Whallon[140], A.M. Wharton[75], A.S. White[92], A. White[8], M.J. White[1], R. White[34b], D. Whiteson[166], B.W. Whitmore[75], F.J. Wickens[133], W. Wiedenmann[176], M. Wielers[133], C. Wiglesworth[39], L.A.M. Wiik-Fuchs[51], A. Wildauer[103], F. Wilk[87], H.G. Wilkens[32], H.H. Williams[124], S. Williams[109], C. Willis[93], S. Willocq[89], J.A. Wilson[19], I. Wingerter-Seez[5], E. Winkels[151], F. Winklmeier[118], O.J. Winston[151], B.T. Winter[23], M. Wittgen[145], M. Wobisch[82,u], A. Wolf[86], T.M.H. Wolf[109], R. Wolff[88], M.W. Wolter[42], H. Wolters[128a,128c], V.W.S. Wong[171], N.L. Woods[139], S.D. Worm[19], B.K. Wosiek[42], J. Wotschack[32], K.W. Wozniak[42], M. Wu[33], S.L. Wu[176], X. Wu[52], Y. Wu[92], T.R. Wyatt[87], B.M. Wynne[49], S. Xella[39], Z. Xi[92], L. Xia[35c], D. Xu[35a], L. Xu[27], T. Xu[138], W. Xu[92], B. Yabsley[152], S. Yacoob[147a], D. Yamaguchi[159], Y. Yamaguchi[159], A. Yamamoto[69], S. Yamamoto[157], T. Yamanaka[157], F. Yamane[70], M. Yamatani[157], T. Yamazaki[157], Y. Yamazaki[70], Z. Yan[24], H. Yang[36c], H. Yang[16], Y. Yang[153], Z. Yang[15], W-M. Yao[16], Y.C. Yap[45], Y. Yasu[69], E. Yatsenko[5], K.H. Yau Wong[23], J. Ye[43], S. Ye[27], I. Yeletskikh[68], E. Yigitbasi[24], E. Yildirim[86], K. Yorita[174], K. Yoshihara[124], C. Young[145], C.J.S. Young[32], J. Yu[8], J. Yu[67], S.P.Y. Yuen[23], I. Yusuff[30,aw], B. Zabinski[42], G. Zacharis[10], R. Zaidan[13], A.M. Zaitsev[132,aj], N. Zakharchuk[45], J. Zalieckas[15], A. Zaman[150], S. Zambito[59], D. Zanzi[91], C. Zeitnitz[178], G. Zemaityte[122], A. Zemla[41a], J.C. Zeng[169], Q. Zeng[145], O. Zenin[132], T. Ženiš[146a], D. Zerwas[119], D. Zhang[36b], D. Zhang[92], F. Zhang[176], G. Zhang[36a,av], H. Zhang[119], J. Zhang[6], L. Zhang[51], L. Zhang[36a], M. Zhang[169], P. Zhang[35b], R. Zhang[23], R. Zhang[36a,at], X. Zhang[36b], Y. Zhang[35a,35d], Z. Zhang[119], X. Zhao[43], Y. Zhao[36b,ax], Z. Zhao[36a],

A. Zhemchugov[68], B. Zhou[92], C. Zhou[176], L. Zhou[43], M. Zhou[35a,35d], M. Zhou[150], N. Zhou[36c], Y. Zhou[7], C.G. Zhu[36b], H. Zhu[35a], J. Zhu[92], Y. Zhu[36a], X. Zhuang[35a], K. Zhukov[98], A. Zibell[177], D. Zieminska[64], N.I. Zimine[68], C. Zimmermann[86], S. Zimmermann[51], Z. Zinonos[103], M. Zinser[86], M. Ziolkowski[143], L. Živković[14], G. Zobernig[176], A. Zoccoli[22a,22b], R. Zou[33], M. zur Nedden[17], L. Zwalinski[32].

[1] Department of Physics, University of Adelaide, Adelaide, Australia
[2] Physics Department, SUNY Albany, Albany NY, United States of America
[3] Department of Physics, University of Alberta, Edmonton AB, Canada
[4] [(a)] Department of Physics, Ankara University, Ankara; [(b)] Istanbul Aydin University, Istanbul; [(c)] Division of Physics, TOBB University of Economics and Technology, Ankara, Turkey
[5] LAPP, CNRS/IN2P3 and Université Savoie Mont Blanc, Annecy-le-Vieux, France
[6] High Energy Physics Division, Argonne National Laboratory, Argonne IL, United States of America
[7] Department of Physics, University of Arizona, Tucson AZ, United States of America
[8] Department of Physics, The University of Texas at Arlington, Arlington TX, United States of America
[9] Physics Department, National and Kapodistrian University of Athens, Athens, Greece
[10] Physics Department, National Technical University of Athens, Zografou, Greece
[11] Department of Physics, The University of Texas at Austin, Austin TX, United States of America
[12] Institute of Physics, Azerbaijan Academy of Sciences, Baku, Azerbaijan
[13] Institut de Física d'Altes Energies (IFAE), The Barcelona Institute of Science and Technology, Barcelona, Spain
[14] Institute of Physics, University of Belgrade, Belgrade, Serbia
[15] Department for Physics and Technology, University of Bergen, Bergen, Norway
[16] Physics Division, Lawrence Berkeley National Laboratory and University of California, Berkeley CA, United States of America
[17] Department of Physics, Humboldt University, Berlin, Germany
[18] Albert Einstein Center for Fundamental Physics and Laboratory for High Energy Physics, University of Bern, Bern, Switzerland
[19] School of Physics and Astronomy, University of Birmingham, Birmingham, United Kingdom
[20] [(a)] Department of Physics, Bogazici University, Istanbul; [(b)] Department of Physics Engineering, Gaziantep University, Gaziantep; [(d)] Istanbul Bilgi University, Faculty of Engineering and Natural Sciences, Istanbul; [(e)] Bahcesehir University, Faculty of Engineering and Natural Sciences, Istanbul, Turkey
[21] Centro de Investigaciones, Universidad Antonio Narino, Bogota, Colombia
[22] [(a)] INFN Sezione di Bologna; [(b)] Dipartimento di Fisica e Astronomia, Università di Bologna, Bologna, Italy
[23] Physikalisches Institut, University of Bonn, Bonn, Germany
[24] Department of Physics, Boston University, Boston MA, United States of America
[25] Department of Physics, Brandeis University, Waltham MA, United States of America
[26] [(a)] Universidade Federal do Rio De Janeiro COPPE/EE/IF, Rio de Janeiro; [(b)] Electrical Circuits Department, Federal University of Juiz de Fora (UFJF), Juiz de Fora; [(c)] Federal University of Sao Joao del Rei (UFSJ), Sao Joao del Rei; [(d)] Instituto de Fisica, Universidade de Sao Paulo, Sao Paulo, Brazil
[27] Physics Department, Brookhaven National Laboratory, Upton NY, United States of America
[28] [(a)] Transilvania University of Brasov, Brasov; [(b)] Horia Hulubei National Institute of Physics and Nuclear Engineering, Bucharest; [(c)] Department of Physics, Alexandru Ioan Cuza University of Iasi, Iasi; [(d)] National Institute for Research and Development of Isotopic and Molecular Technologies, Physics Department, Cluj Napoca; [(e)] University Politehnica Bucharest, Bucharest; [(f)] West University in Timisoara, Timisoara, Romania

[29] Departamento de Física, Universidad de Buenos Aires, Buenos Aires, Argentina
[30] Cavendish Laboratory, University of Cambridge, Cambridge, United Kingdom
[31] Department of Physics, Carleton University, Ottawa ON, Canada
[32] CERN, Geneva, Switzerland
[33] Enrico Fermi Institute, University of Chicago, Chicago IL, United States of America
[34] [(a)] Departamento de Física, Pontificia Universidad Católica de Chile, Santiago; [(b)] Departamento de Física, Universidad Técnica Federico Santa María, Valparaíso, Chile
[35] [(a)] Institute of High Energy Physics, Chinese Academy of Sciences, Beijing; [(b)] Department of Physics, Nanjing University, Jiangsu; [(c)] Physics Department, Tsinghua University, Beijing 100084; [(d)] University of Chinese Academy of Science (UCAS), Beijing, China
[36] [(a)] Department of Modern Physics and State Key Laboratory of Particle Detection and Electronics, University of Science and Technology of China, Anhui; [(b)] School of Physics, Shandong University, Shandong; [(c)] School of Physics and Astronomy, Key Laboratory for Particle Physics, Astrophysics and Cosmology, Ministry of Education; Shanghai Key Laboratory for Particle Physics and Cosmology, Tsung-Dao Lee Institute, Shanghai Jiao Tong University, China
[37] Université Clermont Auvergne, CNRS/IN2P3, LPC, Clermont-Ferrand, France
[38] Nevis Laboratory, Columbia University, Irvington NY, United States of America
[39] Niels Bohr Institute, University of Copenhagen, Kobenhavn, Denmark
[40] [(a)] INFN Gruppo Collegato di Cosenza, Laboratori Nazionali di Frascati; [(b)] Dipartimento di Fisica, Università della Calabria, Rende, Italy
[41] [(a)] AGH University of Science and Technology, Faculty of Physics and Applied Computer Science, Krakow; [(b)] Marian Smoluchowski Institute of Physics, Jagiellonian University, Krakow, Poland
[42] Institute of Nuclear Physics Polish Academy of Sciences, Krakow, Poland
[43] Physics Department, Southern Methodist University, Dallas TX, United States of America
[44] Physics Department, University of Texas at Dallas, Richardson TX, United States of America
[45] DESY, Hamburg and Zeuthen, Germany
[46] Lehrstuhl für Experimentelle Physik IV, Technische Universität Dortmund, Dortmund, Germany
[47] Institut für Kern- und Teilchenphysik, Technische Universität Dresden, Dresden, Germany
[48] Department of Physics, Duke University, Durham NC, United States of America
[49] SUPA - School of Physics and Astronomy, University of Edinburgh, Edinburgh, United Kingdom
[50] INFN e Laboratori Nazionali di Frascati, Frascati, Italy
[51] Fakultät für Mathematik und Physik, Albert-Ludwigs-Universität, Freiburg, Germany
[52] Departement de Physique Nucleaire et Corpusculaire, Université de Genève, Geneva, Switzerland
[53] [(a)] INFN Sezione di Genova; [(b)] Dipartimento di Fisica, Università di Genova, Genova, Italy
[54] [(a)] E. Andronikashvili Institute of Physics, Iv. Javakhishvili Tbilisi State University, Tbilisi; [(b)] High Energy Physics Institute, Tbilisi State University, Tbilisi, Georgia
[55] II Physikalisches Institut, Justus-Liebig-Universität Giessen, Giessen, Germany
[56] SUPA - School of Physics and Astronomy, University of Glasgow, Glasgow, United Kingdom
[57] II Physikalisches Institut, Georg-August-Universität, Göttingen, Germany
[58] Laboratoire de Physique Subatomique et de Cosmologie, Université Grenoble-Alpes, CNRS/IN2P3, Grenoble, France
[59] Laboratory for Particle Physics and Cosmology, Harvard University, Cambridge MA, United States of America
[60] [(a)] Kirchhoff-Institut für Physik, Ruprecht-Karls-Universität Heidelberg, Heidelberg; [(b)] Physikalisches Institut, Ruprecht-Karls-Universität Heidelberg, Heidelberg, Germany
[61] Faculty of Applied Information Science, Hiroshima Institute of Technology, Hiroshima, Japan
[62] [(a)] Department of Physics, The Chinese University of Hong Kong, Shatin, N.T., Hong Kong; [(b)]

Department of Physics, The University of Hong Kong, Hong Kong; [(c)] Department of Physics and Institute for Advanced Study, The Hong Kong University of Science and Technology, Clear Water Bay, Kowloon, Hong Kong, China
[63] Department of Physics, National Tsing Hua University, Taiwan, Taiwan
[64] Department of Physics, Indiana University, Bloomington IN, United States of America
[65] Institut für Astro- und Teilchenphysik, Leopold-Franzens-Universität, Innsbruck, Austria
[66] University of Iowa, Iowa City IA, United States of America
[67] Department of Physics and Astronomy, Iowa State University, Ames IA, United States of America
[68] Joint Institute for Nuclear Research, JINR Dubna, Dubna, Russia
[69] KEK, High Energy Accelerator Research Organization, Tsukuba, Japan
[70] Graduate School of Science, Kobe University, Kobe, Japan
[71] Faculty of Science, Kyoto University, Kyoto, Japan
[72] Kyoto University of Education, Kyoto, Japan
[73] Research Center for Advanced Particle Physics and Department of Physics, Kyushu University, Fukuoka, Japan
[74] Instituto de Física La Plata, Universidad Nacional de La Plata and CONICET, La Plata, Argentina
[75] Physics Department, Lancaster University, Lancaster, United Kingdom
[76] [(a)] INFN Sezione di Lecce; [(b)] Dipartimento di Matematica e Fisica, Università del Salento, Lecce, Italy
[77] Oliver Lodge Laboratory, University of Liverpool, Liverpool, United Kingdom
[78] Department of Experimental Particle Physics, Jožef Stefan Institute and Department of Physics, University of Ljubljana, Ljubljana, Slovenia
[79] School of Physics and Astronomy, Queen Mary University of London, London, United Kingdom
[80] Department of Physics, Royal Holloway University of London, Surrey, United Kingdom
[81] Department of Physics and Astronomy, University College London, London, United Kingdom
[82] Louisiana Tech University, Ruston LA, United States of America
[83] Laboratoire de Physique Nucléaire et de Hautes Energies, UPMC and Université Paris-Diderot and CNRS/IN2P3, Paris, France
[84] Fysiska institutionen, Lunds universitet, Lund, Sweden
[85] Departamento de Fisica Teorica C-15, Universidad Autonoma de Madrid, Madrid, Spain
[86] Institut für Physik, Universität Mainz, Mainz, Germany
[87] School of Physics and Astronomy, University of Manchester, Manchester, United Kingdom
[88] CPPM, Aix-Marseille Université and CNRS/IN2P3, Marseille, France
[89] Department of Physics, University of Massachusetts, Amherst MA, United States of America
[90] Department of Physics, McGill University, Montreal QC, Canada
[91] School of Physics, University of Melbourne, Victoria, Australia
[92] Department of Physics, The University of Michigan, Ann Arbor MI, United States of America
[93] Department of Physics and Astronomy, Michigan State University, East Lansing MI, United States of America
[94] [(a)] INFN Sezione di Milano; [(b)] Dipartimento di Fisica, Università di Milano, Milano, Italy
[95] B.I. Stepanov Institute of Physics, National Academy of Sciences of Belarus, Minsk, Republic of Belarus
[96] Research Institute for Nuclear Problems of Byelorussian State University, Minsk, Republic of Belarus
[97] Group of Particle Physics, University of Montreal, Montreal QC, Canada
[98] P.N. Lebedev Physical Institute of the Russian Academy of Sciences, Moscow, Russia
[99] Institute for Theoretical and Experimental Physics (ITEP), Moscow, Russia
[100] National Research Nuclear University MEPhI, Moscow, Russia

[101] D.V. Skobeltsyn Institute of Nuclear Physics, M.V. Lomonosov Moscow State University, Moscow, Russia
[102] Fakultät für Physik, Ludwig-Maximilians-Universität München, München, Germany
[103] Max-Planck-Institut für Physik (Werner-Heisenberg-Institut), München, Germany
[104] Nagasaki Institute of Applied Science, Nagasaki, Japan
[105] Graduate School of Science and Kobayashi-Maskawa Institute, Nagoya University, Nagoya, Japan
[106] [(a)] INFN Sezione di Napoli; [(b)] Dipartimento di Fisica, Università di Napoli, Napoli, Italy
[107] Department of Physics and Astronomy, University of New Mexico, Albuquerque NM, United States of America
[108] Institute for Mathematics, Astrophysics and Particle Physics, Radboud University Nijmegen/Nikhef, Nijmegen, Netherlands
[109] Nikhef National Institute for Subatomic Physics and University of Amsterdam, Amsterdam, Netherlands
[110] Department of Physics, Northern Illinois University, DeKalb IL, United States of America
[111] Budker Institute of Nuclear Physics, SB RAS, Novosibirsk, Russia
[112] Department of Physics, New York University, New York NY, United States of America
[113] Ohio State University, Columbus OH, United States of America
[114] Faculty of Science, Okayama University, Okayama, Japan
[115] Homer L. Dodge Department of Physics and Astronomy, University of Oklahoma, Norman OK, United States of America
[116] Department of Physics, Oklahoma State University, Stillwater OK, United States of America
[117] Palacký University, RCPTM, Olomouc, Czech Republic
[118] Center for High Energy Physics, University of Oregon, Eugene OR, United States of America
[119] LAL, Univ. Paris-Sud, CNRS/IN2P3, Université Paris-Saclay, Orsay, France
[120] Graduate School of Science, Osaka University, Osaka, Japan
[121] Department of Physics, University of Oslo, Oslo, Norway
[122] Department of Physics, Oxford University, Oxford, United Kingdom
[123] [(a)] INFN Sezione di Pavia; [(b)] Dipartimento di Fisica, Università di Pavia, Pavia, Italy
[124] Department of Physics, University of Pennsylvania, Philadelphia PA, United States of America
[125] National Research Centre "Kurchatov Institute" B.P.Konstantinov Petersburg Nuclear Physics Institute, St. Petersburg, Russia
[126] [(a)] INFN Sezione di Pisa; [(b)] Dipartimento di Fisica E. Fermi, Università di Pisa, Pisa, Italy
[127] Department of Physics and Astronomy, University of Pittsburgh, Pittsburgh PA, United States of America
[128] [(a)] Laboratório de Instrumentação e Física Experimental de Partículas - LIP, Lisboa; [(b)] Faculdade de Ciências, Universidade de Lisboa, Lisboa; [(c)] Department of Physics, University of Coimbra, Coimbra; [(d)] Centro de Física Nuclear da Universidade de Lisboa, Lisboa; [(e)] Departamento de Fisica, Universidade do Minho, Braga; [(f)] Departamento de Fisica Teorica y del Cosmos, Universidad de Granada, Granada; [(g)] Dep Fisica and CEFITEC of Faculdade de Ciencias e Tecnologia, Universidade Nova de Lisboa, Caparica, Portugal
[129] Institute of Physics, Academy of Sciences of the Czech Republic, Praha, Czech Republic
[130] Czech Technical University in Prague, Praha, Czech Republic
[131] Charles University, Faculty of Mathematics and Physics, Prague, Czech Republic
[132] State Research Center Institute for High Energy Physics (Protvino), NRC KI, Russia
[133] Particle Physics Department, Rutherford Appleton Laboratory, Didcot, United Kingdom
[134] [(a)] INFN Sezione di Roma; [(b)] Dipartimento di Fisica, Sapienza Università di Roma, Roma, Italy
[135] [(a)] INFN Sezione di Roma Tor Vergata; [(b)] Dipartimento di Fisica, Università di Roma Tor Vergata,

Roma, Italy
[136] [(a)] INFN Sezione di Roma Tre; [(b)] Dipartimento di Matematica e Fisica, Università Roma Tre, Roma, Italy
[137] [(a)] Faculté des Sciences Ain Chock, Réseau Universitaire de Physique des Hautes Energies - Université Hassan II, Casablanca; [(b)] Centre National de l'Energie des Sciences Techniques Nucleaires, Rabat; [(c)] Faculté des Sciences Semlalia, Université Cadi Ayyad, LPHEA-Marrakech; [(d)] Faculté des Sciences, Université Mohamed Premier and LPTPM, Oujda; [(e)] Faculté des sciences, Université Mohammed V, Rabat, Morocco
[138] DSM/IRFU (Institut de Recherches sur les Lois Fondamentales de l'Univers), CEA Saclay (Commissariat à l'Energie Atomique et aux Energies Alternatives), Gif-sur-Yvette, France
[139] Santa Cruz Institute for Particle Physics, University of California Santa Cruz, Santa Cruz CA, United States of America
[140] Department of Physics, University of Washington, Seattle WA, United States of America
[141] Department of Physics and Astronomy, University of Sheffield, Sheffield, United Kingdom
[142] Department of Physics, Shinshu University, Nagano, Japan
[143] Department Physik, Universität Siegen, Siegen, Germany
[144] Department of Physics, Simon Fraser University, Burnaby BC, Canada
[145] SLAC National Accelerator Laboratory, Stanford CA, United States of America
[146] [(a)] Faculty of Mathematics, Physics & Informatics, Comenius University, Bratislava; [(b)] Department of Subnuclear Physics, Institute of Experimental Physics of the Slovak Academy of Sciences, Kosice, Slovak Republic
[147] [(a)] Department of Physics, University of Cape Town, Cape Town; [(b)] Department of Physics, University of Johannesburg, Johannesburg; [(c)] School of Physics, University of the Witwatersrand, Johannesburg, South Africa
[148] [(a)] Department of Physics, Stockholm University; [(b)] The Oskar Klein Centre, Stockholm, Sweden
[149] Physics Department, Royal Institute of Technology, Stockholm, Sweden
[150] Departments of Physics & Astronomy and Chemistry, Stony Brook University, Stony Brook NY, United States of America
[151] Department of Physics and Astronomy, University of Sussex, Brighton, United Kingdom
[152] School of Physics, University of Sydney, Sydney, Australia
[153] Institute of Physics, Academia Sinica, Taipei, Taiwan
[154] Department of Physics, Technion: Israel Institute of Technology, Haifa, Israel
[155] Raymond and Beverly Sackler School of Physics and Astronomy, Tel Aviv University, Tel Aviv, Israel
[156] Department of Physics, Aristotle University of Thessaloniki, Thessaloniki, Greece
[157] International Center for Elementary Particle Physics and Department of Physics, The University of Tokyo, Tokyo, Japan
[158] Graduate School of Science and Technology, Tokyo Metropolitan University, Tokyo, Japan
[159] Department of Physics, Tokyo Institute of Technology, Tokyo, Japan
[160] Tomsk State University, Tomsk, Russia
[161] Department of Physics, University of Toronto, Toronto ON, Canada
[162] [(a)] INFN-TIFPA; [(b)] University of Trento, Trento, Italy
[163] [(a)] TRIUMF, Vancouver BC; [(b)] Department of Physics and Astronomy, York University, Toronto ON, Canada
[164] Faculty of Pure and Applied Sciences, and Center for Integrated Research in Fundamental Science and Engineering, University of Tsukuba, Tsukuba, Japan
[165] Department of Physics and Astronomy, Tufts University, Medford MA, United States of America

[166] Department of Physics and Astronomy, University of California Irvine, Irvine CA, United States of America
[167] [(a)] INFN Gruppo Collegato di Udine, Sezione di Trieste, Udine; [(b)] ICTP, Trieste; [(c)] Dipartimento di Chimica, Fisica e Ambiente, Università di Udine, Udine, Italy
[168] Department of Physics and Astronomy, University of Uppsala, Uppsala, Sweden
[169] Department of Physics, University of Illinois, Urbana IL, United States of America
[170] Instituto de Fisica Corpuscular (IFIC), Centro Mixto Universidad de Valencia - CSIC, Spain
[171] Department of Physics, University of British Columbia, Vancouver BC, Canada
[172] Department of Physics and Astronomy, University of Victoria, Victoria BC, Canada
[173] Department of Physics, University of Warwick, Coventry, United Kingdom
[174] Waseda University, Tokyo, Japan
[175] Department of Particle Physics, The Weizmann Institute of Science, Rehovot, Israel
[176] Department of Physics, University of Wisconsin, Madison WI, United States of America
[177] Fakultät für Physik und Astronomie, Julius-Maximilians-Universität, Würzburg, Germany
[178] Fakultät für Mathematik und Naturwissenschaften, Fachgruppe Physik, Bergische Universität Wuppertal, Wuppertal, Germany
[179] Department of Physics, Yale University, New Haven CT, United States of America
[180] Yerevan Physics Institute, Yerevan, Armenia
[181] Centre de Calcul de l'Institut National de Physique Nucléaire et de Physique des Particules (IN2P3), Villeurbanne, France
[182] Academia Sinica Grid Computing, Institute of Physics, Academia Sinica, Taipei, Taiwan
[a] Also at Department of Physics, King's College London, London, United Kingdom
[b] Also at Institute of Physics, Azerbaijan Academy of Sciences, Baku, Azerbaijan
[c] Also at Novosibirsk State University, Novosibirsk, Russia
[d] Also at TRIUMF, Vancouver BC, Canada
[e] Also at Department of Physics & Astronomy, University of Louisville, Louisville, KY, United States of America
[f] Also at Physics Department, An-Najah National University, Nablus, Palestine
[g] Also at Department of Physics, California State University, Fresno CA, United States of America
[h] Also at Department of Physics, University of Fribourg, Fribourg, Switzerland
[i] Also at II Physikalisches Institut, Georg-August-Universität, Göttingen, Germany
[j] Also at Departament de Fisica de la Universitat Autonoma de Barcelona, Barcelona, Spain
[k] Also at Departamento de Fisica e Astronomia, Faculdade de Ciencias, Universidade do Porto, Portugal
[l] Also at Tomsk State University, Tomsk, and Moscow Institute of Physics and Technology State University, Dolgoprudny, Russia
[m] Also at The Collaborative Innovation Center of Quantum Matter (CICQM), Beijing, China
[n] Also at Universita di Napoli Parthenope, Napoli, Italy
[o] Also at Institute of Particle Physics (IPP), Canada
[p] Also at Horia Hulubei National Institute of Physics and Nuclear Engineering, Bucharest, Romania
[q] Also at Department of Physics, St. Petersburg State Polytechnical University, St. Petersburg, Russia
[r] Also at Borough of Manhattan Community College, City University of New York, New York City, United States of America
[s] Also at Department of Financial and Management Engineering, University of the Aegean, Chios, Greece
[t] Also at Centre for High Performance Computing, CSIR Campus, Rosebank, Cape Town, South Africa
[u] Also at Louisiana Tech University, Ruston LA, United States of America
[v] Also at Institucio Catalana de Recerca i Estudis Avancats, ICREA, Barcelona, Spain

[w] Also at Department of Physics, The University of Michigan, Ann Arbor MI, United States of America
[x] Also at Graduate School of Science, Osaka University, Osaka, Japan
[y] Also at Fakultät für Mathematik und Physik, Albert-Ludwigs-Universität, Freiburg, Germany
[z] Also at Institute for Mathematics, Astrophysics and Particle Physics, Radboud University Nijmegen/Nikhef, Nijmegen, Netherlands
[aa] Also at Department of Physics, The University of Texas at Austin, Austin TX, United States of America
[ab] Also at Institute of Theoretical Physics, Ilia State University, Tbilisi, Georgia
[ac] Also at CERN, Geneva, Switzerland
[ad] Also at Georgian Technical University (GTU),Tbilisi, Georgia
[ae] Also at Ochadai Academic Production, Ochanomizu University, Tokyo, Japan
[af] Also at Manhattan College, New York NY, United States of America
[ag] Also at The City College of New York, New York NY, United States of America
[ah] Also at Departamento de Fisica Teorica y del Cosmos, Universidad de Granada, Granada, Portugal
[ai] Also at Department of Physics, California State University, Sacramento CA, United States of America
[aj] Also at Moscow Institute of Physics and Technology State University, Dolgoprudny, Russia
[ak] Also at Departement de Physique Nucleaire et Corpusculaire, Université de Genève, Geneva, Switzerland
[al] Also at Institut de Física d'Altes Energies (IFAE), The Barcelona Institute of Science and Technology, Barcelona, Spain
[am] Also at School of Physics, Sun Yat-sen University, Guangzhou, China
[an] Also at Institute for Nuclear Research and Nuclear Energy (INRNE) of the Bulgarian Academy of Sciences, Sofia, Bulgaria
[ao] Also at Faculty of Physics, M.V.Lomonosov Moscow State University, Moscow, Russia
[ap] Also at National Research Nuclear University MEPhI, Moscow, Russia
[aq] Also at Department of Physics, Stanford University, Stanford CA, United States of America
[ar] Also at Institute for Particle and Nuclear Physics, Wigner Research Centre for Physics, Budapest, Hungary
[as] Also at Giresun University, Faculty of Engineering, Turkey
[at] Also at CPPM, Aix-Marseille Université and CNRS/IN2P3, Marseille, France
[au] Also at Department of Physics, Nanjing University, Jiangsu, China
[av] Also at Institute of Physics, Academia Sinica, Taipei, Taiwan
[aw] Also at University of Malaya, Department of Physics, Kuala Lumpur, Malaysia
[ax] Also at LAL, Univ. Paris-Sud, CNRS/IN2P3, Université Paris-Saclay, Orsay, France
* Deceased